

# Improving Accuracy and Computational Efficiency of the Load Flow Computation of an Active/Passive Distribution Network

Rishabh Verma

A Thesis Submitted to  
Indian Institute of Technology Hyderabad  
In Partial Fulfillment of the Requirements for  
The Degree of Doctor of Philosophy



Department of Electrical Engineering

April 2019

## Declaration

I declare that this written submission represents my ideas in my own words, and where ideas or words of others have been included, I have adequately cited and referenced the original sources. I also declare that I have adhered to all principles of academic honesty and integrity and have not misrepresented or fabricated or falsified any idea/data/fact/source in my submission. I understand that any violation of the above will be a cause for disciplinary action by the Institute and can also evoke penal action from the sources that have thus not been properly cited, or from whom proper permission has not been taken when needed.

Rishabh Verma

(Signature)

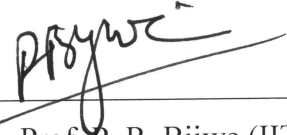
(Rishabh Verma)

EE13P1011

(Roll No.)

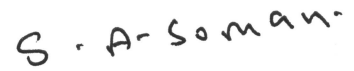
## Approval Sheet

This thesis entitled – Improving Accuracy and Computational Efficiency of the Load Flow Computation of an Active/Passive Distribution Network by Rishabh Verma is approved for the degree of Doctor of Philosophy from IIT Hyderabad.



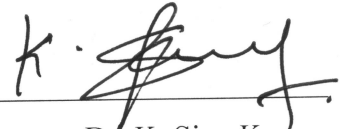
Prof. P. R. Bijwe (IITD)

Examiner 1



Prof. S. A. Soman (IITB)

Examiner 2



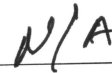
Dr. K. Siva Kumar

Internal Examiner



Dr. Vaskar Sarkar

Adviser/Guide



-Name and affiliation-

Co-Adviser



Dr. Raja Banarjee

Chairman

# Acknowledgements

First of all, I would like to express my sincere gratitude towards my supervisor Dr. Vaskar Sarkar for his continuous guidance and encouragement, especially, during turbulent times. He provided all the required inputs to complete my research in spite of his remaining commitments. I have enjoyed my doctorate tenure working with him. His immense knowledge in Power System has helped me to understand the subject more closely. His dedication towards work inspired me a lot. I am really fortunate to work under his guidance.

I am thankful to my doctoral committee members Dr. K. Sivakumar, Dr. RaviKumar Bhimasingu and Dr. Raja Banerjee for providing valuable inputs to improve the work.

I would like to thank the Indian Institute of Technology, Hyderabad and the Ministry of Human Resource Development for the financial supports.

I am lucky to have a good research group who bear me for almost 6 years. They helped me in many aspects.

I am indebted to my parents, wife and kid for their constant support. It is not possible to thanks them using words.

**Rishabh Verma**

# Dedication

To all the teachers

# Abstract

Over the last couple of decades, there has been a growing trend to make a paradigm shift from the passive distribution network to the active distribution network. With the rapid enlargement of network and installation of distributed generation (DG) units into distribution network, new technical challenges have arisen for load flow computation. The available techniques for the active distribution load flow calculation have limited scope of application and, sometimes, suffer from computational complexity. The complexity level of the distribution system power flow calculation is higher because of the issues of phase imbalance and high  $R/X$  ratios of feeder lines. The phase-imbalance increases computational complexity, whereas, the high  $R/X$  ratio makes time-consuming derivative based solver such as Newton-Raphson inviable for such large system. The motivation behind this work is to propose distinct mathematical approach for accurate modeling of network components, and leads to reduce computational time with improve accuracy. The applicability of an existing technique remains limited either by DG control modes, or by transformer configurations. The objective of this work is basically to develop an active distribution load flow (ADLF) algorithm with the following features.

- Improved computational efficiency.
- Applicability to any feeder network.
- Accurate modeling of loads.
- Applicability to different mode of operations of distributed generators (DGs).

Typically, distributed generators are power-electronically interfaced sources that can be operated either in the current-balanced or in the voltage-balanced mode. The integration of DGs to the feeder network enables the distribution system to have bidirectional power exchange with the transmission grid. Which, also improve the voltage profile of the distribution network by providing additional sources of reactive power compensation.

The contribution of the first work is to carry out the load flow analysis of a distribution network in the case of the dominant presence of induction motor loads. For a given operating condition, the load representation of an induction motor on the distribution network is made by analyzing its exact equivalent circuit. Thus, the induction motor is precisely represented as a voltage and frequency dependent load. The necessity of representing an induction motor by means of its precise load model

is verified through a detailed case study. The convergence of the load flow solution with the precise modeling of induction motor loads is ensured by carrying out the load flow analysis over a complex distribution network containing several loops and distributed generations.

The specific contribution of the second work is to improve the accuracy of the results obtained from the load flow analysis of a distribution network via forward-backward sweeps. Specific attention is paid to the two-port modeling of a transformer with precise consideration for the zero sequence components of its port voltages. The zero sequence voltages at transformer ports are often ignored in the conventional load flow analyses. A new two-port network model is derived, which is generalized enough for the accurate representation of a transformer in the cascaded connection. Based upon the novel two-port representation made, a new set of iteration rules is established to carry out the forward-backward sweeps for solving the load flow results. All possible transformer configurations are taken into account. It is shown that the load flow analysis technique proposed is suitable for both active and passive distribution networks. The accuracy analysis of the load flow results is also carried out. For a given load flow result, by assessing the nodal current imbalances are evaluated based upon the admittance matrix representation of the network. Extensive case studies are performed to demonstrate the utility of the proposed load flow analysis technique.

The contribution of the third work is to develop a computationally efficient and generalised algorithm for the load flow calculation in an active distribution network. The available techniques for the active distribution load flow calculation have limited scope of application and, sometimes, suffer from computational complexity. The applicability of an existing technique remains limited either by DG control modes or by transformer configurations. In this chapter, the load flow calculation is carried out by using the concept of Gauss- $Z_{bus}$  iterations, wherein the DG buses are modeled via the technique of power/current compensation. The specific distinctness of the proposed Gauss- $Z_{bus}$  formulation lies in overcoming the limitations imposed by DG control modes for the chosen DG bus modeling as well as in having optimized computational performance. The entire load flow calculation is carried out in the symmetrical component domain by decoupling all the sequence networks. Furthermore, a generalised network modeling is carried out to define decoupled and tap-invariant sequence networks along with maintaining the integrity of the zero sequence network under any transformer configurations. The computational efficiency and accuracy of the methodology proposed are verified through extensive case studies.

The contribution of the fourth work is to identify and eliminate unnecessary it-

eration loops in the load flow analysis of an active distribution network so as to improve its overall computational efficiency. The number of iteration loops is minimized through the integrated modeling of a distributed generator (DG) and the associated coupling transformer. The DG bus is not preserved in the load flow calculation and the aforementioned DG-transformer assembly is represented in the form of a voltage dependent negative load at the point of connection to the main distribution network. Thus, the iteration stage that is involved in indirectly preserving the DG in the form of a voltage source or negative constant power load can be got rid of. This, in turn, eliminates the need for multiple rounds of forward-backward sweep iterations to determine the bus voltages. The power characteristics of the DG-transformer assembly are thoroughly investigated through a carefully performed case study so as to assess the potential convergence performance of the proposed.



# Contents

Declaration . . . . .	ii
Approval Sheet . . . . .	iii
Acknowledgements . . . . .	iv
Abstract . . . . .	vi
<b>1 Introduction</b>	<b>1</b>
1.1 Preamble . . . . .	1
1.2 Evolution of Distribution Network . . . . .	2
1.3 Distribution Network Challenges . . . . .	2
1.4 Scope and Objectives . . . . .	3
1.5 Organization of the Thesis . . . . .	5
<b>2 Literature Survey</b>	<b>6</b>
2.1 Introduction . . . . .	6
2.2 Load Flow Analysis of Distribution Networks . . . . .	7
2.2.1 Passive Distribution Network Load Flow . . . . .	7
2.2.2 Phase-domain and Symmetrical-domain Approaches . . . . .	8
2.2.3 Feeder Bus Numbering Scheme . . . . .	9
2.2.4 Meshed Network Treatment . . . . .	9
2.2.5 Single Slack Gauss- $Z_{bus}$ Technique . . . . .	10
2.3 Load Flow Analysis of Active Distribution Networks . . . . .	10
2.3.1 Distributed Generators Modeling . . . . .	11
2.3.2 Sensitivity Matrix Based Approach . . . . .	12
2.3.3 Multi Slack and Newton-Raphson Technique . . . . .	12
2.3.4 DG with Droop Characteristics . . . . .	13
2.4 Summary . . . . .	13
<b>3 Two-Port Admittance Matrix Modeling of Network Elements</b>	<b>14</b>
3.1 Introduction . . . . .	14

3.2	Feeder Two-Port Model . . . . .	15
3.3	Transformer Two-Port Modeling . . . . .	16
3.4	Voltage Regulator Two-Port Modeling . . . . .	20
3.5	Summary . . . . .	22
<b>4</b>	<b>Load Flow Analysis with Accurate Modeling of Induction Motor</b>	
	<b>Loads</b>	<b>23</b>
4.1	Background . . . . .	23
4.2	Forward-Backward Load Flow Technique . . . . .	24
4.3	Induction Motor Load Modeling . . . . .	25
4.4	Case Study . . . . .	26
4.5	Summary . . . . .	28
<b>5</b>	<b>FBS Algorithm with Accurate Modeling of Zero Sequence Voltages</b>	<b>30</b>
5.1	Introduction . . . . .	30
5.2	Proposed Two-Port Cascade/Hybrid Parameter Modeling of Trans- formers . . . . .	31
	5.2.1 Cascade Parameter Model . . . . .	32
	5.2.2 Hybrid Parameter Model . . . . .	34
5.3	Proposed FBS algorithm . . . . .	36
	5.3.1 Modified Forward-Backward Sweeps . . . . .	36
	5.3.2 Accuracy Assessment . . . . .	37
5.4	Case Study . . . . .	38
5.5	Summary . . . . .	46
<b>6</b>	<b>Active Distribution Network via Single-Slack Gauss-<math>Z_{bus}</math> Iterations and Canonical Network Transformation</b>	<b>48</b>
6.1	Introduction . . . . .	48
6.2	Organization and Operational Characteristics of a DG . . . . .	50
6.3	The General Template of the ADLF Calculation . . . . .	52
6.4	Transformer/Voltage Regulator Modeling . . . . .	55
6.5	Proposed Load Flow Algorithm . . . . .	56
6.6	Case study . . . . .	60
	6.6.1 Case Study 1 (Verification of the Solution Accuracy): . . . . .	61
	6.6.2 Case Study 2 (Comparison of the Computational Performance):	63
	6.6.3 Case Study 3 (Scalability Verification): . . . . .	65
6.7	Summary . . . . .	66

<b>7</b>	<b>Load Flow Analysis via Integrated DG and Transformer Modeling</b>	<b>68</b>
7.1	Introduction . . . . .	68
7.2	Proposed DG Modeling . . . . .	69
7.2.1	Load Model A . . . . .	72
7.2.2	Load Model B . . . . .	72
7.3	ADLF Algorithm with the Proposed DG Modeling . . . . .	73
7.4	Case Study: . . . . .	75
7.4.1	Case Study 1 (Verification of the Convergence Performance) . . . . .	76
7.4.2	Case Study 2 (Verification of the Computational Efficiency and Solution Accuracy) . . . . .	79
7.5	Summary . . . . .	82
<b>8</b>	<b>Conclusions</b>	<b>84</b>
8.1	Overall Summary . . . . .	84
8.1.1	Load flow Analysis with Accurate Modeling of IM Loads . . . . .	84
8.1.2	FBS Algorithm with Accurate Modeling of Zero Sequence Voltages . . . . .	85
8.1.3	Modified Gauss- $Z_{bus}$ Iterations for Solving ADLF Problem . . . . .	86
8.1.4	LF Analysis via Integrated DG and Transformer Modeling . . . . .	87
8.1.5	Merits of Proposed Work . . . . .	87
8.2	Future Scopes of Work . . . . .	87
8.2.1	OPF Analysis of an Unbalanced Active Distribution Network . . . . .	88
8.2.2	Network-Constrained Consumer Load Aggregation Over Distribution System . . . . .	88
8.2.3	Power Flow Analysis of an AC-DC Distribution Network . . . . .	88
	<b>APPENDICES</b>	<b>89</b>
	<b>A Smaller Test System</b>	<b>89</b>
	<b>B Bigger Test System</b>	<b>92</b>
	<b>References</b>	<b>93</b>

# List of Figures

3.1	General two port representation of an element. . . . .	15
3.2	Feeder equivalent three-wire representation. . . . .	16
3.3	Transformer connection bank. . . . .	17
3.4	Sequence network model of a transformer. . . . .	19
3.5	Winding arrangement of a star-connected voltage regulator. . . . .	21
4.1	Equivalent circuit of induction motor. . . . .	25
4.2	Thevenin's representation of the equivalent circuit. . . . .	25
4.3	Bus voltage magnitudes for the P-V controlled generator operation. . . . .	27
4.4	Bus voltage angles for the P-V controlled generator operation. . . . .	27
4.5	Bus voltage magnitudes for the droop controlled generator operation. . . . .	28
4.6	Bus voltage angles for the droop controlled generator operation. . . . .	28
5.1	Comparison of BCMIs for the 34-bus system. . . . .	40
5.2	Comparison of BCMIs for the 123-bus system. . . . .	41
5.3	Comparison of actual and perceived bus voltage profiles corresponding to the capacitor switching schedule obtained from the conventional FBS algorithm in the 34-bus system. . . . .	44
5.4	Comparison of actual and perceived bus voltage profiles corresponding to the capacitor switching schedule obtained from the conventional FBS algorithm in the 123-bus system. . . . .	45
6.1	Organization of a power electronically interfaced DG unit. . . . .	50
6.2	Symmetrical domain representation of the DG unit. a) Zero sequence, b) negative sequence under current balance, c) negative sequence under voltage balance, d) positive sequence. . . . .	51
6.3	Flowchart for the ADLF calculation with indirect representation of DG buses. . . . .	53
6.4	General two port representation of a transformer or voltage regulator. . . . .	55

6.5	Equivalent circuit representation of a two-port element. . . . .	56
6.6	Nodal active power mismatches in the main feeder network under the current-balanced operation of DGs. . . . .	62
6.7	Nodal reactive power mismatches in the main feeder network under the current-balanced operation of DGs. . . . .	62
6.8	Nodal active power mismatches in the main feeder network under the voltage-balanced operation of DGs. . . . .	62
6.9	Nodal reactive power mismatches in the main feeder network under the voltage-balanced operation of DGs. . . . .	63
6.10	Network arrangement for the scalability test systems. . . . .	66
7.1	Organization of a power electronically interfaced DG unit. . . . .	70
7.2	Symmetrical domain representation of the DG plant. a) Positive sequence, b) zero sequence, c) negative sequence under current balance, d) negative sequence under voltage balance. . . . .	71
7.3	Flowchart of the proposed ADLF algorithm. . . . .	74
7.4	Absolute errors between actual and quadratically approximated load characteristics of DG1 for different POC bus voltages. a) Active power, b) reactive power. . . . .	78
7.5	Plant power characteristics for DG1. a) Active power, b) reactive power. . . . .	79
7.6	IEEE 123-bus system with the locations of DGs, transformers and regulators in referred bus numbering. . . . .	80
A.1	30 bus weakly meshed distribution system with induction motor and generator. . . . .	89
B.1	Single line diagram of the modified 123-bus system with DGs and links. . . . .	92

# List of Tables

4.1	Generator data . . . . .	29
4.2	Induction motor data . . . . .	29
5.1	Load Flow Solutions for Bus Voltage Magnitudes in the 34-bus System	42
5.2	Load Flow Solutions for Bus Voltage Angles in the 34-bus System . .	43
6.1	Link data for the modified 123-bus system . . . . .	61
6.2	DG data for the modified 123-bus system . . . . .	61
6.3	Power/voltage mismatches at DG buses . . . . .	64
6.4	Comparison of computation time requirements among different meth- ods for the current-balanced DG operation . . . . .	64
6.5	Comparison of computation time requirements among different meth- ods for the voltage-balanced DG operation . . . . .	65
6.6	Computational performance of the proposed ADLF algorithm in larger systems . . . . .	66
7.1	DG plant information . . . . .	76
7.2	Parameters of the quadratically approximated active power character- istics of DG plants . . . . .	77
7.3	Parameters of the quadratically approximated reactive power charac- teristics of DG plants . . . . .	77
7.4	Comparison of computation time requirements by different ADLF al- gorithms corresponding to the current-balanced DG operation . . . .	81
7.5	Comparison of computation time requirements by different ADLF al- gorithms corresponding to the voltage-balanced DG operation . . . .	81
7.6	Results for the maximum bus power mismatch at the load flow solution	82
A.1	System line data . . . . .	90
A.2	System nominal load data . . . . .	91

# List of Symbols

## Indices:

$\mathbf{3}\phi$	Three-phase vector/matrix
$abc$	Three-phase matrix
$bw$	Backward sweep
$fw$	Forward sweep
$k$	$k^{th}$ iteration
$ld$	Load
$m$	Bus $m$
$n$	Bus $n$
$N$	Neutral
$p1$	Port 1 (upstream port)
$p2$	Port 2 (downstream port)
$s$	Sequence network (superscript)
$tr$	Transformer
$w$	Transformer terminal winding

## Variables and Parameters:

$\alpha$	Downstream-to-upstream voltage transformation ratio
$A_I$	Current transformation matrix
$A_v$	Voltage transformation matrix
$C$	Fortescue's transformation matrix
$\mathbf{f}_{3\phi}$	Three-phase vector
$\mathbf{F}_{3\phi}$	Three-phase matrix
$\mathbf{H}_{blo}$	Lower triangular components
$\mathbf{H}_{bup}$	Upper triangular components
$\bar{I}$	Current vector

$\bar{\mathbf{I}}_{3\phi,bus,i}$	Bus current injection vector (A)
$N_{pole}$	Number of poles in induction motor
$P_{dg}^{sp}$	Fixed DG active power output (W)
$P_{DG}^{sp(1)}$	Positive sequence active power output (W)
$Q_{dg}^{sp}$	Fixed DG reactive power output (VAr)
$Q_{DG}^{sp(1)}$	Positive sequence reactive power output (VAr)
$Q_{G,max}$	Maximum DG reactive power (VAr)
$Q_{G,min}$	Minimum DG reactive power (VAr)
$Q_{DG}^{(1),(k)}$	Positive sequence reactive power at $k^{th}$ iteration (VAr)
$R_2$	Induction motor rotor resistance (ohm)
$R_{th}$	Thevenin's equivalent resistance (ohm)
$t$	Transformer winding turns ratio
$T$	Load torque applied on induction motor
$\mathbf{U}$	Identity matrix
$\bar{\mathbf{V}}$	Voltage vector
$\bar{V}_{0,m}$	Zero sequence voltage at Bus $m$ (V)
$V_{DG}^{sp(1)}$	Positive sequence terminal voltage (V)
$\mathbf{V}_{DG}^{(1),(k)}$	Positive sequence voltage magnitudes at $k^{th}$ iteration (V)
$V_{poc}^{(1)}$	POC bus voltage magnitude (positive sequence)
$V_{th}$	Thevenin's equivalent voltage (V)
$\omega_g$	Grid frequency (rad/s)
$X_{th}$	Thevenin's equivalent reactance (ohm)
$Y$	Admittance matrix (S)
$z_{tr}^{(s)}$	Sequence domain transformer impedance



## Abbreviations:

ADLF	Active distribution load flow
ADNs	Active distribution networks
BCBV	Branch Current to Bus Voltage
BCMI	bus current mismatch index
BFS	Backward/forward sweep
BIBC	Bus injection to branch current
DG	Distributed generator.
DNLF	Distribution network load flow
ECI	Equivalent current injection
FBS	Forward backward sweep
KCL	Kirchhoff's current law
LTC	Load tap changing
NR	Newton-Raphson
OPF	Optimal power flow
PDLF	Passive distribution load flow
PDN	Passive distribution networks
POC	Point-of-connection
PQ	Constant active and reactive power terminal
PV	Constant power voltage terminal
VSC	Voltage source converter
ZIP	Constant impedance, constant current and constant power

# Chapter 1

## Introduction

### 1.1 Preamble

Electric power distribution network is a crucial link in the electricity supply chain. The electric power distribution system is the infrastructure that is required to serve the end consumer loads at low voltage levels. It carries electricity from the step-down transmission substation to individual end consumers. More substantial power consuming consumers are directly connected to medium voltage step-down transmission substation. While, smaller industrial, commercial and residential customers are connected to low voltage level distribution substation. These low voltage level distribution substations are always located near to the end consumer. In general, distribution network is designed for one way traffic of energy from transmission level down to distribution consumer level.

Generally, distribution system has prominent phase imbalance that may happen either because of unbalanced load distribution over different phases at a bus or because of the presence of single-phase, two-phase and untransposed three-phase feeders in the network [1]. Unlike the transmission network, distribution network is a low voltage system with high  $R/X$  ratio. Some of the specific attributes of the electric distribution systems are:

- Radial or weakly meshed structure
- Multi-phase, phase-imbalance nature
- High  $R/X$  ratio
- Extremely large structure

The traditional distribution networks contain only consumer loads; therefore, always have to draw power from the transmission grid. Such a distribution network is said to be passive in nature.

## 1.2 Evolution of Distribution Network

Over the last couple of decades, there has been a growing trend to make a paradigm shift from the passive distribution network to the active distribution network. The motivation behind the introduction of the active distribution network is to reduce the energy deficiency by harvesting power locally from renewables [2]. The active distribution network is a smart solution for serving power to the consumers by deploying locally available generating resources along with the grid power supply. Thus, an active distribution network is featured by the integration of small-scale generators to the feeder network after the same originates from the transmission grid. The development of such small-scale generating plants, referred to as distributed generators (DGs), is useful to harvest power from the renewable energy sources that are naturally available within a locality. Typically, these distributed generators are power-electronically interfaced sources that can be operated either in the current-balanced or in the voltage-balanced mode [3].

The concept of active distribution network was born as a cost-efficient and timely solution to reliably meet the increasing power demand of the society [4]. The deployment of these local power generations helps in reducing the stress on the main grid. The integration of DGs to the feeder network enables the distribution system to have bidirectional power exchange with the transmission grid. With surplus power from DGs embedded into it, an active distribution network can also reverse its role by providing power supply to the main grid so as to fill the energy deficiencies at other locations [5–8]. This, in turn, renders more flexibility in the distribution system operation along with supporting the transmission grid with the available excess power. In addition, DGs can also improve the voltage profile of the distribution network by providing additional sources of reactive power compensation.

## 1.3 Distribution Network Challenges

The load flow calculation in a distribution system is necessary to evaluate the network loss as well as for scheduling reactive power compensators. With the increased distribution system automation possibility for optimal performance of the network is

increased. Optimum performance can be in terms of loss minimization, no overloading of transformer, reduction in phase imbalance etc. With the help of automation loss minimization and fault isolation can be achieved with network reconfiguration [9,10]. Phase imbalance, overloading and unequal utilization of phases are major issues in distribution network operation. However, in actual operations, the entire distribution network parameters need to be updated in real time to ensure safe and optimal operation [11,12]. So, efficient and computationally fast load flow technique is highly desirable. Optimal operational related computational challenges are listed as follows.

1. Desire of efficient and computationally fast load flow technique.
2. Optimal reconfiguration for loss minimization [13–15].
3. Network reconfiguration for fault isolation [16].
4. Optimal power flow for distribution network [17–19].
5. Optimal voltage regulation to ensure safe operation [20–23].

To efficiently utilize the resources optimal power flow (OPF) models are proposed [24–28]. OPF problem focus on to determine the best operating levels for electric distribution network, usually with the objective of minimizing operating cost or loss minimization. Because electrical power flow equations are nonlinear in nature, nonconvex functions of the OPF are difficult problem to handle specially for distribution network. Power theft is also one of the major issue in electricity distribution system [29]. Distribution network expansion planning is also a multistage problem. Expansion aspects like reliability and economic need to assess for optimized decision [30].

## 1.4 Scope and Objectives

Load flow analysis is one of the fundamental tools for numerical analysis of power flow in an interconnected network, it is important for grid planning, operation or future expansion. The load flow study is mainly carried out to obtain the magnitude and the phase angle of the voltage at each load bus and the real and the reactive power flow through each line.

The load flow analysis of a distribution network is well-known for its complexity and distinctness compared to the load flow analysis of the high voltage transmission network. Because of high  $R/X$  ratios of distribution feeders and prominent phase

imbalance traditional transmission network load flow approaches, such as Newton-Raphson and Gauss-Seidel methods, are observed to be inefficient for distribution network. Traditional load flow techniques suffer from following issues.

1. Convergence issue due to feeder high  $R/X$  ratio.
2. Applicability issues due to feeder structure (weakly meshed network).
3. Computationally expensive.
4. Inaccurate modeling of loads.
5. Inapplicability to incorporate various characteristic DGs.

These are the fundamental issues of distribution network load flow techniques [31]. To cope up with these issues in the past researchers worked to improve the accuracy of existing techniques. Still multiple research gaps are found in existing techniques on the following points.

- Problem of inaccuracy due to negligence of zero sequence components.
- Most of available techniques are computationally inefficient to handle bigger network.
- In correct load modeling especially in the dominant presence of induction motor (IM) loads.
- Incompetency to integrate different characteristic generators

Based on the network configuration distribution network is classified as passive/active network. In active distribution network, integration of DGs requires special attention due to different operating characteristics. The conventional structure that is followed by active distribution load flow (ADLF), is to represent a DG bus into its equivalent load bus. In general, DG reactive power output is updated by using iterative current/power compensation techniques. This conventional approach adds an additional loop of iteration for transforming the original active distribution network into a form that resembles a passive distribution network. Subsequently, the regular steps for the passive distribution network load flow analysis are followed to determine the bus voltage profile. In each iteration of the DG reactive power updation loop, one passive distribution load flow (PDLF) problem is solved. Thus, the ADLF problem is effectively formulated as a series of several PDLF problems. This, in turn, makes

the computation time requirement of the load flow analysis of an active distribution network several times higher than that for its passive counterpart. By keeping these issues in mind modified version of ADLF and PDLF have been design in forthcoming chapters. Therefore, final goals here are to improve the accuracy and computational efficiency of power flow analysis for both active/passive distribution networks.

## 1.5 Organization of the Thesis

The flow of work is carried out as follows. Initially feeder modeling is performed including different network elements in two port format. Specific attention is paid for the zero sequence port voltages. Precise load modeling of induction motor is performed for accurate load flow results. Distributed generators modeling in various control modes are further modified to enhance the scope of application. The applicability of developed generalised algorithm is investigated for the load flow calculation in an active/passive distribution network. The computational efficiency of proposed methodologies are verified through extensive case studies and compared with existing algorithm reported in literature. The performances of proposed algorithms are thoroughly investigated on different IEEE standard test feeders and convergence of algorithm is verified.

The remaining part of the thesis is organized as follows. An elaborative literature survey on load flow analysis of active/passive distribution network is discussed in Chapter 2. In Chapter 3, modeling of various network elements in two-port admittance matrix form is explained. Load flow analysis with accurate modeling of induction motor loads in ZIP form is proposed in Chapter 4. In Chapter 5, forward-backward sweep (FBS) algorithm with accurate modeling of zero sequence voltages of network components is proposed. Modified Gauss- $Z_{bus}$  algorithm for solving the load flow problem in active distribution network is proposed in Chapter 6. Active distribution network load flow analysis through Non-Repetitive FBS iterations with integrated DG and transformer is performed in Chapter 7. Finally, the thesis is concluded in Chapter 8.

# Chapter 2

## Literature Survey

### 2.1 Introduction

The electric power distribution system is the infrastructure that is required to serve the end consumer loads at low voltage levels. The load flow calculation in a distribution system is necessary to evaluate the network loss as well as for scheduling reactive power compensators [32,33] for grid planning, operation, economic scheduling and power exchange between utilities. The objective of power flow analysis is to calculate voltage phasor at every bus and the active and reactive power flow through the feeder. However, the complexity level of the distribution system power flow calculation is higher because of the issues of phase imbalance and high  $R/X$  ratios of feeder lines. The phase-imbalance increases computational complexity, whereas, the high  $R/X$  ratio makes the Jacobian matrix ill-conditioned in the Newton-Raphson (N-R) iteration [1, 34–37]. The traditional distribution networks contain only consumer loads; therefore, always have to draw power from the transmission grid. Such a distribution network is said to be passive in nature.

Over the decades, various load flow methodologies were proposed for distribution networks. Here, an extensive chronological survey of the evolution of the distribution network load flow (DNLf) is presented in this chapter. The evolution of the load flow technique from balanced three-phase network to unbalanced three-phase network [38], from passive distribution network to active distribution network with multiple feeding sources of different nature have been traced and discussed in this literature. Aim of this survey to cover the following topics.

1. Load flow technique for Passive distribution network.
2. Phase-domain and symmetrical domain load flow approaches.

3. Treatment of weakly meshed network.
4. Network organization and PDLF discussion.
5. Active distribution network and generator classification.
6. Active distribution load flow discussion.

Traditional distribution networks always draw power from the slack bus and classified as passive in nature. While, recent trend is to generate power locally with grid power and this kind of network classified as active in nature.

## 2.2 Load Flow Analysis of Distribution Networks

The load flow analysis of a distribution network is well-known for its complexity and distinctness compared to the load flow analysis of the high voltage transmission network. One specific attribute of the distribution network that makes these two load flow analysis problems different is the high  $R/X$  ratios of distribution feeders [1]. In addition, the distribution system has prominent phase imbalance that may happen either because of unbalanced load distribution over different phases at a bus or because of the presence of single-phase, two-phase and untransposed three-phase feeders in the network [39]. Due to high  $R/X$  and prominent phase imbalance the conventional load flow approaches such as Gauss-Seidel and Newton Raphson is failed to meet the requirement of essential solution in terms of convergence. Therefore techniques like Newton-Raphson are not suitable for the purpose.

### 2.2.1 Passive Distribution Network Load Flow

Basically the load flow analysis of a passive distribution network is simply based upon iteratively updating the load currents according to the nature of voltage dependence of a load element. The basic techniques that are used in the literature to carry out the load flow analysis of a distribution network is the ladder iterative technique or forward-backward sweep (FBS) [40,41] in which the load currents and node voltages are sequentially updated by tracing the nodes from leaves to the root and root to leaves vice versa. In FBS, or ladder technique load flow process start with end nodes with nominal voltages and reach back to the slack bus. In the presence of multiple laterals go downstream from the same bus, that node is considered as junction node, at which current is calculated as sum of current (KCL) from laterals while voltage is calculated from the most recent voltage from adjacent node.



Also Ladder and forward-backward technique require additional treatment for weakly meshed network. This extra calculation for weakly meshed link which are required for ladder technique and forward-backward technique are based on current or power compensation technique, which are proposed in literature [1, 42–44].

### 2.2.2 Phase-domain and Symmetrical-domain Approaches

The prominent number of imbalanced single-phase loads and non symmetrical components of three-phase load causes the unbalances situation in distribution feeders [45]. This imbalance and mutual coupling between phases causes larger problem size and increased computational burden [46]. Due to the merits of symmetrical domain to convert three mutually coupled networks into three independent networks. Using the sequence-components frame in the power-flow analysis effectively reduces the problem size and the computational burden as compared to the phase-frame approach [47].

Moreover, due to the separation between the three sequence networks, the system equations can be solved independently irrespective of mutual coupling between phases. While, phase-frame approach is sufficient for radial unbalanced three phase passive distribution network solution it is insufficient in the presence of DGs, so use of sequence components is mandatory for active distribution network.

The load flow calculation in a passive distribution network is usually carried out by means of the forward-backward sweep (FBS) technique [35], which is based upon simple Kirchoff's current and voltage equations. To conduct this transformation from phase-domain including 3-phase, 2-phase and 1-phase feeders into symmetrical domain to convert the unbalance three-phase distribution network into three phase balance network, firstly network is transformed into symmetrical balance network and remaining unsymmetrical residue network. This unsymmetrical residue network is converted as three phase load, lumped between two terminals.

In [48–50], the forward-backward sweeps are carried out in the symmetrical component domain. Distinct treatments of three-phase, two-phase and single-phase feeders are carried out in [51] to improve the computational efficiency of the load flow analysis. With regard to the treatment of an unbalanced distributions feeder in the symmetrical component domain, it is shown in [48] that the particular feeder can be modeled as the combination of a balanced feeder and a couple of voltage dependent current sources at the terminal nodes.

Different versions of the FBS technique is available in literature [52–63]. In [51], forward-backward sweeps are carried out in the symmetrical component domain. A

mixed domain implementation of the FBS technique is shown in [50] by decomposing the entire network into balanced and unbalanced subnetworks. In order to improve the speed of computation, the forward sweep is replaced in [42] with simple voltage scaling based upon the linear proportion principle. A different form of voltage scaling is employed in [44] for the power equation-based forward sweep that was originally proposed in [1]. The methodologies proposed in [1] and [44] are applicable only to a balanced system. The backward/forward sweep technique can also be applied to a weakly meshed system. This requires the incorporation of one more level of iteration in which a link is to be replaced with some current compensations at terminal nodes [52,64]. Apart from the BFS, the use of the Gauss- $Z_{bus}$  iteration technique has also been reported in literature to carry out the load flow calculation for a passive distribution network [65,66].

### 2.2.3 Feeder Bus Numbering Scheme

Distribution network consist thousand of buses in real world scenario, so proper numbering of bus is integral part of load flow computation. In literature different algorithm based on different number schemes are presented. In 1990, G.X. Luo and A. Semlyen uses buses number from slack node to end node of longest laterals then next number to laterals nearest to slack node till end node. Similar method is proposed in Kersting and Mendive (1976) where iteration starts from the first lateral to the end lateral. Ordering network in form of layers instead of buses was proposed by [59], where each lateral in the same layer section were given consecutive numbering. Similarly [67] also proposed fast decoupled load flow technique, where ‘laterals’ orders the network instead of ‘buses’ into ‘layers’, which reduces the problem size and computation time upto greater extend.

### 2.2.4 Meshed Network Treatment

Generally distribution network are not purely radial in nature, they are mostly in weakly meshed configuration. This added link needs extra iterative calculation with radial network load flow approach. The main two methodologies which are proposed in literature are as follows.

1. Current compensation technique [52].
2. Power compensation technique [59].

These techniques use breakpoints to convert weakly meshed network into equivalent radial network, this breaking of network causes addition of two new pseudo nodes in the network. These nodes are injected with the equal current with opposite polarity, current injection is calculated in way so that, the physical source and load currents remain unaltered and the voltage difference between two corresponding breakpoints will become zero.

Then with the help of this equivalent radial network load flow calculation can be done with any available technique. Further, unlike forward-backward sweep technique, the Gauss- $Z_{bus}$  iteration technique does not require any separate treatment of the links for a meshed distribution network.

### 2.2.5 Single Slack Gauss- $Z_{bus}$ Technique

The load flow analysis of a passive distribution network is simply based upon iteratively updating the load currents according to the nature of voltage dependence of a load element. The Gauss- $Z_{bus}$  technique simultaneously updates the load current at all nodes in each load flow iterations. Apart from the FBS, the use of the Gauss- $Z_{bus}$  iteration technique has also been reported in literature to carry out the load flow calculation for a passive distribution network.

Since, the load flow calculation approaches, such as Newton-Raphson and Gauss-Seidel methods, are observed to be inefficient or incompetent to produce the load flow solution for a distribution network. So, to compensate the drawback of these techniques single-slack Gauss- $Z_{bus}$  technique was reported in [56]. This Single-slack Gauss- $Z_{bus}$  technique uses admittance matrix based approach or Equivalent Current Injection (ECI) based approach and it works well as long as feeder components can be modeled in the form Y-matrix or can be converted into ECI. Based on similar topology a new approach [60] was proposed in form of Bus Injection to Branch Current (BIBC) matrix, and Branch Current to Bus Voltage (BCBV) matrix. These methods work efficiently with radial and weakly meshed networks for both balanced and unbalanced distribution networks.

## 2.3 Load Flow Analysis of Active Distribution Networks

With the rapid installation of distributed generators (DGs) passive distribution networks (PDN) have evolved into active distribution networks (ADNs). Based on op-

erating characteristics DGs are usually specified as *PV* generators, *PQ* generators, and droop generators. Adding constant power (*PQ*) generators are easy as it can represent as negative load at node and can be added directly as load in FBS load flow algorithm. While adding a constant power voltage (*PV*) generator needs extra effort, since reactive power injection is unknown. The load flow analysis for such active distribution network can be carried out either by converting the *PV* generator buses either into *PQ* generator buses [52] or into  $V\delta$  buses [3]. In principle, the *PV* buses can be directly addressed by formulating nodal power balance equations and solving those through Newton-Raphson (N-R) iterations. The similar approach is followed in [48] and [49]. However, the N-R technique is, in general, not suitable for the distribution system because of high  $R/X$  ratios of feeder lines [1]. In [52], [68] the DG buses are indirectly modeled in the load flow analysis. Although, originally derived for radial and passive distribution networks, the forward-backward sweep technique has also been found to be applicable for an active and/or meshed distribution network [71, 72] through the addition of one more level of iteration. The additional level of iteration is required to convert the active and/or meshed distribution network into an equivalent passive and radial network.

The sensitivity method was introduced to solve the *PV*-node into the *PQ*-node for forward-backward sweep method [52], where sensitivity approach calculates reactive power injection in each iteration to update the reactive power of the *PV* nodes. To deal with three-phase imbalance load flow positive sequence sensitivity reactance matrices have been proposed in [52] and [61], where reactive power injection at *PV* nodes was chosen as the variable and need to be updated using a sensitivity analysis. The same is carried out by means of a sensitivity analysis over the positive sequence network [50, 59].

### 2.3.1 Distributed Generators Modeling

The conventional structure that is followed by ADLF, is to represent a DG bus into its equivalent load bus. In general, DG reactive power output is updated by using iterative current/power compensation techniques [73]. This conventional approach adds an additional loop of iteration for transforming the original active distribution network into a form that resembles a passive distribution network. Subsequently, the regular steps for the passive distribution network load flow analysis are followed to determine the bus voltage profile. In each iteration of the DG reactive power updation loop, one passive distribution load flow (PDLF) problem is solved. Thus,

the ADLF problem is effectively formulated as a series of several PDLF problems. This, in turn, makes the computation time requirement of the load flow analysis of an active distribution network several times higher than that for its passive counterpart.

### 2.3.2 Sensitivity Matrix Based Approach

For the generators, which are represented by constant power and voltage source, reactive power is needed to maintain the specified voltage value. The most popular technique for handling  $PV$  nodes reactive power calculation is sensitivity matrix technique which are given in literature [52]. In this technique  $PV$  nodes are transformed into  $PQ$  nodes in an iterative manner. Here, sensitivity reactance matrix is used for injected reactive power calculation. This method considers interaction between the  $PV$  nodes into the account, which leads to improved and accurate result.

To cope up with the concept of unbalance generation scenario, sensitivity reactance matrix concept is also used in symmetrical domain frame-work. To incorporate the constant  $PV$  mode of generators into three phase unbalance network, additional process is required in load flow calculation. In sequence transformation different approach is required for negative, zero sequence and positive sequence. As only positive sequence voltage magnitude and active power are usually controlled so only positive sequence reactive power is calculated in iterative manner. After each iteration, the reactive power at positive sequence  $PV$  nodes is updated until it will reach to the convergence criteria.

Based on the sensitivity approach reactive current injection at the  $PV$  nodes was proposed in [52, 56]. A similar method also proposed, which uses the branch impedance magnitude instead of the branch reactance. A modified version of sensitivity approach was proposed in [50, 56] to improve convergence.

### 2.3.3 Multi Slack and Newton-Raphson Technique

In the other approach, the  $PV$  is transformed into a  $V\delta$  (or slack) bus via voltage compensation [3]. By computational approach, the  $PV$  buses can be directly converted to  $PQ$  nodes by utilizing nodal power balance equations and terminal voltage equation and solving those equation by Newton-Raphson (N-R) method.

Although, N-R technique is not suitable for the active distribution system because of high  $R/X$  ratios of feeder lines [1]. Still many researchers worked on N-R and modified N-R [36, 74] techniques for active distribution network load flow. N-R technique is a jacobian matrix based approach where high  $R/X$  makes it ill-condition.

In the literature, researchers proposed modified version of N-R technique to tackle ill-condition distribution network [75].

### **2.3.4 DG with Droop Characteristics**

In grid connected case or islanded case, it is very common to operate DGs in droop characteristic mode [76]. In the case of droop mode of operation, the active power produced by a generator is linked to the system frequency and the reactive power produced is linked to the terminal voltage magnitude. The drooping mode of operation is defined with respect to a reference set of frequency, voltage magnitude, active power and reactive power. A detail description about droop generator operation is discussed in [77]. Radial distribution networks need slack bus for facilitating the computation by means of conventional methods. While, in droop mode of operation rather having the stiff bus that provides a voltage reference and supplies the necessary power, the voltage and power regulation must be shared among the distributed resources as a function of their frequency and voltage droop functions. In presence of multiple droop based generators real and reactive power is shared by all the generators, in the inversely proportion of their droop coefficients.

## **2.4 Summary**

This chapter provides a comprehensive literature survey on the load flow analysis of distribution networks. Extensive discussion from conventional passive distribution network to evolved active distribution network is presented. Merit and demerits of available PDLF techniques are explained in elaborated manner. Structural evolution such as link addition and different characteristic generator addition is also explained. Techniques to tackle these changes such as load flow technique for weakly mesh network and ADLF for different mode of DGs operation are explained and compared on the basis of their advantages and limitations. This survey provides a clear picture of available passive and active distribution network load flow techniques.

# Chapter 3

## Two-Port Admittance Matrix Modeling of Network Elements

### 3.1 Introduction

The load flow algorithm of an active distribution network requires to be generalized for different network configuration. For an unbalanced three-phase network, it is necessary to combine single-phase, two-phase, and three-phase network components in power flow equations. While exploring the representation methodologies the novel two-port representation was found suitable for iterative equation of power flow equations. There are different ways to express two-port relationships based upon network parameters. Based on form representation two-port presentation can be classified as impedance, admittance, cascade or hybrid form. The fundamental way to model distribution network elements as two-port elements is to use the admittance form and the other forms, in exist, can be derived from the admittance form.

The general two-port representation of an element within a distribution network is shown in Fig. 3.1. The element is placed between Bus  $m$  and Bus  $n$ . Without losing generality, Bus  $m$  can be taken as the upstream bus and Bus  $n$  can be taken as the downstream bus. The upstream and downstream ports are named as Port 1 and Port 2 (symbolized with  $p1$  and  $p2$  in subscripts), respectively. The admittance parameter model of the particular element can be written as,

$$\bar{I}_{3\phi,p1} = Y_{3\phi,11}\bar{V}_{3\phi,m} + Y_{3\phi,12}\bar{V}_{3\phi,n} \quad (3.1)$$

$$\bar{I}_{3\phi,p2} = -Y_{3\phi,21}\bar{V}_{3\phi,m} - Y_{3\phi,22}\bar{V}_{3\phi,n}. \quad (3.2)$$

The cascade and hybrid parameter models are obtained through some simple algebraic manipulations of Equations (3.1) and (3.2).

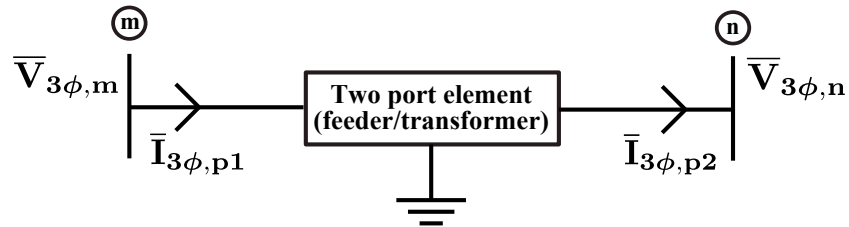


Figure 3.1: General two port representation of an element.

## 3.2 Feeder Two-Port Model

For load flow computation application the general two port model of a feeder line need to present in cascade format to update voltage and current equations in iterative process. With reference to Fig. 3.1 general feeder two port model can introduce in the following format.

$$\bar{V}_{3\phi,m} = A_{3\phi}\bar{V}_{3\phi,n} + B_{3\phi}\bar{I}_{3\phi,p2} \quad (3.3)$$

$$\bar{I}_{3\phi,p1} = C_{3\phi}\bar{V}_{3\phi,n} + D_{3\phi}\bar{I}_{3\phi,p2} \quad (3.4)$$

where, to find parameter  $A_{3\phi}$ ,  $B_{3\phi}$ ,  $C_{3\phi}$  and  $D_{3\phi}$  feeder physical 4-wire or 3-wire feeder line need to present with equivalent 3-wire representation with ground being represented as an equipotential.

Since distribution network is inherently unbalanced consist of single-phase, two-phase, and untransposed three-phase lines serving unbalanced loads, the most accurate representation of a feeder line should not make any assumptions regarding the spacing between conductors, conductor sizes, and transposition. In 1962 John R. Carson developed a technique to calculate self and mutual impedances of conductors. Where, line resistance was directly taken from conductor data. The Carson's equations are applicable to both overhead and underground cables. In formulation Carson also consider the ground return path for the unbalanced currents. A physical 4-wire feeder line will result in a  $4 \times 4$  primitive impedance matrix. For equivalent representation purpose this  $4 \times 4$  primitive impedance matrix is reduce to  $4 \times 4$  primitive impedance matrix by Kron reduction technique. Similar to series impedance matrix calculation, line shunt admittance matrix can also be determined. Finally 4-wire or 3-wire feeder line can be reduced to the equivalent form as shown in Fig. 3.2.



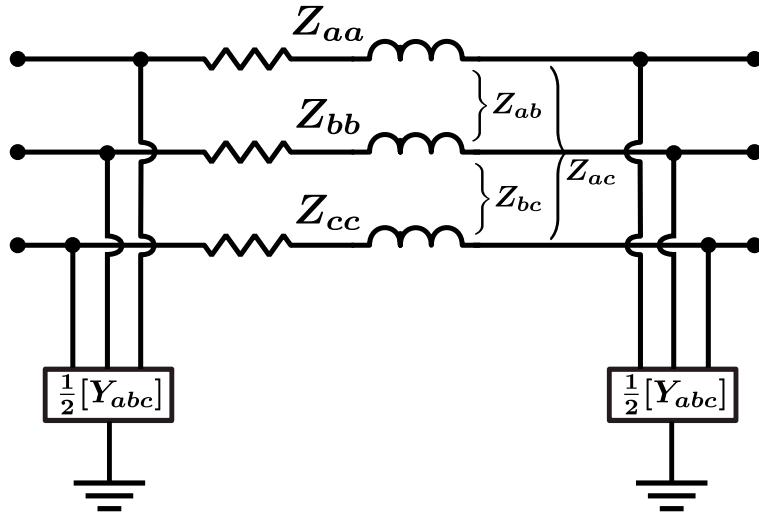


Figure 3.2: Feeder equivalent three-wire representation.

For two-phase or single-phase feeder, the primitive impedance matrices obtained after Carson's equations will be in the dimension of  $3 \times 3$  and  $2 \times 2$ . After Kron's reduction matrices will reduce to the dimension of  $2 \times 2$  and a single element. Finally equivalent admittance matrices can be expanded to  $3 \times 3$  phase frame matrices by the addition of rows and columns of zero elements for the missing phases.

### 3.3 Transformer Two-Port Modeling

A transformer is essentially a two-port element with three-phase ports [78]. Here, to establish a generalized transformer equivalent two-port model for different connection configuration, a generalized transformer connection bank is shown in Fig. 3.3.

Here, the lower case letters  $a, b, c, n$  is referred as the source side (Node  $m$ ) of the bank and the capital letters  $A, B, C, N$  is referred as the load side (Node  $n$ ) of the bank. In general determining transformer equivalent admittance parameter is a straightforward task, afterward two-port model can be achieved by simply using mathematical equations. For transformer terminal winding input and output current equation can be written in generalized form as follows.

$$\bar{I}_{w,abc} = Y_{w,abc}^{abc} \bar{V}_{w,abc} + Y_{w,abc}^{ABC} \bar{V}_{w,ABC} \quad (3.5)$$

$$\bar{I}_{w,ABC} = Y_{w,ABC}^{abc} \bar{V}_{w,abc} + Y_{w,ABC}^{ABC} \bar{V}_{w,ABC}. \quad (3.6)$$

In case of star ground connection configuration on the load side of transformer,

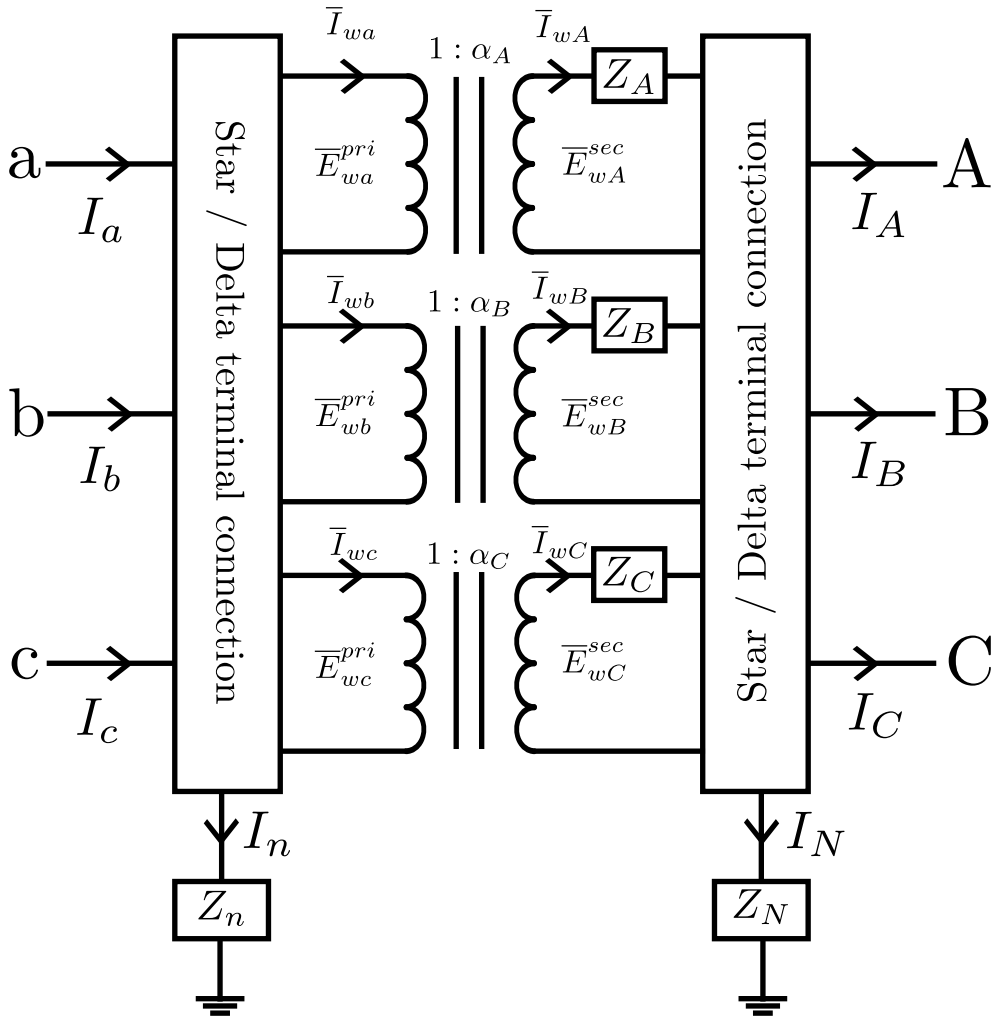


Figure 3.3: Transformer connection bank.

the voltage equations can be written as follows.

$$\bar{V}_{ABC} = \bar{V}_{w,ABC} + \bar{V}_N I_3 \quad (3.7)$$

$$\bar{V}_{abc} = \bar{V}_{w,abc} + \bar{V}_N I_3 \quad (3.8)$$

Since,  $I_3 \bar{I}_{w,ABC} = 0$ , in case of star grounded connection.

Voltage equation can be further translate into generalized form of  $V_N$ ,  $V_n$ ,  $V_{abc}$  and  $V_{ABC}$  as follows.

$$C_{11} \bar{V}_n + C_{12} \bar{V}_N = K_{11} \bar{V}_{abc} + K_{12} \bar{V}_{ABC} \quad (3.9)$$

similarly,

$$C_{21} \bar{V}_n + C_{22} \bar{V}_N = K_{21} \bar{V}_{abc} + K_{22} \bar{V}_{ABC}. \quad (3.10)$$

By using these generalized equations  $V_N$  and  $V_n$  can be written in form of  $V_{abc}$  and  $V_{ABC}$ .

$$\begin{aligned}\bar{V}_N &= a_{11}\bar{V}_{abc} + a_{12}\bar{V}_{ABC} \\ \bar{V}_n &= a_{21}\bar{V}_{abc} + a_{22}\bar{V}_{ABC}.\end{aligned}\tag{3.11}$$

Finally, using the values of  $V_N$  and  $V_n$  from eqn.3.10, eqn.3.5 and 3.6 can be written in the generalized form of  $I_{abc}$  and  $I_{ABC}$ . For star connected transformer bank terminal input and output terminal current can be written as follows:

$$\bar{I}_{abc} = A_I Y_{w,abc}^{abc} A_v \bar{V}_{abc} + A_I Y_{w,abc}^{ABC} A_v \bar{V}_{ABC}\tag{3.12}$$

$$\bar{I}_{ABC} = A_I Y_{w,ABC}^{abc} A_v \bar{V}_{abc} + A_I Y_{w,ABC}^{ABC} A_v \bar{V}_{ABC}.\tag{3.13}$$

Where,  $A_I$  and  $A_v$  are current and voltage transformation matrix. These matrix can be generated by using simple transformer circuit analysis.

$$\begin{aligned}\bar{V}_{abc} &= A_v \bar{V}_{w,abc} \\ \bar{I}_{ABC} &= A_I \bar{I}_{w,ABC}\end{aligned}\tag{3.14}$$

$$\begin{aligned}A_v &= \begin{pmatrix} 1 & -1 & 0 \\ 0 & 1 & -1 \\ -1 & 0 & -1 \end{pmatrix} \\ A_I &= \begin{pmatrix} 1 & 0 & -1 \\ -1 & 1 & 0 \\ 0 & -1 & 1 \end{pmatrix}.\end{aligned}\tag{3.15}$$

Using these generalized current equations of star and delta transformer terminal connection other combination of terminal connection's equations can be generated as per the need. After processing these equations transformer equivalent two-port network parameter can be computed.

Furthermore, a distribution network load transformer is essentially a symmetrical element with identical winding turns ratio for each phase (i.e.,  $t^{(a)}=t^{(b)}=t^{(c)}=t$ ). Therefore, it is possible to decompose a load transformer into positive, negative and zero sequence networks. Any sequence network for a load transformer can, in general, be represented as is shown in Fig. 3.4. The above sequence network representation can be found by following the same procedure as is shown in [79]. The positive and

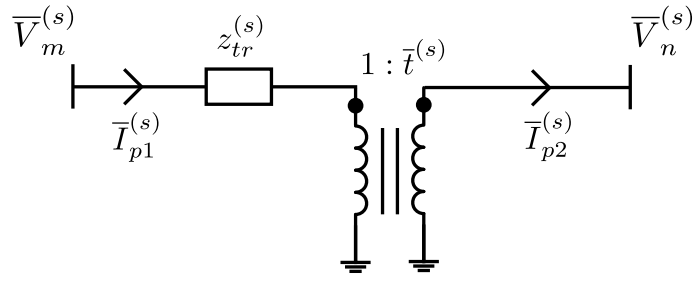


Figure 3.4: Sequence network model of a transformer.

negative sequence network parameters can be obtained through following equations.

$$z_{tr}^{(1)} = z_{tr}^{(2)} = z_{tr}. \quad (3.16)$$

$$\bar{t}^{(1)} = \bar{t}^{(2)*} = t e^{j\theta}. \quad (3.17)$$

The zero sequence network parameters directly depend upon the transformer configuration. The expressions of those parameters are shown below.

$$\begin{aligned} \bar{t}^{(0)} &= \pm t && \text{for star-star} \\ &= \infty && \text{otherwise.} \end{aligned} \quad (3.18)$$

$$\begin{aligned} z_{tr}^{(0)} &= z_{tr} + 3(z_{gp} + t^{-2}z_{gs}) && \text{for star-star} \\ &= z_{tr} + 3z_{gp} && \text{for star-delta} \\ &= \infty && \text{for delta-delta.} \end{aligned} \quad (3.19)$$

From Fig. 3.4, the two-port equation for any sequence network of a load transformer can be written down in admittance form as follows [80].

$$\bar{I}_{p1}^{(s)} = \frac{1}{z_{tr}^{(s)}} \bar{V}_m^{(s)} - \frac{1}{\bar{t}^{(s)} z_{tr}^{(s)}} \bar{V}_n^{(s)} \quad (3.20)$$

$$\bar{I}_{p2}^{(s)} = \frac{1}{\bar{t}^{(s)*} z_{tr}^{(s)}} \bar{V}_m^{(s)} - \frac{1}{|\bar{t}^{(s)}|^2 z_{tr}^{(s)}} \bar{V}_n^{(s)}. \quad (3.21)$$

Based upon Equations (3.20) and (3.21), the combined sequence-domain two-port admittance matrix parameters of a transformer can be found as follows.

$$\mathbf{Y}_{11}^{(012)} = \begin{bmatrix} z_{tr}^{(0)} & 0 & 0 \\ 0 & z_{tr}^{(1)} & 0 \\ 0 & 0 & z_{tr}^{(2)} \end{bmatrix}^{-1} \quad (3.22)$$

$$\mathbf{Y}_{12}^{(012)} = - \begin{bmatrix} \bar{t}^{(0)} z_{tr}^{(0)} & 0 & 0 \\ 0 & \bar{t}^{(1)} z_{tr}^{(1)} & 0 \\ 0 & 0 & \bar{t}^{(2)} z_{tr}^{(2)} \end{bmatrix}^{-1} \quad (3.23)$$

$$\mathbf{Y}_{21}^{(012)} = - \begin{bmatrix} \bar{t}^{(0)*} z_{tr}^{(0)} & 0 & 0 \\ 0 & \bar{t}^{(1)*} z_{tr}^{(1)} & 0 \\ 0 & 0 & \bar{t}^{(2)*} z_{tr}^{(2)} \end{bmatrix}^{-1} \quad (3.24)$$

$$\mathbf{Y}_{22}^{(012)} = \begin{bmatrix} |\bar{t}^{(0)}|^2 z_{tr}^{(0)} & 0 & 0 \\ 0 & |\bar{t}^{(1)}|^2 z_{tr}^{(1)} & 0 \\ 0 & 0 & |\bar{t}^{(2)}|^2 z_{tr}^{(2)} \end{bmatrix}^{-1}. \quad (3.25)$$

Finally, the following equations need to be used to convert the admittance matrix parameters from sequence-domain to the phase-domain.

$$\mathbf{Y}_{11}^{(abc)} = \mathbf{C} \mathbf{Y}_{11}^{(012)} \mathbf{C}^{-1} \quad (3.26)$$

$$\mathbf{Y}_{12}^{(abc)} = \mathbf{C} \mathbf{Y}_{12}^{(012)} \mathbf{C}^{-1} \quad (3.27)$$

$$\mathbf{Y}_{21}^{(abc)} = \mathbf{C} \mathbf{Y}_{21}^{(012)} \mathbf{C}^{-1} \quad (3.28)$$

$$\mathbf{Y}_{22}^{(abc)} = \mathbf{C} \mathbf{Y}_{22}^{(012)} \mathbf{C}^{-1} \quad (3.29)$$

where,  $\mathbf{C}$  is the Fortescue's transformation matrix for a three-phase system.

### 3.4 Voltage Regulator Two-Port Modeling

Voltage regulation is an important operation on a distribution network. As voltage profile keep changing with variation in the consumer's load, so it very important to keep terminal or consumer end voltage within the acceptable level with the help of voltage regulators. Generally steptype voltage regulators, load tap changing transformers (LTC), and shunt capacitors are used for regulating the voltage. Steptype voltage regulator is fundamentally an autotransformer with load tap changing mechanism. The voltage change can be obtained by changing the taps of the autotransformer in winding sections.

A three-phase voltage regulator is basically a star-connected or delta-connected autotransformer [35]. Unlike a load transformer, a voltage regulator may not operate under the phase symmetry since the voltage winding turns ratio can be different for different phases. The winding arrangement of a star-connected voltage regulator

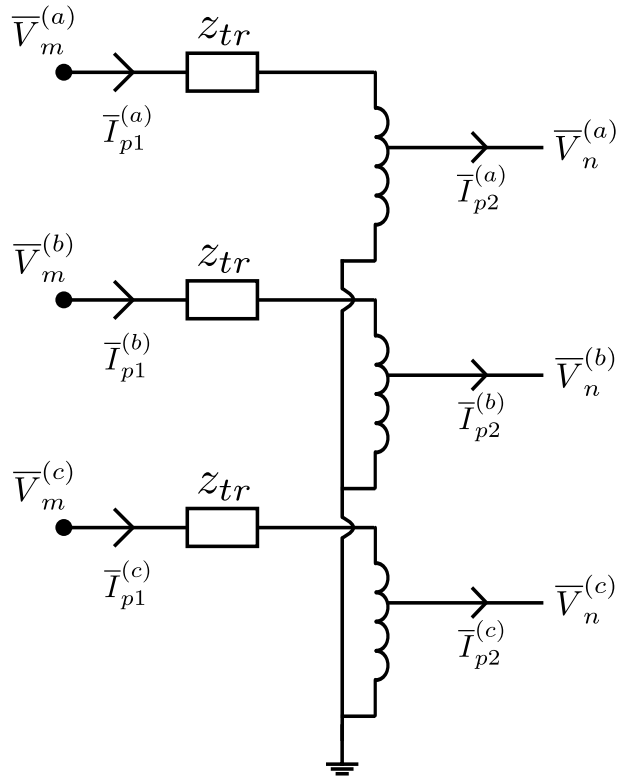


Figure 3.5: Winding arrangement of a star-connected voltage regulator.

(which is considered in the case study) is shown in Fig. 3.5. Here, the neutral point is taken to be solidly grounded. For the voltage regulator presented in Fig. 3.5 the two-port admittance matrix parameters in the phase-domain can be directly obtained as follows.

$$\mathbf{Y}_{11}^{(abc)} = \begin{bmatrix} z_{tr} & 0 & 0 \\ 0 & z_{tr} & 0 \\ 0 & 0 & z_{tr} \end{bmatrix}^{-1} \quad (3.30)$$

$$\mathbf{Y}_{12}^{(abc)} = - \begin{bmatrix} t^{(a)} z_{tr} & 0 & 0 \\ 0 & t^{(b)} z_{tr} & 0 \\ 0 & 0 & t^{(c)} z_{tr} \end{bmatrix}^{-1} \quad (3.31)$$

$$\mathbf{Y}_{21}^{(abc)} = - \begin{bmatrix} t^{(a)} z_{tr} & 0 & 0 \\ 0 & t^{(b)} z_{tr} & 0 \\ 0 & 0 & t^{(c)} z_{tr} \end{bmatrix}^{-1} \quad (3.32)$$

$$\mathbf{Y}_{22}^{(abc)} = \begin{bmatrix} t^{(a)2} z_{tr} & 0 & 0 \\ 0 & t^{(b)2} z_{tr} & 0 \\ 0 & 0 & t^{(c)2} z_{tr} \end{bmatrix}^{-1} . \quad (3.33)$$

## 3.5 Summary

This chapter provides a comprehensive discussion on two-port modeling of feeder line and network components. The necessity of representing network components in two-port equivalent model is to bring all components in same data format for ease of network voltage and current iterative updation. The final objective of this conversion is to represent three phase network elements such as transformer, voltage regulator into two port model so that this equivalent two-port model can be converted into distribution equivalent  $\pi$  model with network up-stream and down-stream connection. This component equivalent  $\pi$  model with line series and shunt admittance will be integrated into feeder network and treated as equivalent network line model.

Finally, complete system can be considered as equivalent radial network without any extra non-linear components. By using sequence domain transformation this imbalance network will be converted into three balanced sequence network. This conversion of transformer and voltage regulator as equivalent line model reduce computational burden and ease network iterative updation. In addition, on the basis of two port matrix formulation, transformer configuration can be categorized into cascade and hybrid parameters. This categorization will be done on the basis of the singularity or non-singularity characteristic of different matrices. Finally, conversion of feeder elements as equivalent line model helps in reduction extra calculation steps and reduces computational time by good margin.

# Chapter 4

## Load Flow Analysis with Accurate Modeling of Induction Motor Loads

### 4.1 Background

Appropriate load modeling is a vital concern to accurately perform the load flow analysis of a power network. The typical load models that are employed in the load flow analysis of a distribution network are the constant impedance, constant current and constant power (i.e., ZIP) loads [44]. Conventionally, an induction motor is represented as a constant power load in the load flow analysis [81]. The particular approach can work well with the minimal presence of induction motor loads. However, the scenario can be significantly different in the case of an active distribution network or microgrid. For example, there can be large number of induction motor loads over the microgrid established for an industrial park. With the dominant presence of induction motor loads, there may be sufficient inaccuracy in the load flow solution in the case induction motors are represented as constant power loads, which may, in turn, lead to incorrect operational decisions.

With the motivation to improve the accuracy of the load flow solution, the precise modeling of induction motor loads in the distribution system power flow analysis is addressed in this chapter. A particular operating condition of an induction motor is represented by means of the load torque that is applied on it. Subsequently, the power drawn by the induction motor is derived as the function of the terminal voltage and system frequency. Thus, an induction motor is precisely represented as a voltage



and frequency dependent load. The closed form of expression obtained for the power drawn by an induction motor can be easily fit into any of the available load flow analysis techniques. The load flow analysis is carried out for an active distribution network by considering different modes of the generator operation with and without system frequency variation.

## 4.2 Forward-Backward Load Flow Technique

This approach is an iterative technique which involves two steps of calculation. In first step currents are calculated using the load given at the node buses. Then in second step voltages are updated using the current derived from the previous iteration. Convergence occurs when the difference between calculated node voltages of the two consecutive iterations is within the specified tolerance limit. Admittance matrix  $Y$  for  $n$  node bus system:

$$\begin{pmatrix} I_1 \\ I_2 \\ \vdots \\ I_n \end{pmatrix} = \begin{pmatrix} Y_{11} & \cdots & Y_{1n} \\ Y_{21} & \cdots & Y_{2n} \\ \vdots & \ddots & \vdots \\ Y_{n1} & \cdots & Y_{nn} \end{pmatrix} \begin{pmatrix} V_1 \\ V_2 \\ \vdots \\ V_n \end{pmatrix} \quad (4.1)$$

With the assumption of only one slack bus with fixed voltage magnitude and angle of  $1\angle 0$ , remaining all nodes are PQ nodes.

$$\begin{bmatrix} I_{slack} \\ I_{PQbus} \end{bmatrix} = \begin{pmatrix} \zeta_{11} & \zeta_{12} \\ \zeta_{21} & \zeta_{22} \end{pmatrix} \begin{bmatrix} V_{slack} \\ V_{PQbus} \end{bmatrix}$$

Current and voltage updation equation for any domain will remain similar and given as follows: Current updation,

$$I = \left\{ \frac{S}{V} \right\}^* \quad (4.2)$$

Voltage updation,

$$[V_{PQbus}] = -(\zeta_{22})^{-1} I_{PQbus} - (\zeta_{22})^{-1} (\zeta_{21}) V_{slack} \quad (4.3)$$

where,  $\zeta_{21} = (Y_{12} \cdots Y_{1n})^t$  and  $\zeta_{22} = \begin{pmatrix} Y_{22} & \cdots & Y_{2n} \\ \vdots & \ddots & \vdots \\ Y_{n2} & \cdots & Y_{nn} \end{pmatrix}$  are admittance matrix components.  $I_{PQbus}$  is combination of all node current except slack node. Here slack node

voltage will remain fixed so only remaining all other nodes voltage will be updated.

### 4.3 Induction Motor Load Modeling

The equivalent circuit of induction motor [82] is shown in Fig. 4.1. By representing the induction motor equivalent circuit in Thevenin's form as in Fig. 4.2, the torque equation can be derived as follows.

$$T = \frac{V_{th}^2}{\left(R_{th} + \frac{R_2}{s}\right)^2 + (X_{th})^2} \times \frac{R_2}{s} \times \frac{1}{\omega_g} \times \frac{N_{pole}}{2}. \quad (4.4)$$

Here,  $N_{pole}$  indicates the number of poles in induction motor and  $\omega_g$  is grid frequency in radian per second.

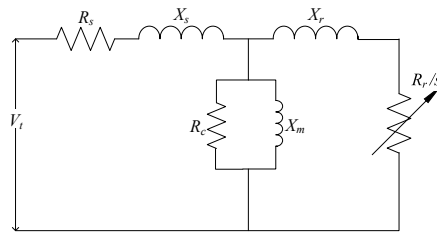


Figure 4.1: Equivalent circuit of induction motor.

As mentioned previously, the operating condition of an induction motor is specified by the load torque applied on it. For particular values of grid frequency and the motor terminal voltage, the induction motor slip can be determined by solving the following quadratic equation.

$$as^2 + bs + c = 0 \quad (4.5)$$

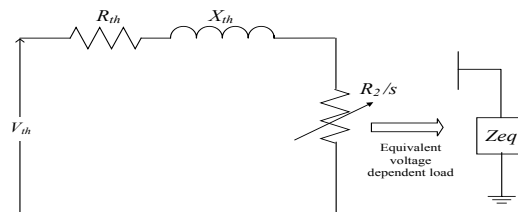


Figure 4.2: Thevenin's representation of the equivalent circuit.

where,

$$a = \left( R_{th}^2 + (X_{th} + X_2)^2 \right) T \omega_g \quad (4.6)$$

$$b = 2R_2 R_{th} \omega_g T - V_{th}^2 R_2 \quad (4.7)$$

$$c = R_2^2 \omega_g T. \quad (4.8)$$

Here,  $T$  indicates the load torque applied on the induction motor. There, exist two solution of the slip, out of which, the smallest positive value is to be considered.

After calculating the slip, the equivalent impedance of the induction motor can be derived, from which, the current drawn by the induction motor for the given grid frequency and terminal voltage can be easily determined. Therefore, the steps to include induction motor loads in the load flow analysis appear as follows.

**Step1:** For the presently calculated grid frequency and bus voltage, determine the induction motor slip by solving the above mention quadratic equation.

**Step2:** After calculating the slip, calculate the induction motor equivalent impedance.

**Step3:** Determine the current drawn by the induction motor and add it to the net nodal load current.

## 4.4 Case Study

The particular case study is performed to justify the need for precise induction motor modeling in the distribution system load flow analysis. A 30 bus distribution network is considered for case study which is shown in Appendix Fig. A.1. The line and load data of the particular system are provided in Appendix Tables A.1 and A.2 respectively. While, generator data of the particular system are presented in Tables 4.1. The induction motor parameters are also provided in Table 4.2. The stator and rotor parameters are taken to be the same for all the induction motors.

In specific, the inaccuracy in load flow results that is introduced because of the conventional representation of the induction motor as a constant power load is investigated. Results are produced for both the P-V and drooping modes of generator operation. The control settings of different generators corresponding to the drooping mode of operation are presented in Table 4.1. For the present study, no additional shunt compensation is considered. Bus 1 is taken as the slack bus. Fig. 4.3 and 4.4

show the comparison of results that are obtained with conventional and precise load models of induction motors for the P-V mode of generator operation.

From Fig. 4.3, it is very obvious that the voltage magnitudes calculated for Buses 9, 10, 11, 12, 28, 29 and 30 with the constant power model of the induction model significantly differ from the actual values. The practical consequence of such inaccuracy in the load flow calculation can be the voltage collapse at certain buses because of insufficiently arranging the reactive power compensation. Results corresponding to the droop controlled generator operation are produced in Fig. 4.5 and 4.6.

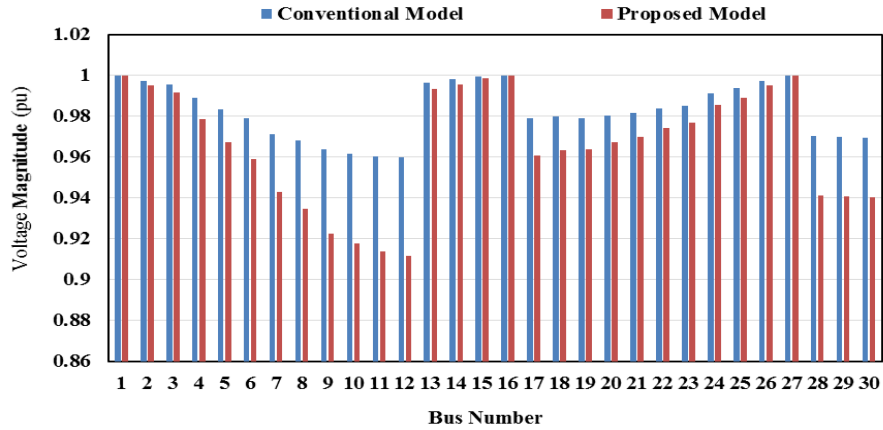


Figure 4.3: Bus voltage magnitudes for the P-V controlled generator operation.

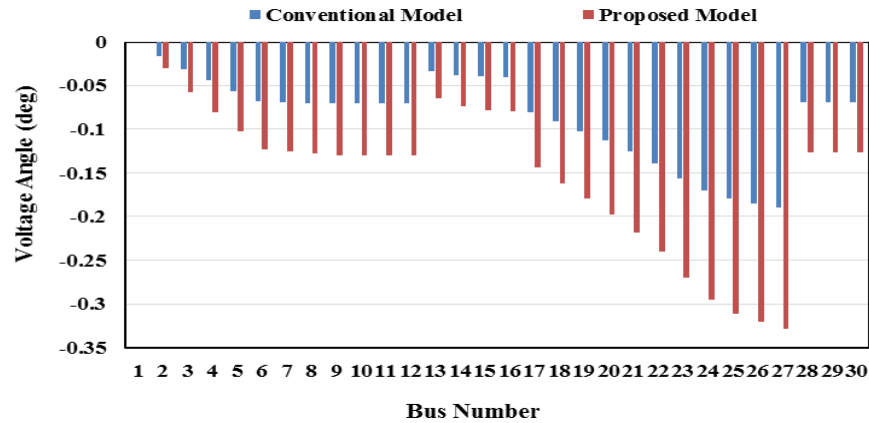


Figure 4.4: Bus voltage angles for the P-V controlled generator operation.

The error introduced in the load flow calculation because of the constant power modeling of induction motor is more prominent in the case of droop controlled generator operation. The inaccurate calculation of bus voltage magnitudes and angles also has a strong concern with the stability of a renewable-driven microgrid. There are

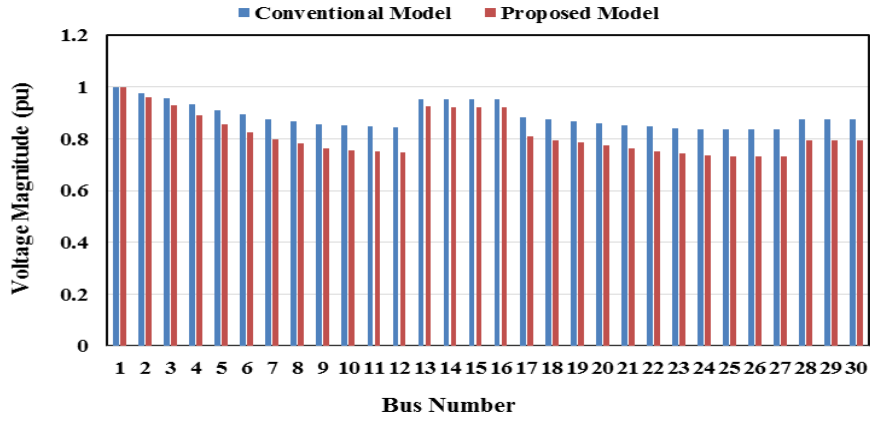


Figure 4.5: Bus voltage magnitudes for the droop controlled generator operation.

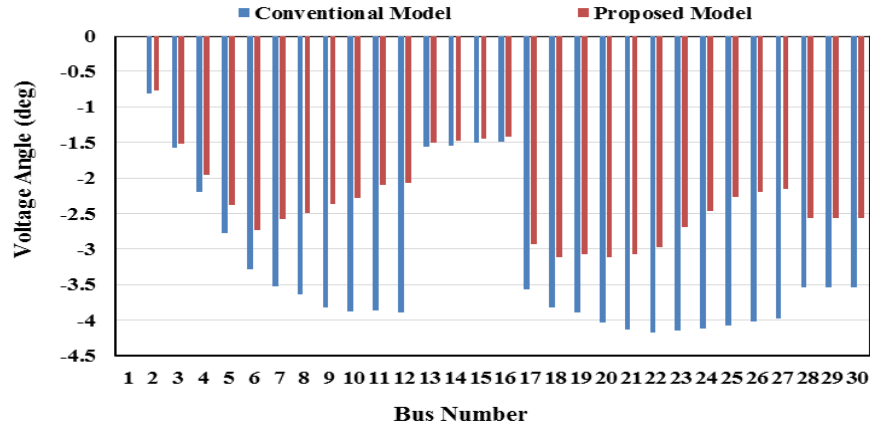


Figure 4.6: Bus voltage angles for the droop controlled generator operation.

controller parameters that are to be tuned by carrying out a system level study, in which the system dynamics is initially to be linearized around the equilibrium that is obtained from a load flow analysis. Therefore, the inaccuracy in the load flow calculation is translated into the inaccuracy in determining the system equilibrium. This, in turn, results in inappropriate parameter tuning with the final effect of degrading the system stability.

## 4.5 Summary

The chapter reports a detailed procedure for the load flow analysis of a distribution network with induction motor loads. Unlike the conventional constant power model, an induction motor is precisely represented in the form of a voltage dependent load.

Table 4.1: Generator data

Bus no.	PV mode of operation		Droop mode of operation		
	Active power output (pu)	Terminal voltage (pu)	Active power output (pu)	Voltage droop coefficient (pu)	frequency droop coefficient (pu)
1	-	1	0.1	0.05	0.05
16	0.1	1	0.1	0.1	0.1
27	0.1	1	0.1	0.2	0.2

Table 4.2: Induction motor data

Machine parameters (pu)	Values (pu)
$R_s$	0.031
$X_s$	0.1
$X_m$	3.2
$R_r$	0.018
$X_r$	0.18
$T$	1

Simple steps are established for determining the induction motor current at each iteration of the load flow calculation. Specific attention is paid on the active distribution network. Studies are performed both for the P-V and drooping mode of generator operation. The frequency dependence of induction motor loads is also recognized. Despite the added complexity in the induction motor modeling over an active distribution network, converged load flow solutions are always obtained. It is revealed from the case studies, there can be significant inaccuracy in the load flow results in the case induction motors are represented as constant power loads.

# Chapter 5

## FBS Algorithm with Accurate Modeling of Zero Sequence Voltages

### 5.1 Introduction

The forward-backward sweep methodology requires the two-port model of each element in terms of both cascade and hybrid parameters. The cascade parameters are required for the backward sweep and the hybrid parameters are required for the forward sweep [40,83]. It is necessary to express all the phase voltages with respect to a common reference node (such as the ground) so as to correctly apply the Kirchhoff's voltage law within a set of electrically connected components. The need for choosing a common voltage reference node makes the standard cascade/hybrid parameter representation, impossible for certain transformer configurations when zero sequence components are present in transformer port voltages. Therefore, the conventional FBS algorithm is based upon the following assumptions.

1. The zero sequence bus voltage component of the phase voltages (with respect to the given common reference) across the port of a delta connected 3-phase winding is zero.
2. For an ungrounded star-connected 3-phase winding, the neutral point voltage is equal to the common reference node voltage.

Although there can be convergence in the load flow solution in terms of the back-calculated substation bus voltage, the overall solution obtained may be inaccurate

because of the above mentioned simplifications of zero sequence voltages at transformer ports. Apart from the FBS technique, the Gauss  $\mathbf{Z}_{bus}$  technique is available to carry out the distribution load flow analysis [60,65]. However, the problem of zero sequence persists since the 3-phase  $\mathbf{Z}_{bus}$  matrix of the complete network does not exist in the presence of certain transformer configurations.

The contribution of this chapter lies in prescribing a modified forward-backward sweep technique that can produce a very accurate load flow picture of the distribution network with due consideration for zero sequence voltages. The work starts with redefining the cascade and hybrid parameter representation of a 3-phase element through the introduction of some zero-sequence voltage offsets, whenever necessary. Detailed mathematical derivation is carried out to determine the new cascade and hybrid parameters. The FBS technique proposed specifically addresses the treatment of those zero-sequence voltage offsets. Suitable steps are followed to evaluate the accuracy of the proposed methodology. It is to be emphasized once again the objective of this chapter is not to improve the convergence performance, but to improve the accuracy of the load flow solution.

## 5.2 Proposed Two-Port Cascade/Hybrid Parameter Modeling of Transformers

A transformer is essentially a two-port element with single-phase or three-phase ports. Typically, two types of transformers are used in the distribution system network. Those are the load transformers and voltage regulators. A voltage regulator is, in essence, an autotransformer. The two-port modeling carried out in this chapter is applicable to both load transformers and voltage regulators, and for all possible configurations. The cascade and hybrid parameter models required are directly derived from the admittance parameter model. The derivation of the admittance parameter model is a straightforward task, which is extensively addressed in literature [84,85].

There are a few general notations that are followed in this chapter. A three-phase vector/matrix is indicated by  $\mathbf{3}\phi$  in subscripts. The structures of a three-phase vector ( $\mathbf{f}_{\mathbf{3}\phi}$ ) and a three-phase matrix ( $\mathbf{F}_{\mathbf{3}\phi}$ ) appear as follows.

$$\mathbf{f}_{\mathbf{3}\phi} = \begin{bmatrix} f_a & f_b & f_c \end{bmatrix}^T \quad (5.1)$$



$$\mathbf{F}_{3\phi} = \begin{bmatrix} F_{aa} & F_{ab} & F_{ac} \\ F_{ba} & F_{bb} & F_{bc} \\ F_{ca} & F_{cb} & F_{cc} \end{bmatrix}. \quad (5.2)$$

For a block matrix over several three-phase elements, subscript  $\mathbf{3}\Phi$  is used. Such a block vector/matrix is composed of blocks each of which is a three-phase subvector/submatrix. All the parameter vectors would be represented by small letters in bold scripts. For parameter matrices, boldscripted capital letters are used. However, for current and voltage vectors, capital letters are used instead of small letters.

### 5.2.1 Cascade Parameter Model

In the cascade parameter model, the voltage and current vectors at Port 1 (as shown in Fig. 3.1) should be expressed in terms of the voltage and current vectors at Port 2, or vice versa. Two cases are to be considered depending upon the invertibility of matrix  $\mathbf{Y}_{3\phi,21}$ .

#### Case 1: $\mathbf{Y}_{3\phi,21}$ is invertible

For a transformer with  $\times$  connections on both the sides, matrix  $\mathbf{Y}_{3\phi,21}$  is always invertible. The cascade parameter model of the particular transformer configuration can simply be derived as follows,

$$\bar{\mathbf{V}}_{3\phi,m} = \mathbf{A}_{3\phi} \bar{\mathbf{V}}_{3\phi,n} + \mathbf{B}_{3\phi} \bar{\mathbf{I}}_{3\phi,p2} \quad (5.3)$$

$$\bar{\mathbf{I}}_{3\phi,p1} = \mathbf{C}_{3\phi} \bar{\mathbf{V}}_{3\phi,n} + \mathbf{D}_{3\phi} \bar{\mathbf{I}}_{3\phi,p2} \quad (5.4)$$

where,

$$\mathbf{A}_{3\phi} = \left\{ -\mathbf{Y}_{3\phi,21} \right\}^{-1} \mathbf{Y}_{3\phi,22} \quad (5.5)$$

$$\mathbf{B}_{3\phi} = \left\{ -\mathbf{Y}_{3\phi,21} \right\}^{-1} \quad (5.6)$$

$$\mathbf{C}_{3\phi} = \left[ \mathbf{Y}_{3\phi,11} \left\{ -\mathbf{Y}_{3\phi,21} \right\}^{-1} \mathbf{Y}_{3\phi,22} + \mathbf{Y}_{3\phi,12} \right] \quad (5.7)$$

$$\mathbf{D}_{3\phi} = \mathbf{Y}_{3\phi,11} \left\{ -\mathbf{Y}_{3\phi,21} \right\}^{-1}. \quad (5.8)$$

Equations (5.3) and (5.4) show the standard form of the cascade parameter model that the conventional FBS algorithm is solely based upon.

**Case 2:  $Y_{3\phi,21}$  is non-invertible**

In the case matrix  $Y_{3\phi,21}$  is non-invertible, one additional equation is required to determine the voltage and current vectors at Port 2 for given voltage and current information at Port 1. Let the zero sequence voltage at Port 2 be known. Therefore, the following equation can be introduced.

$$\bar{V}_{0,m} = \mathbf{1}^T \bar{V}_{3\phi,m}. \quad (5.9)$$

Here,  $\mathbf{1}$  is a  $(3 \times 1)$  vector of all ones. The voltage quantity  $\bar{V}_{0,m}$  indicates the zero sequence component of any phase voltage at Bus  $m$ . By replacing the third row of Equation (5.3) with Equation (5.9) and Equation (5.3) can be modified as follows.

$$\Theta \bar{I}_{3\phi,p2} + \rho \bar{V}_{0,m} = -\hat{Y}_{3\phi,21} \bar{V}_{3\phi,m} - \tilde{Y}_{3\phi,22} \bar{V}_{3\phi,n} \quad (5.10)$$

where,

$$\Theta = \begin{bmatrix} 1 & 0 & 0 \\ 0 & 1 & 0 \\ 0 & 0 & 0 \end{bmatrix} \quad (5.11)$$

$$\rho = \begin{bmatrix} 0 & 0 & 1 \end{bmatrix}^T \quad (5.12)$$

$$\hat{Y}_{3\phi,21} = \begin{bmatrix} Y_{aa,21} & Y_{ab,21} & Y_{ac,21} \\ Y_{ba,21} & Y_{bb,21} & Y_{bc,21} \\ -1 & -1 & -1 \end{bmatrix} \quad (5.13)$$

$$\tilde{Y}_{3\phi,22} = \begin{bmatrix} Y_{aa,22} & Y_{ab,22} & Y_{ac,22} \\ Y_{ba,22} & Y_{bb,22} & Y_{bc,22} \\ 0 & 0 & 0 \end{bmatrix}. \quad (5.14)$$

Therefore, the cascade parameter model of the respective transformer can be formulated as,

$$\bar{V}_{3\phi,m} = A_{3\phi} \bar{V}_{3\phi,n} + B_{3\phi} \bar{I}_{3\phi,p2} + \gamma_{3\phi} \bar{V}_{0,m} \quad (5.15)$$

$$\bar{I}_{3\phi,p1} = C_{3\phi} \bar{V}_{3\phi,n} + D_{3\phi} \bar{I}_{3\phi,p2} + \eta_{3\phi} \bar{V}_{0,m} \quad (5.16)$$

where,

$$\mathbf{A}_{3\phi} = \left\{ -\widehat{\mathbf{Y}}_{3\phi,21} \right\}^{-1} \widetilde{\mathbf{Y}}_{3\phi,22} \quad (5.17)$$

$$\mathbf{B}_{3\phi} = \left\{ -\widehat{\mathbf{Y}}_{3\phi,21} \right\}^{-1} \boldsymbol{\Theta} \quad (5.18)$$

$$\boldsymbol{\gamma}_{3\phi} = \left\{ -\widehat{\mathbf{Y}}_{3\phi,21} \right\}^{-1} \boldsymbol{\rho} \quad (5.19)$$

$$\mathbf{C}_{3\phi} = \left[ \mathbf{Y}_{3\phi,11} \left\{ -\widehat{\mathbf{Y}}_{3\phi,21} \right\}^{-1} \widetilde{\mathbf{Y}}_{3\phi,22} + \widehat{\mathbf{Y}}_{3\phi,12} \right] \quad (5.20)$$

$$\mathbf{D}_{3\phi} = \mathbf{Y}_{3\phi,11} \left\{ -\widehat{\mathbf{Y}}_{3\phi,21} \right\}^{-1} \boldsymbol{\Theta} \quad (5.21)$$

$$\boldsymbol{\eta}_{3\phi} = \mathbf{Y}_{3\phi,11} \left\{ -\widehat{\mathbf{Y}}_{3\phi,21} \right\}^{-1} \boldsymbol{\rho}. \quad (5.22)$$

Note that the cascade parameter model derived above differs from the standard cascade parameter model because of the involvement of the zero sequence voltage offsets  $\boldsymbol{\gamma}_{3\phi} \overline{\mathbf{V}}_{0,m}$  and  $\boldsymbol{\eta}_{3\phi} \overline{\mathbf{V}}_{0,m}$ .

## 5.2.2 Hybrid Parameter Model

In the hybrid parameter model, the voltage vector at Port 2 and the current vector at Port 1 are to be expressed in terms of the current vector at Port 2 and the voltage vector at Port 1, or vice versa. Similarly to the previous derivation, two cases are to be considered with regard to the invertibility of matrix  $\mathbf{Y}_{3\phi,22}$ . However, only the voltage equation at Port 2 is required for the purpose of load flow analysis of a distribution network. Therefore, the derivation of the current equation is not presented.

### Case 1: $\mathbf{Y}_{3\phi,22}$ is invertible

Matrix  $\mathbf{Y}_{3\phi,22}$  is always invertible for the  $\nabla$  connection on the downstream side and  $\Delta$  or  $\nabla$  connection on the upstream side. The hybrid parameter model equation for these transformer configurations is show below.

$$\overline{\mathbf{V}}_{3\phi,n} = \mathbf{G}_{3\phi,21} \overline{\mathbf{V}}_{3\phi,m} + \mathbf{G}_{3\phi,22} \overline{\mathbf{I}}_{3\phi,p2} \quad (5.23)$$

where,

$$\mathbf{G}_{3\phi,21} = \left\{ -\mathbf{Y}_{3\phi,22} \right\}^{-1} \mathbf{Y}_{3\phi,21} \quad (5.24)$$

$$\mathbf{G}_{3\phi,22} = \left\{ -\mathbf{Y}_{3\phi,22} \right\}^{-1}. \quad (5.25)$$

Again, Equation (5.23) represents the standard form of the hybrid parameter model. The conventional FBS algorithm is formulated only based upon this standard form.

### Case 2: $\mathbf{Y}_{3\phi,22}$ is non-invertible

For non-invertible  $\mathbf{Y}_{3\phi,22}$ , the zero sequence voltage of Bus  $n$  is to be considered. Thus, Equation (5.4) is to be modified as is shown below.

$$\Theta \bar{\mathbf{I}}_{3\phi,p2} + \rho \bar{\mathbf{V}}_{0,n} = -\tilde{\mathbf{Y}}_{3\phi,21} \bar{\mathbf{V}}_{3\phi,m} - \hat{\mathbf{Y}}_{3\phi,22} \bar{\mathbf{V}}_{3\phi,n}. \quad (5.26)$$

Matrices  $\hat{\mathbf{Y}}_{3\phi,22}$  and  $\tilde{\mathbf{Y}}_{3\phi,21}$  are obtained in the same way as matrices  $\hat{\mathbf{Y}}_{3\phi,21}$  and  $\tilde{\mathbf{Y}}_{3\phi,22}$  are obtained. Finally, the hybrid parameter representation, with a zero sequence voltage offset, is obtained as follows.

$$\bar{\mathbf{V}}_{3\phi,n} = \mathbf{G}_{3\phi,21} \bar{\mathbf{V}}_{3\phi,m} + \mathbf{G}_{3\phi,22} \bar{\mathbf{I}}_{3\phi,p2} + \boldsymbol{\xi}_{3\phi} \bar{\mathbf{V}}_{0,n} \quad (5.27)$$

where,

$$\mathbf{G}_{3\phi,21} = \left\{ -\hat{\mathbf{Y}}_{3\phi,22} \right\}^{-1} \tilde{\mathbf{Y}}_{3\phi,21} \quad (5.28)$$

$$\mathbf{G}_{3\phi,22} = \left\{ -\hat{\mathbf{Y}}_{3\phi,22} \right\}^{-1} \Theta \quad (5.29)$$

$$\boldsymbol{\xi}_{3\phi} = \left\{ -\hat{\mathbf{Y}}_{3\phi,22} \right\}^{-1} \rho. \quad (5.30)$$

The cascade and hybrid parameter models derived above reduce to the standard models (i.e., models that are normally considered) if the following assumptions are made.

1.  $\bar{\mathbf{V}}_{0,m} = 0$ , if the upstream winding connection is delta, or the upstream winding connection is star (either grounded or ungrounded) and the downstream winding connection is delta.
2.  $\bar{\mathbf{V}}_{0,m} = \alpha \bar{\mathbf{V}}_{0,n} = \alpha \mathbf{1}^T \bar{\mathbf{V}}_{3\phi,n}$ , if the upstream winding connection is ungrounded star and the downstream winding connection is grounded star. Here,  $\alpha$  is the downstream-to-upstream voltage transformation ratio.
3.  $\bar{\mathbf{V}}_{0,n} = 0$ , if the downstream winding connection is delta, or the downstream winding connection is ungrounded star and the upstream winding connection is delta.

4.  $\bar{V}_{0,n} = \alpha^{-1}\bar{V}_{0,m} = \alpha^{-1}\mathbf{1}^T\bar{\mathbf{V}}_{3\phi,m}$ , if the upstream winding connection is ungrounded star and the downstream winding connection is grounded star. Here,  $\alpha$  is the downstream-to-upstream voltage transformation ratio.

Albeit Assumptions 2 and 4 look exactly the same, the first one is basically related to the cascade parameter model, whereas, the second one is related to the hybrid parameter model. The particular assumptions may, however, not be realistic if phase imbalances are high at certain buses.

## 5.3 Proposed FBS algorithm

The detailed transformer modeling in terms of admittance, cascade and hybrid parameters is presented in the previous section. The new cascade and hybrid parameter models derived to perform the to upgrade forward-backward sweep across a transformer. The accuracy assessment of load flow results is carried out by using the admittance parameter model. It is to be noted the two-port models of a feeder line remain unaltered. In this chapter, however, a single-phase or two-phase feeder is equivalently represented as a three-phase feeder with no load and no shunt charging capacitances for the phases that are originally not present. Nonetheless, it is possible to treat a single-phase or two-phase feeder in the original form (as in [51]), since only the FBS steps across a transformer are revised in this chapter.

### 5.3.1 Modified Forward-Backward Sweeps

The overall structure of FBS algorithm remains unaltered. Each iteration comprises of a backward sweep and a forward sweep. The backward sweep starts from the leaf nodes and gradually goes upstream till the substation bus by updating element currents and bus voltages. Following the backward sweep, the forward sweep is carried out to re-update the bus voltages based upon the element currents calculated during the backward sweep and with known substation bus voltage. The iteration stops when substation bus voltage calculated by the backward sweep closely matches the specified value.

With the general algorithmic procedure stated, the only change that is to be made is to revise the forward and reverse sweep equations across a transformer so as to appropriately take into account the zero sequence offsets that are derived in the previous section. Let the updated voltage and current values during the backward sweep in the  $k$ th iteration be indicated by  $(k, bw)$  in superscripts. Similarly,  $(k, fw)$

is used in superscripts to indicate the re-updated voltage values during the forward sweep. Equations for backward sweep to update upstream port voltage and current of a transformer can, thus, be written as follows.

$$\bar{V}_{3\phi,m}^{(k,bw)} = A_{3\phi} \bar{V}_{3\phi,n}^{(k,bw)} + B_{3\phi} \bar{I}_{3\phi,p2}^{(k,bw)} + \gamma_{3\phi} \bar{V}_{0,m}^{(k-1,fw)} \quad (5.31)$$

$$\bar{I}_{3\phi,p1}^{(k,bw)} = C_{3\phi} \bar{V}_{3\phi,n}^{(k,bw)} + D_{3\phi} \bar{I}_{3\phi,p2}^{(k,bw)} + \eta_{3\phi} \bar{V}_{0,m}^{(k-1,fw)}. \quad (5.32)$$

In order to re-update the downstream port bus voltage during forward sweep, the following equation is to be used.

$$\bar{V}_{3\phi,n}^{(k,fw)} = G_{3\phi,21} \bar{V}_{3\phi,m}^{(k,fw)} + G_{3\phi,22} \bar{I}_{3\phi,p2}^{(k,bw)} + \xi_{3\phi} \bar{V}_{0,n}^{(k,bw)}. \quad (5.33)$$

It is again to be mentioned the above zero sequence voltage offsets are not present in the conventional FBS equations. Iterations are carried out based upon latest updated zero sequence voltages. Thus, the zero sequence voltage offsets used during a backward sweep are derived from the results of the forward sweep in the previous iteration. On the other hand, the zero sequence voltage offsets used during a forward sweep are derived from the backward sweep results of the same iteration. The zero sequence voltages of all the buses are to be initialized to zeros at the start of the load flow calculation.

### 5.3.2 Accuracy Assessment

The accuracy of a load flow solution can be assessed by verifying the Kirchhoff's current law (KCL) at each bus (except for the substation bus). According to the KCL, the following relationship should hold good.

$$\bar{I}_{3\phi,ld,i} + \bar{I}_{3\phi,bus,i} = \mathbf{0} \quad \forall i > 1. \quad (5.34)$$

Here,  $\bar{I}_{3\phi,ld,i}$  is the total three-phase load current drawn at Bus  $i$ . The total three-phase current flowing away from Bus  $i$  via the distribution feeders and transformers connected to it is indicated by  $\bar{I}_{3\phi,bus,i}$ . The load current can, in general, be expressed as a function of bus voltage as follows.

$$\bar{I}_{3\phi,ld,i} = f_{ld,i}(\bar{V}_{3\phi,i}). \quad (5.35)$$

The bus current injection vector  $\bar{\mathbf{I}}_{3\phi,bus,i}$  is obtained through the following equation.

$$\bar{\mathbf{I}}_{3\phi,bus} = \mathbf{Y}_{3\phi,bus} \bar{\mathbf{V}}_{3\phi,bus} \quad (5.36)$$

where,

$$\bar{\mathbf{I}}_{3\phi,bus} = \left[ \bar{\mathbf{I}}_{3\phi,bus,1}^T \quad \bar{\mathbf{I}}_{3\phi,bus,2}^T \quad \cdots \quad \bar{\mathbf{I}}_{3\phi,bus,N_b}^T \right]^T \quad (5.37)$$

$$\bar{\mathbf{V}}_{3\phi,bus} = \left[ \bar{\mathbf{V}}_{3\phi,bus,1}^T \quad \bar{\mathbf{V}}_{3\phi,bus,2}^T \quad \cdots \quad \bar{\mathbf{V}}_{3\phi,bus,N_b}^T \right]^T. \quad (5.38)$$

Here,  $\mathbf{Y}_{3\phi,bus}$  is the three-phase bus admittance matrix and  $N_b$  is the number of three-phase buses in the distribution network. The three-phase bus admittance matrix can be easily determined by using the three-phase admittance matrix models of individual elements. The load flow inaccuracy can be quantified in terms of a bus current mismatch index (BCMI). By indicating the load flow results for bus voltages with “\*” in superscripts, the current mismatch vector at Bus  $i$  (symbolized as  $\Delta \bar{\mathbf{I}}_{3\phi,i}$ ) can be obtained as follows.

$$\Delta \bar{\mathbf{I}}_{3\phi,i} = f_{ld,i}(\bar{\mathbf{V}}_{3\phi,i}^*) + \sum_{j=1}^{N_b} \mathbf{Y}_{3\phi,bus,i,j} \bar{\mathbf{V}}_{3\phi,j}^*. \quad (5.39)$$

The BCMI vector at Bus  $i$  is simply given by the absolute value of  $\Delta \bar{\mathbf{I}}_{3\phi,i}$ . It is obvious that the lower is the BCMI, the higher is the accuracy. For the perfectly accurate load flow solution, the BCMIs at all the buses would be zeros.

## 5.4 Case Study

Case studies are performed on modified IEEE 34-bus and 123-bus passive radial distribution networks. Both the systems contain three-phase, two-phase and single-phase feeders. Both test system has one transformer. Each transformer has the  $\Delta$ - $\nabla$  configuration with the  $\Delta$  on the upstream side. The original data of the particular systems is available in [86]- [87]. The following modifications are carried out.

1. The Phase-b and Phase-c loads at each of the downstream buses of a transformer are increased by 5%.
2. The Phase-a load at each of the downstream buses of transformer is increased

- by 25% to create higher phase imbalance across the transformer ports.
- 3. The total load at each single-phase bus is composed of 80% constant power load, 10% constant impedance load and 10% constant current load.
- 4. The capacitor bank placed at each single-phase bus is assumed to be composed of 10 equal sized capacitors.
- 5. For the sake of simplicity, voltage regulators are ignored.

The upper and lower limits of the bus voltage magnitude for switching off and switching on a capacitor are set to 1.0 p.u. and 0.95 p.u., respectively. Thus, it is attempted to maintain a distribution bus voltage at or below the nominal value. This is because it may be harmful to operate an equipment above the rated terminal voltage. Capacitors are switched on or switched off appropriately so as to maintain bus voltage magnitudes within specified limits. Bus 1 is taken as the substation bus.

The objective of the particular study is threefold such as,

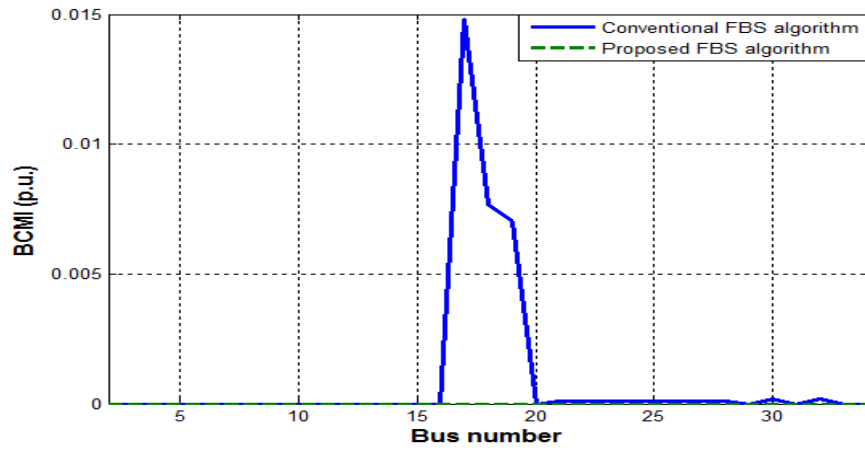
1. to provide a clear illustration of the difference between the conventional and proposed FBS algorithms;
2. to provide evidence of the accuracy improvement caused to the load flow results by proposed algorithm; and,
3. to illustrate the impact of the inaccuracy in the load flow calculation.

In overall, it is attempted to observe the practical benefit of the proposed methodology over the conventional FBS algorithm.

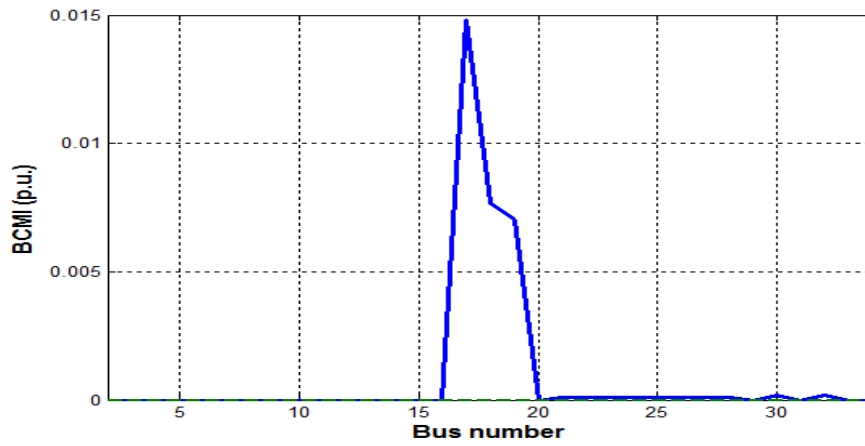
The load flow results obtained from the proposed and conventional algorithms for the 34-bus system are presented in Table 5.1 and Table 5.2. Table 5.1 shows the solutions for bus voltage magnitudes and Table 5.2 shows the solutions for bus voltage angles. Both sets of solutions are obtained by considering the same tolerance (i.e., 0.01 p.u.) for the substation bus voltage magnitude mismatch at the point of convergence. Differences in those two load flow results can be seen from the given tables. Since the load flow solution is supposed to be unique, it is apparent that there is some inaccuracy in either of those two load flow results.

In order to verify the accuracy of load flow results, the BCMIs are plotted in Fig. 5.1 and Fig. 5.2. Fig. 5.1 corresponds to the 34-bus system, where as Fig. 5.2 corresponds to the 123-bus system. The load flow solution produced by the proposed algorithm maintains almost zero BCMIs at all the buses. In contrast, the bus current

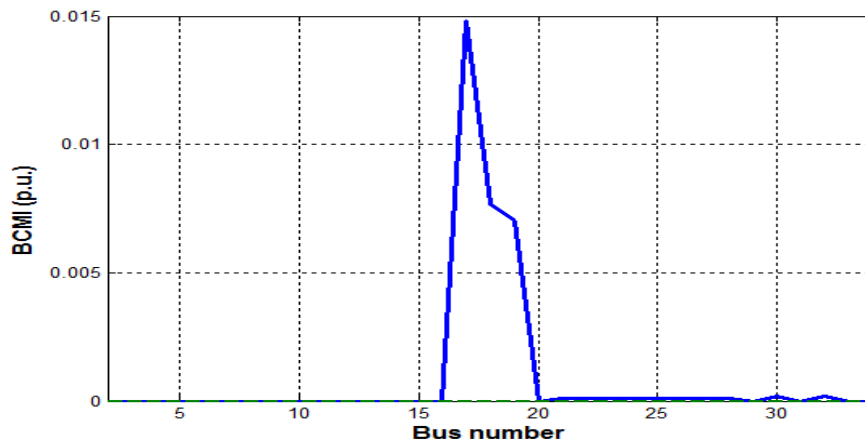




(a) Phase-a



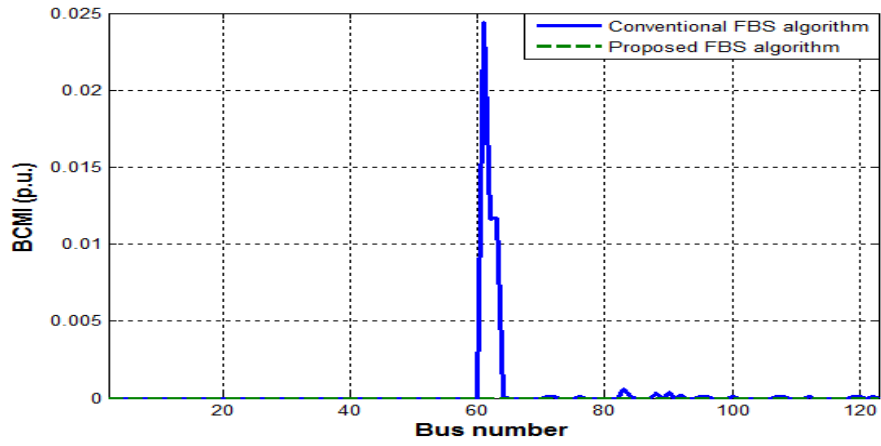
(b) Phase-b



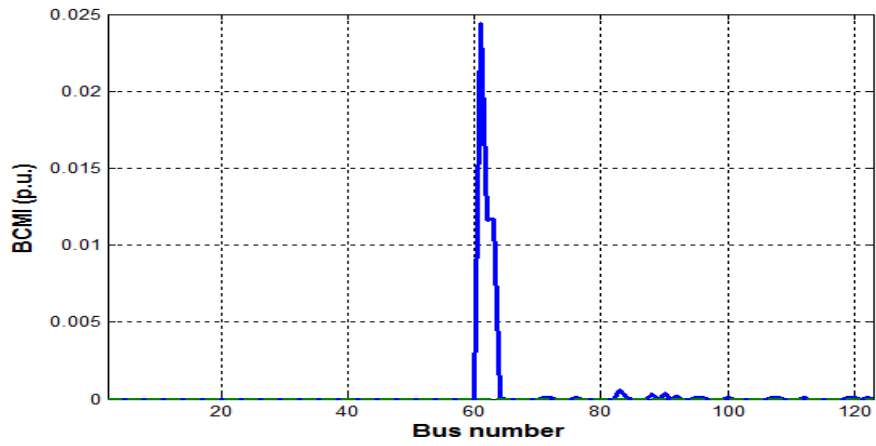
(c) Phase-c

Figure 5.1: Comparison of BCMI for the 34-bus system.

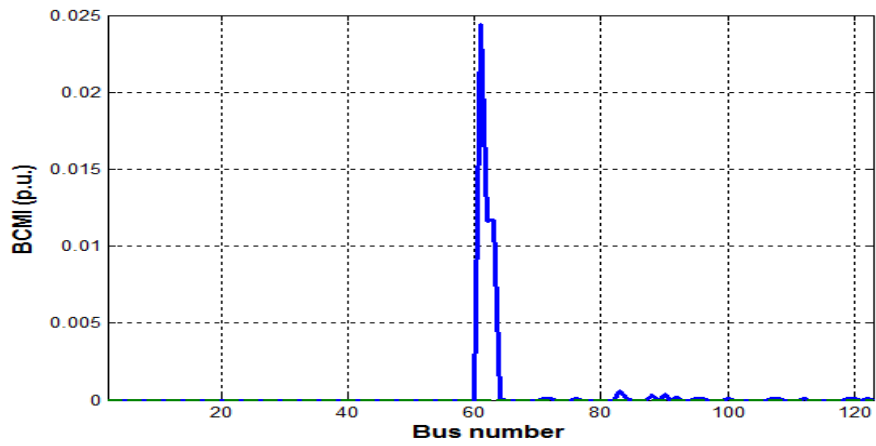
BCMIs are prominent for the conventional algorithm, specially, at buses near the transformers. This, in turn, justifies the ability of the proposed algorithm to produce



(a) Phase-a



(b) Phase-b



(c) Phase-c

Figure 5.2: Comparison of BCMI for the 123-bus system.

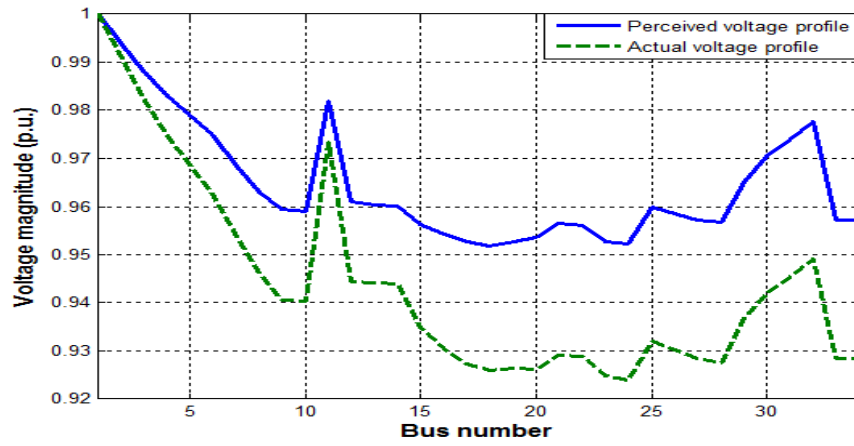
a more accurate load flow solution.

Table 5.1: Load Flow Solutions for Bus Voltage Magnitudes in the 34-bus System

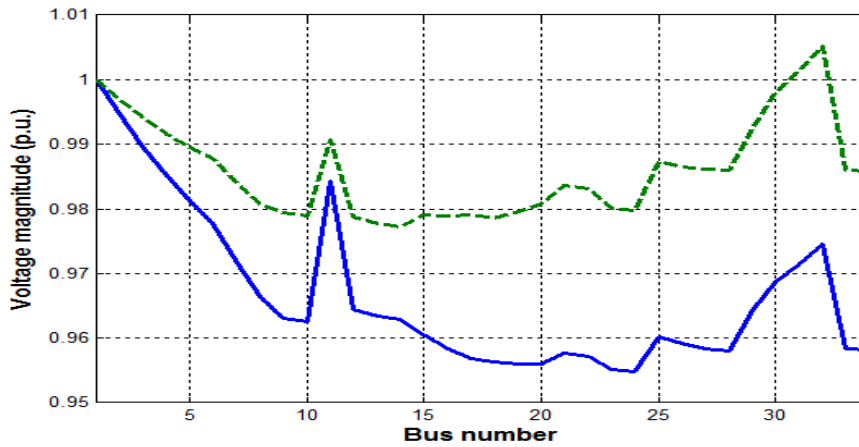
Bus no.	Node ID	Conventional FBS algorithm			Proposed FBS algorithm		
		Phase a (p.u.)	Phase b (p.u.)	Phase c (p.u.)	Phase a (p.u.)	Phase b (p.u.)	Phase c (p.u.)
1	800	1	1	1	1	1	1
2	802	0.9937	0.9947	0.9948	0.9934	0.9959	0.9949
3	806	0.9876	0.9896	0.9899	0.987	0.9922	0.9902
4	808	0.9822	0.985	0.9856	0.9814	0.9886	0.9861
5	812	0.9779	0.9811	0.9817	0.9775	0.9855	0.982
6	814	0.9737	0.9774	0.978	0.9739	0.9828	0.978
7	850	0.9671	0.9714	0.9719	0.9675	0.9778	0.9715
8	816	0.9614	0.9661	0.9664	0.9623	0.9734	0.9657
9	824	0.9578	0.9627	0.963	0.9592	0.9709	0.9618
10	826	0.9575	0.9622	0.9622	0.959	0.9704	0.9609
11	810	0.9809	0.9841	0.9851	0.9799	0.9876	0.986
12	818	0.9594	0.9641	0.9644	0.9605	0.9714	0.9637
13	820	0.9588	0.963	0.963	0.9602	0.9703	0.9618
14	822	0.9584	0.9625	0.9623	0.9601	0.9698	0.9609
15	828	0.9548	0.9601	0.9605	0.9563	0.9692	0.9592
16	832	0.9526	0.9581	0.9588	0.9545	0.9677	0.9574
17	888	0.9513	0.9565	0.9574	0.9541	0.9665	0.9558
18	890	0.9503	0.956	0.957	0.9529	0.966	0.9557
19	830	0.9513	0.9557	0.957	0.9558	0.9657	0.9549
20	854	0.9521	0.9557	0.9574	0.9585	0.9655	0.9548
21	856	0.955	0.9574	0.959	0.9641	0.9669	0.9553
22	852	0.9547	0.9569	0.9583	0.964	0.9664	0.9544
23	858	0.9512	0.9549	0.957	0.957	0.9647	0.955
24	864	0.9507	0.9545	0.9568	0.9562	0.9643	0.955
25	834	0.9584	0.9599	0.9615	0.9699	0.9691	0.9571
26	860	0.957	0.9588	0.9603	0.9682	0.9682	0.956
27	836	0.9558	0.958	0.9594	0.9664	0.9678	0.9555
28	840	0.9552	0.9577	0.9592	0.9655	0.9676	0.9555
29	842	0.9635	0.9639	0.9658	0.9777	0.9726	0.9608
30	844	0.9689	0.9682	0.9703	0.9858	0.9765	0.9647
31	846	0.9725	0.9712	0.9733	0.9911	0.9791	0.9674
32	848	0.9762	0.9742	0.9765	0.9965	0.9818	0.9701
33	862	0.9558	0.9579	0.9594	0.9664	0.9676	0.9555
34	838	0.9557	0.9579	0.9594	0.9664	0.9675	0.9555

Table 5.2: Load Flow Solutions for Bus Voltage Angles in the 34-bus System

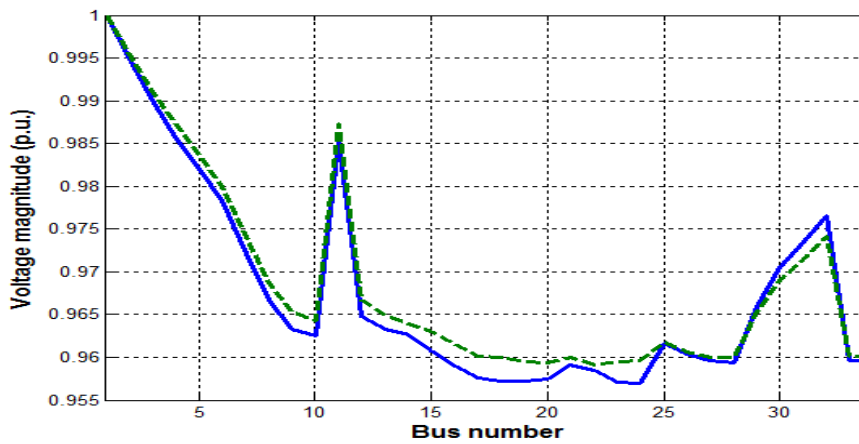
Bus no.	Node ID	Conventional FBS algorithm			Proposed FBS algorithm		
		Phase a (rad)	Phase b (rad)	Phase c (rad)	Phase a (rad)	Phase b (rad)	Phase c (rad)
1	800	0	-2.0944	2.0944	0	-2.0944	2.0944
2	802	-0.0083	-2.102	2.0856	-0.0117	-2.1011	2.0859
3	806	-0.0167	-2.1095	2.0767	-0.0236	-2.108	2.0774
4	808	-0.0252	-2.1172	2.068	-0.0355	-2.1149	2.0688
5	812	-0.0336	-2.1253	2.0593	-0.0475	-2.1215	2.0597
6	814	-0.042	-2.1334	2.0506	-0.0596	-2.128	2.0507
7	850	-0.0524	-2.1437	2.0398	-0.0747	-2.1362	2.039
8	816	-0.0631	-2.1543	2.0287	-0.0901	-2.1446	2.0269
9	824	-0.0741	-2.1653	2.0175	-0.1059	-2.1533	2.0145
10	826	-0.074	-2.1655	2.0176	-0.1059	-2.1533	2.0146
11	810	-0.0253	-2.1167	2.0679	-0.0354	-2.1147	2.0688
12	818	-0.0629	-2.1541	2.0289	-0.0899	-2.1444	2.027
13	820	-0.0627	-2.1545	2.0292	-0.0899	-2.1444	2.0271
14	822	-0.0625	-2.1547	2.0293	-0.0899	-2.1444	2.0271
15	828	-0.0854	-2.1762	2.006	-0.1218	-2.1623	2.0022
16	832	-0.097	-2.1872	1.9946	-0.1379	-2.1713	1.9897
17	888	-0.1086	-2.1987	1.9833	-0.154	-2.1801	1.9768
18	890	-0.1086	-2.1983	1.9831	-0.1538	-2.1801	1.9769
19	830	-0.1203	-2.2104	1.9722	-0.1701	-2.1888	1.9636
20	854	-0.1322	-2.2224	1.961	-0.1863	-2.1976	1.9502
21	856	-0.1441	-2.2351	1.9498	-0.2027	-2.2063	1.9363
22	852	-0.1439	-2.2353	1.95	-0.2027	-2.2063	1.9363
23	858	-0.1325	-2.2221	1.9609	-0.1863	-2.198	1.9504
24	864	-0.1326	-2.222	1.9609	-0.1862	-2.1982	1.9506
25	834	-0.156	-2.2475	1.9385	-0.219	-2.2152	1.9225
26	860	-0.1558	-2.2473	1.9384	-0.2189	-2.2152	1.9228
27	836	-0.1557	-2.247	1.9383	-0.2188	-2.2154	1.9232
28	840	-0.1556	-2.2467	1.9382	-0.2187	-2.2156	1.9234
29	842	-0.1681	-2.26	1.9273	-0.2352	-2.2241	1.9087
30	844	-0.18	-2.2723	1.916	-0.2512	-2.2329	1.895
31	846	-0.1872	-2.2798	1.9093	-0.2607	-2.2382	1.8867
32	848	-0.1942	-2.2872	1.9027	-0.2701	-2.2434	1.8785
33	862	-0.1557	-2.247	1.9383	-0.2187	-2.2154	1.9231
34	838	-0.1557	-2.247	1.9383	-0.2187	-2.2155	1.9231



(a) Phase-a

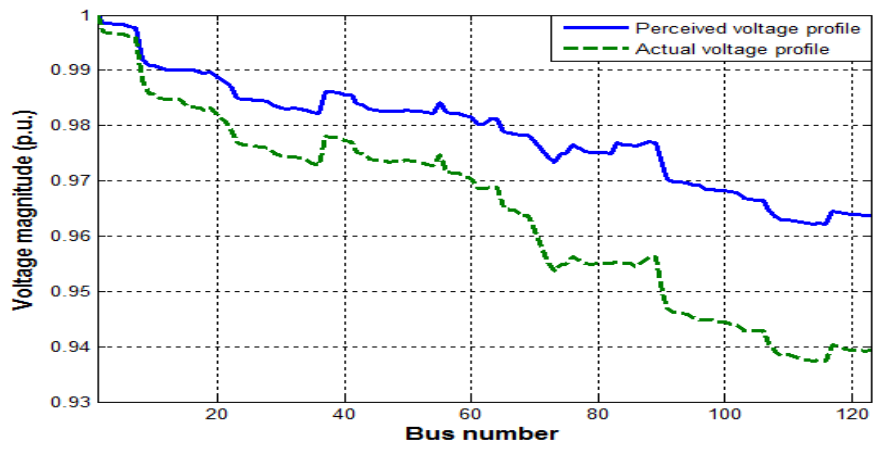


(b) Phase-b

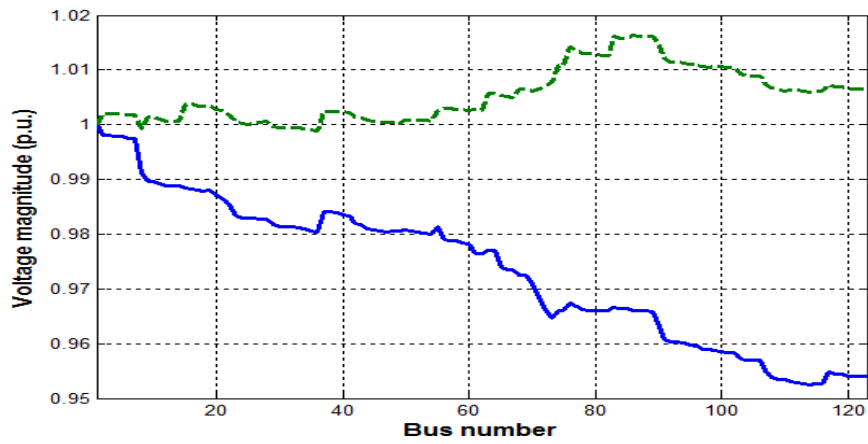


(c) Phase-c

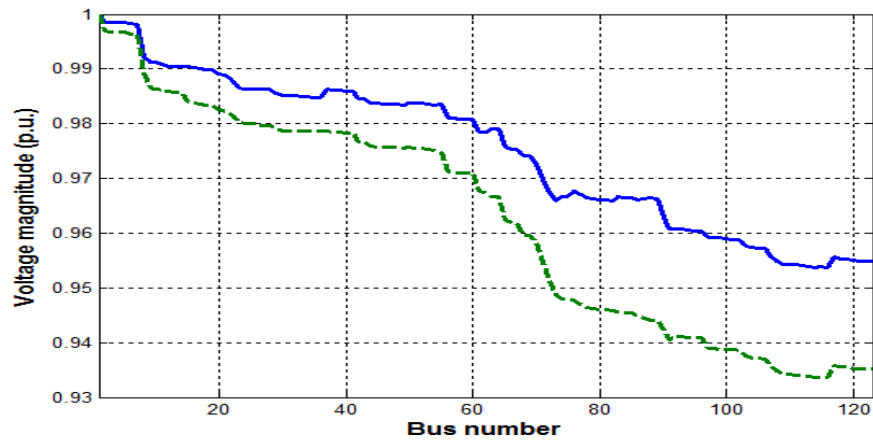
Figure 5.3: Comparison of actual and perceived bus voltage profiles corresponding to the capacitor switching schedule obtained from the conventional FBS algorithm in the 34-bus system.



(a) Phase-a



(b) Phase-b



(c) Phase-c

Figure 5.4: Comparison of actual and perceived bus voltage profiles corresponding to the capacitor switching schedule obtained from the conventional FBS algorithm in the 123-bus system.

In order to verify the impact of the inaccuracy introduced by the conventional algorithm in the load flow calculation, the capacitor switching plan is prepared by carrying out the load flow analysis with the same algorithm. Subsequently, another load flow analysis is carried out by using the proposed algorithm to obtain the exact bus voltage profile corresponding the capacitor switching plan that is already prepared. The comparisons of those two load flow results for the 123-bus system are produced in Fig. 5.4. For the given capacitor switching plan, the bus voltage profile perceived through the conventional FBS calculation and the actual bus voltage profile obtained through the proposed FBS calculation are presented side-by-side. It is to be noted that the result presented in Fig. 5.3 in connection to the proposed FBS algorithm is different from the result produced in Table 5.1. In Table 5.1, the capacitor switching plan is independently prepared by each load flow algorithm. With regard to Fig. 5.3, the proposed load flow algorithm is run by considering an already fixed capacitor switching plan. According to the load flow calculation carried out by the conventional FBS algorithm, all the bus voltage magnitudes were supposed to be within the prescribed limits. In reality, there would be lower voltages at several buses, which is apparent from the actual voltage profile curves in Fig. 5.3 and Fig. 5.4. At some other buses, the actual voltage magnitudes are found to rise above the maximum limit. This is indicative of the fact that the use of the conventional load flow algorithm may cause undervoltage or overvoltage at certain distribution buses because of producing an incorrect capacitor switching plan.

## 5.5 Summary

A novel forward-backward sweep technique is proposed in this chapter to improve the accuracy of the load flow analysis of a distribution network. The methodology proposed is distinct in the sense that it makes an accurate treatment of the zero sequence components of transformer port voltages, especially for the configurations that involve delta or ungrounded star windings. The cascade and hybrid parameter models of a transformer are modified by introducing some offset terms related to zero sequence port voltages. The particular offset terms, however, do not arise for grounded-star connection on both the sides of a transformer. The FBS iterations are modified with due consideration for the above mentioned zero sequence voltage offsets. The correction of the FBS calculation by recognizing the zero sequence voltage offsets in the two-port model of a transformer is the specific novelty of the proposed work. Case studies show the clear difference between the load flow results obtained

from the proposed and existing techniques. In order to verify the accuracy of a load flow solution, the three-phase bus admittance matrix is employed. For the bus voltage profile determined, the imbalance between load currents and current injections (according to line flows) at different buses are calculated. Interestingly, although there can be converged load flow solution from the traditional forward-backward sweep technique, the same is found to violate the KCL according to the admittance matrix model of the network. On the other hand, no inaccuracy is observed in the load flow solution produced by the proposed technique. One potential shortcoming of the inaccurate load flow calculation is shown to be the rise or fall of bus voltages beyond limits because of incorrect capacitor switching.



# Chapter 6

## Active Distribution Network via Single-Slack Gauss- $Z_{bus}$ Iterations and Canonical Network Transformation

### 6.1 Introduction

The load flow calculation in an active distribution network using the backward/forward sweep (BFS) technique, it is necessary to represent a DG bus as an equivalent load bus by iteratively updating the reactive power output of the respective DG. The reactive power output of a DG can be updated by using the current/power compensation technique proposed in [68]- [70]. Alternatively, the shunt capacitance model as was proposed in [41] can be employed. The overall process is a mixed-domain approach in which the reactive power output of a DG is updated by carrying out a sensitivity analysis in the symmetrical component domain [89]. Subsequently, backward/forward sweeps are carried out in the phase domain. Methodologies proposed in [48, 88] perform active distribution load flow (ADLF) calculation purely in the symmetrical component domain. The power flow equations for the positive sequence network are solved by means of N-R iterations, whereas, Gauss- $Z_{bus}$  iterations are performed to update negative and zero sequence bus voltages. Another mixed-domain approach was proposed in [3], which is primarily based upon Gauss- $Z_{bus}$  iterations in the phase domain. During Gauss- $Z_{bus}$  iterations, each DG bus is represented as an independent slack bus. Thus, the Gauss- $Z_{bus}$  iterations of [3] involve multiple slack

buses at a time. The voltage magnitude and angle of such a slack bus are obtained through a local power flow analysis in the symmetrical domain.

The objective of this work is basically to develop an ADLF algorithm with the following features.

1. Improved computational efficiency.
2. Applicability to any feeder network.
3. Applicability to both current-balanced and voltage-balanced operations of DGs.

Out of the available techniques, the BFS methodology cannot deal with voltage-balanced DGs. On the other hand, the multi-slack Gauss- $Z_{bus}$  technique proposed in [3] has the limitation of being computationally expensive because of complex computations involved in finding the equivalent slack bus representation of a DG bus. The N-R technique suffers from the limitations of both BFS and multi-slack Gauss- $Z_{bus}$  techniques. In addition, the existing Gauss- $Z_{bus}$  iteration based techniques (for both passive and active distribution networks) cannot be applied to a general feeder network. There are two major issues to be dealt with while preparing the feeder network model for performing Gauss- $Z_{bus}$  iterations.

1. Treatment of the zero sequence current flow blockages that are present in the original feeder network.
2. Treatment of tap-changing transformers.

In [88], an admittance matrix reduction technique was proposed to resolve the first problem. However, the methodology proposed in [88] is applicable only if each of the islands, except for the one that contains the substation bus, in the zero sequence network comprises of a single bus. In reality, there can be islands of bigger sizes in the zero sequence network. With regard to the second issue, no work is reported so far on the representation of tap-changing transformers in Gauss- $Z_{bus}$  iterations. It is to be noted that, without proper modeling of tap-changing transformers, the bus impedance matrices are to be fully reconstructed every time whenever the tap positions are changed. This may significantly increase the computation time for Gauss- $Z_{bus}$  iterations.

However, as was shown in [3], the Gauss- $Z_{bus}$  iterative technique is promising for building an ADLF algorithm that can take into account both the voltage-balanced and current-balanced operations of a DG. Therefore, the same principle is employed

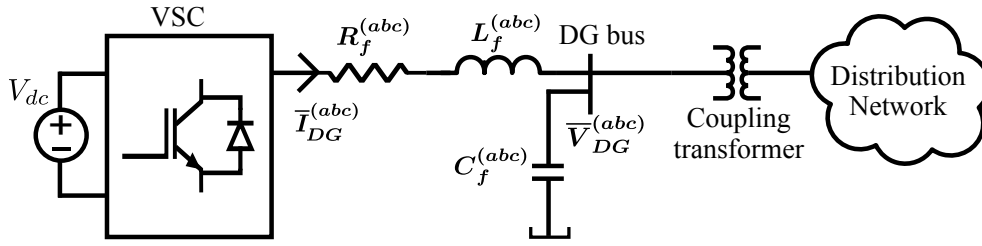


Figure 6.1: Organization of a power electronically interfaced DG unit.

to build the proposed ADLF algorithm. The principal focus of this work is, thus, on attaining the following goals.

1. Prevention of blockages to the zero sequence current flow and elimination of the need for the repeated reconstruction of impedance matrices by means of some suitable modeling of transformers and voltage regulators.
2. Exploring a suitable modification of the Gauss- $Z_{bus}$  iterative formula so as to ensure faster computation and convergence of the ADLF calculation.

Unlike the multi-slack approach taken in [3], the modified Gauss- $Z_{bus}$  iterative formula derived in this work uses only a single slack bus and is independently established for each individual sequence network.

## 6.2 Organization and Operational Characteristics of a DG

The schematic representation of the circuit and connection arrangements of a power-electronically interfaced DG unit is shown in Fig. 6.1 [90]- [91]. Here, the DC side of the DG unit is equivalently represented in the form of a fixed DC voltage source. The acronym “VSC” stands for the voltage source converter. Both the shunt capacitive filter and the DG side winding of the coupling transformer are either delta-connected or star-connected with neutral not grounded. This, in turn, ensures no zero sequence current flow on the DG side of the coupling transformer under any circumstances.

As mentioned earlier, a DG can be operated either in the voltage-balanced or in the current-balanced fashion [92]. The voltage-balanced operation of the DG refers to the case when  $\bar{V}_{DG}^{(abc)}$  does not have any negative sequence component. In the same way, the current-balanced operation indicates the absence of negative sequence component in  $\bar{I}_{DG}^{(abc)}$ . Implementations of voltage balancing and current balancing

controls are discussed in [91]. For both the cases, the negative sequence or zero sequence power supplied by the VSC to the distribution system is zero.

The DG representations in positive, negative and zero sequence networks are shown in Fig. 6.2. As mentioned previously, the zero sequence current on the DG side is always zero. Therefore, the DG always behaves as a zero current source in the zero sequence network. For the voltage-balanced operation, the negative sequence component of the DG terminal voltage is zero, which can be represented by a short circuit to the ground. The current source shown in the negative sequence network under the voltage balancing control does not have any physical significance. It is kept only to maintain uniformity among all the figures. In the case of the current-balanced operation, the only path through which the negative sequence current can flow is the shunt capacitor. In the positive sequence network, the DG should be represented as a single-phase AC generator with either of the following output specifications that pertain to positive sequence only.

1. Fixed active power output and fixed terminal voltage magnitude (i.e.,  $P_{DG}^{sp(1)}$  and  $V_{DG}^{sp(1)}$ ).
2. Both fixed active and reactive power outputs (i.e.,  $P_{DG}^{sp(1)}$  and  $Q_{DG}^{sp(1)}$ ).

The actual power output (in MW or Mvar ) of the DG is three times of the positive sequence power output. Ideally, the positive sequence component of the DG terminal voltage should be maintained at a constant value. However, because of the limited capacity, the reactive power output of the DG may, sometimes, have to be kept fixed. It is to be noted that, for the purpose of load flow analysis, the reactive power output of the DG is to be defined without including the shunt capacitor.

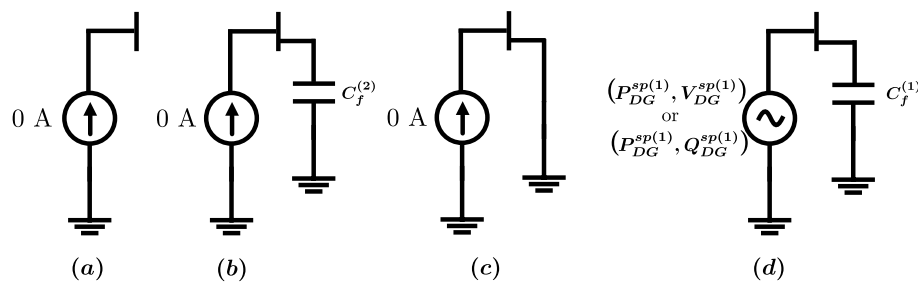


Figure 6.2: Symmetrical domain representation of the DG unit. a) Zero sequence, b) negative sequence under current balance, c) negative sequence under voltage balance, d) positive sequence.

## 6.3 The General Template of the ADLF Calculation

The direct representation of the DG by means of a  $PV$  bus in the positive sequence network requires computationally tedious N-R iterations to solve load flow equations. Therefore, the indirect modelling of DG buses is usually preferred. The general flowchart for the load flow calculation in an active distribution network, with indirect representation of DG buses, is shown in Fig. 6.3. Three levels of iteration are involved. At the outermost level of iteration, the voltage regulators and shunt compensators are suitably adjusted so as to maintain load bus voltage magnitudes within the specified limits. The purpose of the middle loop is to convert  $PV$  buses into non- $PV$  buses through an equivalent representation. Finally, the innermost loop of iteration takes a distribution network with no  $PV$  buses and with fixed voltage regulator/shunt compensator settings. Each iteration in the innermost loop consists of two stages. In the first stage, the load currents are determined based upon the latest updated bus voltages, whereas, in the second stage, bus voltages are determined based upon the latest updated load currents. The convergence of a loop is indicated when the bus voltages obtained after completing a particular iteration of the respective loop do not deviate much from the corresponding result obtained from the previous iteration of the same loop. The flowchart of the N-R method also retains the same looping structure as that in Fig. 6.3. The Newton-Raphson iterations are carried out in the innermost loop only, whereas, the middle loop is required to decompose load power into sequence components. The purpose of the outermost loop is, as usual, to adjust capacitor and voltage regulator settings.

There are two ways to convert a DG bus into a non- $PV$  bus in the middle iteration loop. In the first approach, a  $PV$  bus is converted to a  $PQ$  bus by employing the methodology of current/reactive power compensation. In the other approach, the  $PV$  bus is transformed into a  $V\delta$  (or slack) bus by means of voltage compensation. For the innermost loop also, two different methods can be employed. Those are the BFS and Gauss- $Z_{bus}$  techniques. Till date, only two combinations have been tried between the innermost and middle loops. The ADLF calculation in [39, 68–70] has been implemented by choosing the current/reactive power compensation technique for the middle loop and the BFS technique for the innermost loop [39, 68–70]. In another implementation that can be found in [3], Gauss- $Z_{bus}$  iterations have been carried out in the innermost loop after forming slack buses in the middle loop.

In the present work, the current/reactive power compensation technique is adopted

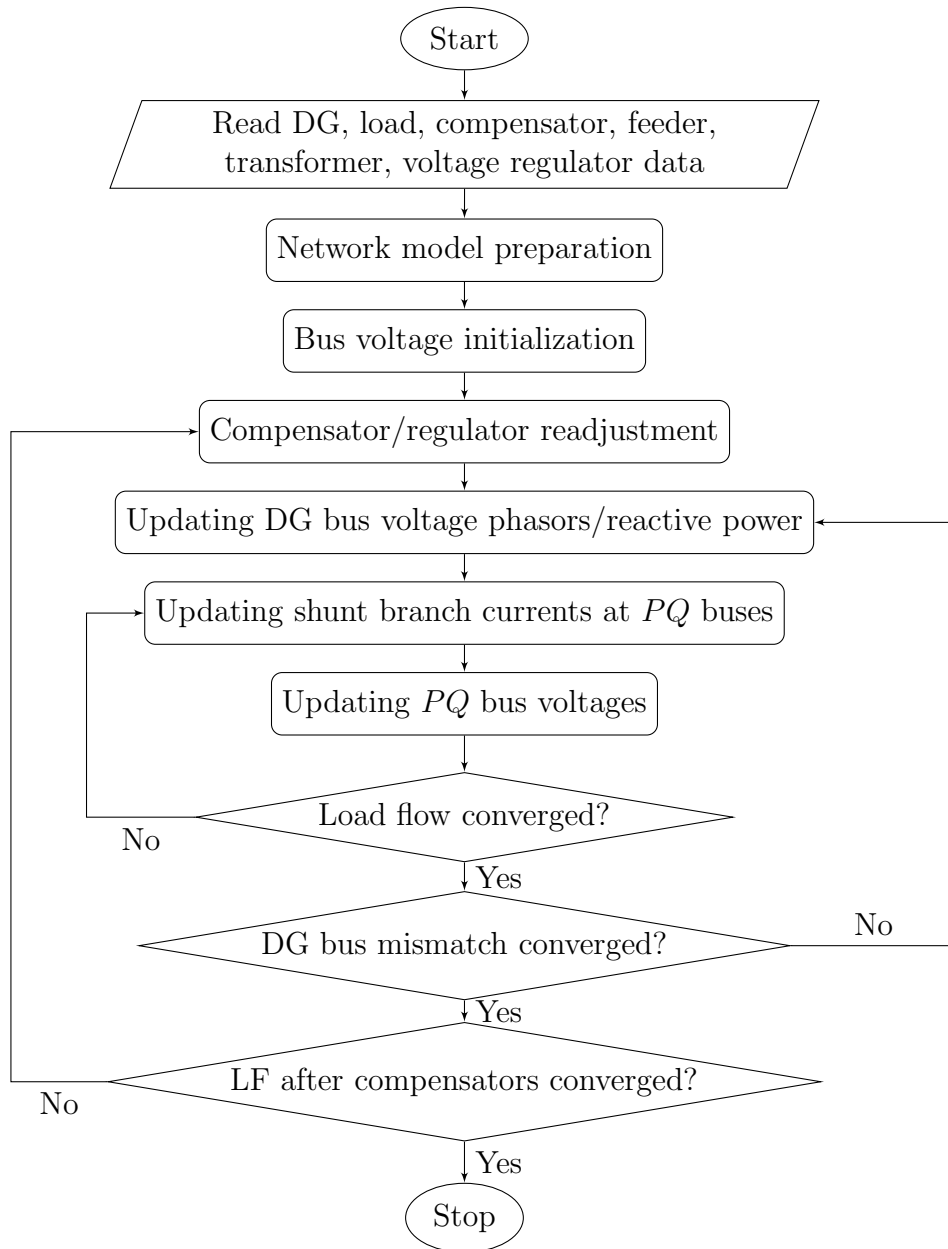


Figure 6.3: Flowchart for the ADLF calculation with indirect representation of DG buses.

to implement the middle loop of iteration. Before entering into the innermost loop, a DG bus can be converted into a  $PQ$  bus by updating its reactive power output through the following equation.

$$Q_{DG}^{(1),(k+1)} = \max \left[ Q_{G,min}, \min \left\{ Q_{G,max}, Q_{DG}^{(1),(k)} + S \left( V_{DG}^{sp(1)} - V_{DG}^{(1),(k)} \right) \right\} \right]. \quad (6.1)$$

Here,  $\mathbf{Q}_{DG}^{(1),(k)}$  indicates the vector of DG reactive power outputs (in the positive sequence network) calculated at the beginning of the  $k$ th iteration in the middle loop of the flowchart shown in Fig. 6.3. The DG bus positive sequence voltage magnitudes obtained at the end of the  $k$ th iteration in the middle loop is indicated by vector  $\mathbf{V}_{DG}^{(1),(k)}$ . The maximum and minimum reactive power capabilities of DGs are indicated by  $\mathbf{Q}_{G,max}$  and  $\mathbf{Q}_{G,min}$ , respectively. The derivation of the sensitivity matrix  $\mathbf{S}$  (which depends only upon network parameters) is provided in [52] and [39]. The particular matrix is essentially given by the reactive part of the positive sequence Thevenin's equivalent impedance matrix as seen from the DG buses. Instead of sensitivity factors, the quadratic equation model as was proposed in [68] can also be used to update the reactive power outputs of generators. Modelling of a DG bus as an equivalent  $PQ$  bus is, however, based upon the assumption that there are only three-phase balanced feeders in the network. Therefore, a single-phase or two-phase feeder is to be equivalently represented as a three-phase feeder with no loads and no shunt charging capacitances for the phases that are originally not present. The particular equivalent representation is possible since the single-phase and two-phase feeders are usually radial in nature. Similarly, an unbalanced feeder can equivalently be represented as a balanced feeder by following the procedure prescribed in [48] and [58].

By employing the current/reactive power compensation technique to model DG buses, the ADLF problem is, in essence, solved through a series of passive distribution load flow (PDLF) calculations. Each of the respective PDLF calculations takes place in the innermost loop. It is to be noted that the DG terminal is represented as a  $PQ$  bus only within the innermost loop. After each round of PDLF calculation through the innermost loop, the reactive power output of a DG is updated in the middle loop based upon the difference between the specified value and the latest solution of its terminal voltage magnitude. The middle loop keeps on adjusting the reactive power output of a DG unless its terminal voltage settles at the specified value provided the DG has adequate reactive power capacity. Therefore, when the program execution comes out of the middle loop, it is ensured that the DG bus has remained voltage-controlled unless its reactive power capacity is exhausted. However, the PDLF calculation that needs to be carried out within the innermost loop is somewhat different from the normal PDLF calculation because of the involvement of DG impedances. Therefore, this chapter specifically contributes towards an efficient implementation of the particular loop through the deployment of Gauss- $Z_{bus}$  iterations.

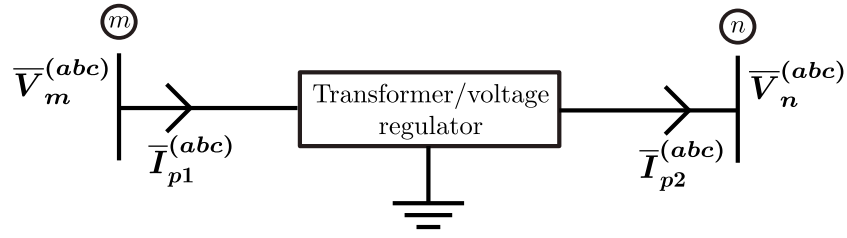


Figure 6.4: General two port representation of a transformer or voltage regulator.

## 6.4 Transformer/Voltage Regulator Modeling

The transformer/voltage regulator modeling is carried out by extending the methodology of [48] and [58] that was originally proposed only for the equivalent balanced representation of a feeder line. A transformer or voltage regulator is essentially a two-port element with three-phase ports. The general two-port representation of a transformer or voltage regulator within a distribution network is shown in Fig. 6.4. Here, the element is placed between Bus  $m$  and Bus  $n$ . The element ports are named as Port 1 and Port 2 (symbolized with  $p1$  and  $p2$  in subscripts), respectively. The admittance parameter model of the particular element can be written as,

$$\bar{I}_{p1}^{(abc)} = \mathbf{Y}_{11}^{(abc)} \bar{V}_m^{(abc)} + \mathbf{Y}_{12}^{(abc)} \bar{V}_n^{(abc)} \quad (6.2)$$

$$\bar{I}_{p2}^{(abc)} = -\mathbf{Y}_{21}^{(abc)} \bar{V}_m^{(abc)} - \mathbf{Y}_{22}^{(abc)} \bar{V}_n^{(abc)}. \quad (6.3)$$

The determination of the admittance parameter model of a transformer or voltage regulator is a straightforward task, which is extensively addressed in literature [61,84, 85]. A brief derivation of these admittance parameters is also provided in Appendix.

Each admittance parameter of the above two-port model can be decomposed into two parts as follows.

$$\mathbf{Y}_{11}^{(abc)} = y_{se} \mathbf{U} + \Delta \mathbf{Y}_{11}^{(abc)} \quad (6.4)$$

$$\mathbf{Y}_{12}^{(abc)} = -y_{se} \mathbf{U} + \Delta \mathbf{Y}_{12}^{(abc)} \quad (6.5)$$

$$\mathbf{Y}_{21}^{(abc)} = -y_{se} \mathbf{U} + \Delta \mathbf{Y}_{21}^{(abc)} \quad (6.6)$$

$$\mathbf{Y}_{22}^{(abc)} = y_{se} \mathbf{U} + \Delta \mathbf{Y}_{22}^{(abc)} \quad (6.7)$$

where,  $\mathbf{U}$  is an identity matrix of appropriate dimension [for the present case, it is  $(3 \times 3)$ ]. After decomposing the admittance parameters as above, the equivalent circuit representation of a two-port element can be found as is shown in Fig. 6.5. Here, the actual transformer or voltage regulator is converted into the combination of a balanced



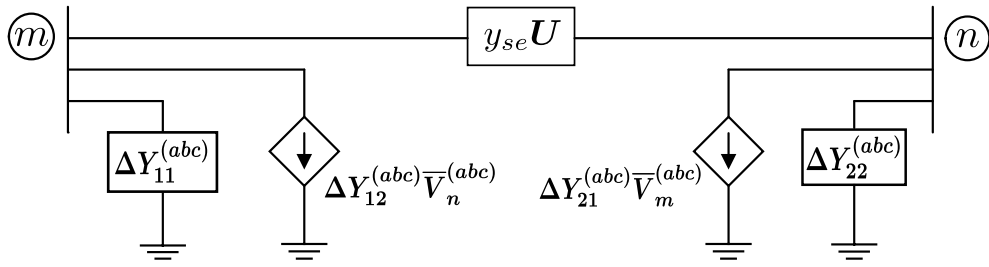


Figure 6.5: Equivalent circuit representation of a two-port element.

feeder and a few shunt elements. The shunt elements of this equivalent representation are treated as external loads in the load flow analysis. It is to be noted that a feeder line can be modelled in the similar manner (but with identical shunt elements on both the sides) since it is also a two port element. Therefore, the system model that is ultimately considered comprises of only a balanced feeder network, but with some additional loads. Since the original unbalanced feeder network is now transformed into a balanced feeder network, it is possible to separate out its positive sequence, negative sequence and zero sequence parts. Moreover, transformers are eliminated and all the nodes become electrically connected in the phase-domain. In addition, by setting the off-diagonal elements of the admittance matrix of an equivalent feeder line to zero, it is ensured that there should not be any blockage to the zero sequence current. That is, the zero sequence impedance of the equivalent feeder line is maintained at a finite value so that the zero sequence network may also remain electrically connected.

The value of  $y_{se}$  can simply be chosen as the average of the diagonal elements of  $\mathbf{Y}_{11}^{(abc)}$ ,  $\mathbf{Y}_{12}^{(abc)}$ ,  $\mathbf{Y}_{21}^{(abc)}$  and  $\mathbf{Y}_{22}^{(abc)}$ . For a voltage regulator,  $y_{se}$  should be evaluated at the nominal transformation ratio and would have to be, subsequently, treated as a fixed parameter. As a result, there is no need to reconstruct bus impedance matrices following a tap change. The effect of voltage regulator tap changes can simply be passed to the shunt branches to be treated as load variations in the load flow calculation.

## 6.5 Proposed Load Flow Algorithm

The load flow algorithm proposed has two components as the novel contribution. First of all, a methodology is introduced to suitably model transformers and voltage regulators in the Gauss- $Z_{bus}$  iterative calculation. In specific, it is attempted to eliminate the complexity caused by tap changing actions and the presence of blockages to zero sequence current flows. Second, a robust and computationally efficient formu-

lation is derived to carry out the ADLF calculation based upon the concept of the Gauss- $Z_{bus}$  iteration. The classical single-slack Gauss- $Z_{bus}$  iterative technique uses a bus impedance matrix that is to formed by placing the voltage reference at the substation bus [80]. For the particular approach, all the shunt elements in the network are to be treated as external loads during the load flow analysis. It is, however, difficult to fit DGs into this classical framework. For example, the short-circuited path in the negative sequence network of a voltage-balanced DG (as is shown in Fig. 6.2) cannot be represented as an external load on the feeder network. Because of the same reason only, it is not possible to perform BFS or N-R iterations with voltage-balanced DGs. The representation of DG impedances as external loads may further lead to the convergence problem as was reported in [37]. Therefore, the Gauss- $Z_{bus}$  iterative formula is redefined in this work by including DG impedances within the network model itself. Only the current/power sources shown in Fig. 6.2 are used to obtain current injections at DG buses.

For the feeder network model employed, the positive, negative and zero sequence bus admittance matrices can be independently formed by separating out all the sequence networks. Initially, the symmetrical-domain bus admittance matrices need to be found by considering only the series elements (i.e., the equivalent feeder lines from Fig. 6.5). The non-zero sequence impedances of DGs are subsequently to be included within the respective sequence admittance matrices. At this stage, any zero shunt impedance from a DG is modelled as a zero voltage source. The respective bus admittance matrix for the  $s$ -th sequence [i.e.,  $s \in \{0, 1, 2\}$ ] is indicated by  $\mathbf{Y}_{bus}^{(s)}$ . The corresponding bus voltage and current injection vectors are indicated by  $\overline{\mathbf{V}}_{bus}^{(s)}$  and  $\overline{\mathbf{I}}_{bus}^{(s)}$ , respectively.

In order to develop the formula for proposed Gauss- $Z_{bus}$  iterations, the network equation needs to be, first, written down as follows.

$$\overline{\mathbf{I}}_{bus}^{(s)} = \mathbf{Y}_{bus}^{(s)} \overline{\mathbf{V}}_{bus}^{(s)}. \quad (6.8)$$

By suitable re-ordering of nodes (that can be separately done for each sequence), vector/matrix  $\overline{\mathbf{V}}_{bus}^{(s)}$ ,  $\overline{\mathbf{I}}_{bus}^{(s)}$  and  $\mathbf{Y}_{bus}^{(s)}$  can be partitioned as follows.

$$\overline{\mathbf{V}}_{bus}^{(s)} = \left[ \overline{\mathbf{V}}_{bus1}^{(s)T} \quad \overline{\mathbf{V}}_{bus2}^{(s)T} \right]^T \quad (6.9)$$

$$\overline{\mathbf{I}}_{bus}^{(s)} = \left[ \overline{\mathbf{I}}_{bus1}^{(s)T} \quad \overline{\mathbf{I}}_{bus2}^{(s)T} \right]^T \quad (6.10)$$

$$\mathbf{Y}_{bus}^{(s)} = \begin{bmatrix} \mathbf{Y}_{bus11}^{(s)} & \mathbf{Y}_{bus12}^{(s)} \\ \mathbf{Y}_{bus21}^{(s)} & \mathbf{Y}_{bus22}^{(s)} \end{bmatrix}. \quad (6.11)$$

Here, vector  $\overline{\mathbf{V}}_{bus1}^{(s)}$  contains bus voltages that are known for the respective sequence. The particular vector can have different dimensions for different sequences. Based upon the vector/matrix partitions made above, the network equation can finally be written as follows.

$$\overline{\mathbf{V}}_{bus2}^{(s)} = \mathbf{H}_{bus21}^{(s)} \overline{\mathbf{V}}_{bus1}^{(s)} + \mathbf{H}_{bus22}^{(s)} \overline{\mathbf{I}}_{bus2}^{(s)} \quad (6.12)$$

where,

$$\mathbf{H}_{bus21}^{(s)} = -\left\{ \mathbf{Y}_{bus22}^{(s)} \right\}^{-1} \mathbf{Y}_{bus21}^{(s)} \quad (6.13)$$

$$\mathbf{H}_{bus22}^{(s)} = \left\{ \mathbf{Y}_{bus22}^{(s)} \right\}^{-1} \quad (6.14)$$

Equation (6.12) can also be seen as the generalisation of the multi-slack Gauss- $Z_{bus}$  iterative formula presented in [3]. Here, the generalisation is made through proper consideration of DG impedances as well as by means of completely independent treatment of different sequences. In the proposed application, however, only the substation bus voltage vector is assumed to be known in the innermost loop of ADLF calculation. This is in line of the typical single-slack version of the Gauss- $Z_{bus}$  calculation. Thus, vectors  $\overline{\mathbf{V}}_{bus1}^{(0)}$ ,  $\overline{\mathbf{V}}_{bus1}^{(1)}$  and  $\overline{\mathbf{V}}_{bus1}^{(2)}$  contain only the substation bus voltage components if all the DGs are operated in the current-balanced mode. In the presence of voltage-balanced DGs, vector  $\overline{\mathbf{V}}_{bus1}^{(2)}$  should contain additional zeros to indicate the corresponding negative sequence short-circuits. Under any circumstances, no non-zero term exists in  $\overline{\mathbf{V}}_{bus1}^{(0)}$  or  $\overline{\mathbf{V}}_{bus1}^{(2)}$ . As a result, the first term on the right hand side of (6.12) can be directly removed for negative and zero sequences. The direct use of Equation (6.12) may not be suitable for the large system application since the particular equation involves a large number of computations. Therefore, a methodology is further proposed to convert the above equation into a computationally efficient format. The proposed conversion is achieved by means of the Doolittle's LU decomposition of the  $\mathbf{H}_{bus22}^{(s)}$  matrix. The lower and upper triangular components of  $\mathbf{H}_{bus22}^{(s)}$  are indicated by  $\mathbf{H}_{blo22}^{(s)}$  and  $\mathbf{H}_{bup22}^{(s)}$ , respectively. Based upon the LU decomposition of  $\mathbf{H}_{bus22}^{(s)}$ , Equation (6.12) can be rewritten as follows.

$$\overline{\mathbf{V}}_{bus2}^{(s)} = \widetilde{\mathbf{H}}_{bus21}^{(s)} \overline{\mathbf{V}}_{bus1}^{(s)} + \mathbf{H}_{bup22}^{(s)} \overline{\mathbf{I}}_{bus2}^{(s)} + \widetilde{\mathbf{H}}_{blo22}^{(s)} \overline{\mathbf{V}}_{bus2}^{(s)} \quad (6.15)$$

where,

$$\widetilde{\mathbf{H}}_{bus21}^{(s)} = \left\{ \mathbf{H}_{blo22}^{(s)} \right\}^{-1} \mathbf{H}_{bus21}^{(s)} \quad (6.16)$$

$$\widetilde{\mathbf{H}}_{blo22}^{(s)} = \mathbf{U} - \left\{ \mathbf{H}_{blo22}^{(s)} \right\}^{-1}. \quad (6.17)$$

As before, matrix  $\mathbf{U}$  in (6.17) indicates an identity matrix of the appropriate dimension. Since  $\mathbf{H}_{blo22}^{(s)}$  is a unit lower triangular matrix, its inverse will also be a unit lower triangular matrix. As a result,  $\widetilde{\mathbf{H}}_{blo22}^{(s)}$  should be a lower triangular matrix with the zero diagonal. Thus, Equation (6.15) effectively expresses a bus voltage variable in terms of its preceding bus voltage variables (as per the bus ordering performed) and the non-preceding bus current variables. The advantage of such representation lies in the following facts.

1. Matrix  $\widetilde{\mathbf{H}}_{blo22}^{(s)}$  is a sparse matrix even in the lower triangular portion itself.
2. Most of the non-zero elements of a row of matrix  $\mathbf{H}_{bup22}^{(s)}$  have the same value.

It can, in fact, be shown that Equation (6.15) is identical to the forward sweep equations of the BFS technique for a radial and passive distribution network. In that case, provided the bus ordering scheme as was proposed in [52] is followed (except for voltage-balanced DG buses), there exists only one non-zero element (whose value is also one) in any row of  $\widetilde{\mathbf{H}}_{blo22}^{(s)}$ . Moreover, all the non-zero elements of a row of  $\mathbf{H}_{bup22}^{(s)}$  remain equal to a specific line impedance. Although the same structures cannot be perfectly achieved for an active and/or weakly meshed distribution network, there may not be significant deviation. The above features of (6.15) enable a computationally efficient implementation of the particular equation.

The iterative representation of (6.15) in the scalar form is shown below.

$$\overline{V}_{bus2,i}^{(s),(l)} = \sum_{j=1}^{N_1^{(s)}} \widetilde{H}_{bus21,i,j}^{(s)} \overline{V}_{bus1,j}^{(s)} + \sum_{j=i}^{N_2^{(s)}} H_{bup22,i,j}^{(s)} \overline{I}_{bus2,j}^{(s),(l)} + \sum_{j=1}^{i-1} \widetilde{H}_{blo22,i,j}^{(s)} \overline{V}_{bus2,j}^{(s),(l)}. \quad (6.18)$$

Here,  $l$  indicates the iteration index for the innermost loop. Indices  $i$  and  $j$  are used to indicate elements of current and voltage vectors. Symbols  $N_1^{(s)}$  and  $N_2^{(s)}$  indicate the number of elements in  $\overline{\mathbf{V}}_{bus1}^{(s)}$  and  $\overline{\mathbf{V}}_{bus2}^{(s)}$  (or  $\overline{\mathbf{I}}_{bus2}^{(s)}$ ), respectively. For each iteration of the innermost loop, the bus currents are to be initially updated. The bus current injection vector is given by load, compensator and other shunt branch currents. The DG currents are directly calculated in the symmetrical component domain

based upon the sequence components of bus voltages. For other shunt branches, currents are first calculated in the phase domain and are, subsequently, transformed to the symmetrical domain. After updating bus currents, the bus voltages need to be sequentially updated by using Equation (6.18).

## 6.6 Case study

Three different case studies are performed. The objective of the first case study is to verify the accuracy of the results obtained from the proposed load flow algorithm. The second case study is performed to compare the computational performance of the proposed methodology with that of the other methodologies. The scalability of the proposed ADLF algorithm is verified through the third case study. All the studies are performed with the help of a modified 123-bus distribution system. The original data of the particular systems can be found in [87]. The system contains three-phase, two-phase and single-phase feeders. Apart from the substation transformer, there is one more transformer in the 123-bus system. The particular transformer is connected in the  $\Delta$ - $Y_n$  configuration with  $\Delta$  on the upstream side. There are also four voltage regulators in the test system. All the voltage regulators are assumed to be solidly grounded star-connected autotransformers. The tap adjustment step size of a voltage regulator is taken to be 2%. The maximum permissible tap adjustment in either (i.e., positive or negative) direction is taken to be 10%. The capacitor bank placed at each single-phase bus is assumed to be composed of 10 equally sized capacitors. The desired lower and upper limits of the bus voltage magnitude are set to 0.95 p.u. and 1.05 p.u., respectively. The capacitor switching or the voltage regulator tap adjustment action is called for if the voltage magnitude at any phase of a bus crosses a limit. Bus 1 is taken as the substation bus.

The original 123-bus system is a radial and passive distribution network. The particular system is converted to a weakly meshed and active distribution network by adding links and DGs as are shown in Appendix Fig. B.1. The respective link and DG data are provided in Table 6.1 and Table 6.2, respectively. The shunt admittance of each link is assumed to be zero. For the sake of simplicity, all the DGs are assumed to be having same parameters. The load (both active power and reactive power) at each phase of any bus is assumed to be composed of 80% constant power load, 10% constant impedance load and 10% constant current load. All the load flow programs are written in MATLAB and are executed in a workstation with Intel(R) Xeon(R) 2.26 GHz processor and 12 GB RAM. The convergence threshold value is taken as

$10^{-6}$  p.u. for all the loops.

Table 6.1: Link data for the modified 123-bus system

Id.	From bus	To bus	Phase self impedance (p.u.)			Phase-phase mutual impedance (p.u.)		
			Zaa	Zbb	Zcc	Zab	Zbc	Zca
Ln1	22	32	0.0024 + 0.0070i	0.0091 + 0.0092i	0.0091 + 0.0093i	0.0011 + 0.0034i	0.0014 + 0.0031i	0.0011 + 0.0029i
Ln2	44	54	0.0082 + 0.0129i	0.0082 + 0.0131i	0.0081 + 0.0133i	0.0017 + 0.0046i	0.0017 + 0.0042i	0.0017 + 0.0055i
Ln3	80	105	0.0103 + 0.0162i	0.0102 + 0.0164i	0.0102 + 0.0166i	0.0022 + 0.0058i	0.0021 + 0.0053i	0.0021 + 0.0069i
Ln4	110	119	0.0066 + 0.0195i	0.0065 + 0.0201i	0.0065 + 0.0198i	0.0030 + 0.0096i	0.0029 + 0.0074i	0.0030 + 0.0081i

Table 6.2: DG data for the modified 123-bus system

Parameter	Value (p.u.)
Active power output	0.05
Terminal voltage magnitude (positive sequence)	1
Coupling transformer resistance	0.0127
Coupling transformer leakage inductance	0.0272
Lower reactive power limit	-0.05
Upper reactive power limit	0.05
Filter capacitance	0.0766

### 6.6.1 Case Study 1 (Verification of the Solution Accuracy):

The solution accuracy of the proposed load flow algorithm is verified through the evaluation of bus power mismatches. The bus power mismatch [93, 94] refers to the difference (in absolute value) between the specified power injection and the calculated power injection at a bus. The specified value of the power injection is basically an input data. On the other hand, the calculated value of the power injection is obtained from the nodal power balance equation (that can be derived by using the bus admittance matrix) at the load flow solution. Results are produced for the case in which DGs are present at all the locations shown in Appendix Fig B.1. The active and reactive power mismatches at the main feeder network buses (except for the substation bus) are produced in Fig. 6.6- 6.9. Fig. 6.6 and Fig. 6.7 are related to the current-balanced DG operation. Similar results for the voltage-balanced operation of DGs are shown in Fig. 6.8 and Fig. 6.9. Calculation of power mismatch is irrelevant for the substation bus. This is because the bus power mismatch can be defined only for those buses that are given with some power injection specifications. So far as the substation bus is concerned, it is basically taken as the slack bus in the load flow analysis. Thus, there cannot be any active power or reactive power specification for the substation bus.

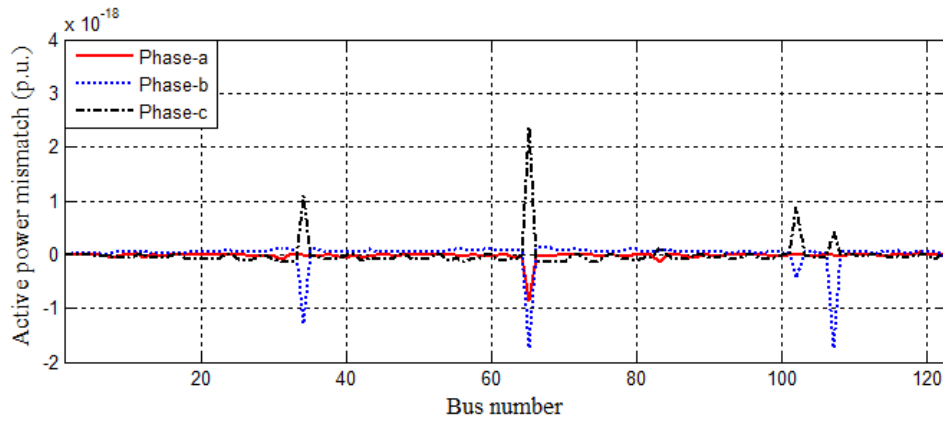


Figure 6.6: Nodal active power mismatches in the main feeder network under the current-balanced operation of DGs.

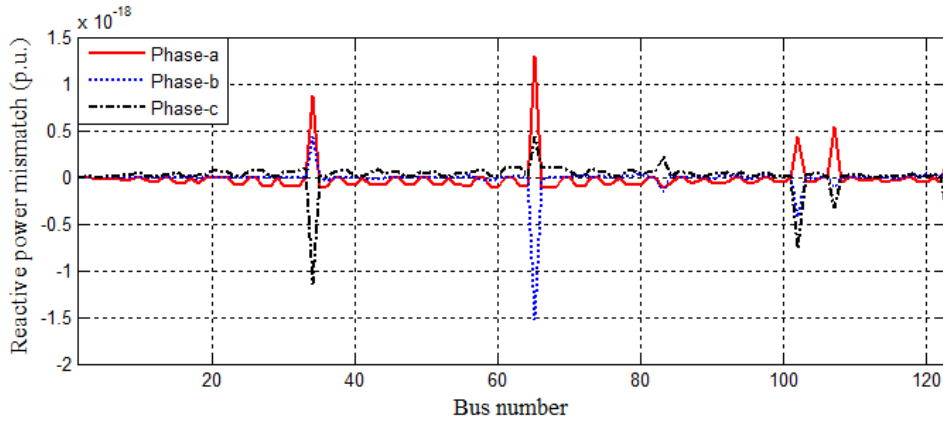


Figure 6.7: Nodal reactive power mismatches in the main feeder network under the current-balanced operation of DGs.

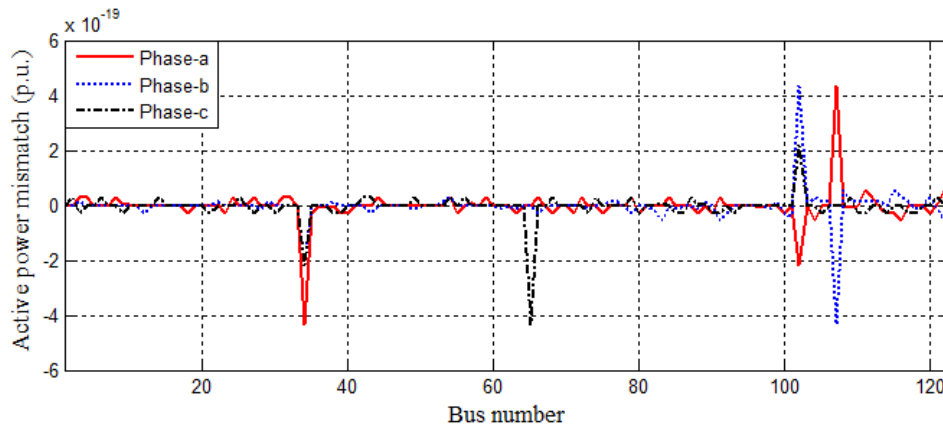


Figure 6.8: Nodal active power mismatches in the main feeder network under the voltage-balanced operation of DGs.

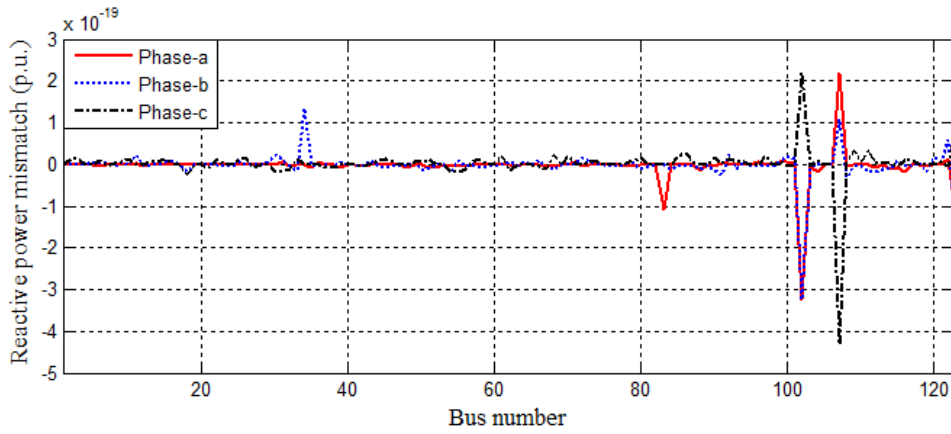


Figure 6.9: Nodal reactive power mismatches in the main feeder network under the voltage-balanced operation of DGs.

Apart from the main feeder network buses, the DG terminals are also treated as separate buses in the load flow calculation. Therefore, it is also necessary to verify the accuracy of calculating those bus quantities. The specified quantities for a DG bus are mainly the positive sequence voltage magnitude and the positive sequence active power injection. However, it is also justified to calculate the reactive power mismatch (in the positive sequence) at a DG bus since the DG bus is modelled as a  $PQ$  bus in the innermost loop of iteration. Here, the reactive power mismatch is to be calculated with reference to the most recently updated reactive power injection specification from the middle loop. Results for the load flow calculation accuracy at DG buses is produced in Table 6.3. Similarly to the main feeder network buses, no perceptible power mismatch is observed at DG buses. The voltage mismatch levels are also insignificant for DG2, DG3 and DG4 that are operated well within the respective reactive power limits. For DG1 and DG2, however, the reactive power capabilities are found to be insufficient to maintain their terminal voltage magnitudes at the specified value. For both the DGs, the upper reactive power limit is hit. Therefore, some voltage mismatches are observed at those DG buses. This is a common phenomenon that happens for any ADLF algorithm.

### 6.6.2 Case Study 2 (Comparison of the Computational Performance):

The relative computational efficiency of the proposed load flow algorithm is verified by considering different numbers of DGs at a time. For this particular study, no computationally efficient implementation of the proposed ADLF algorithm is sought. This



Table 6.3: Power/voltage mismatches at DG buses

Mode	DG id.	Active power mismatch(p.u)	Reactive power mismatch (p.u)	Voltage mismatch (p.u)
Current Balanced	DG1	4.952e-13	2.889e-13	1.0815e-3
	DG2	1.065e-13	1.042e-13	0.4912e-3
	DG3	0.042e-13	0.061e-13	0.0242e-3
	DG4	0.242e-13	0.231e-13	0.0288e-3
	DG5	0.013e-13	0.038e-13	0.0246e-3
Voltage balanced	DG1	7.812e-13	3.046e-13	1.0719e-3
	DG2	1.050e-13	1.370e-13	0.4760e-3
	DG3	0.020e-13	0.007e-13	0.0224e-3
	DG4	0.217e-13	0.216e-13	0.0270e-3
	DG5	0.001e-13	0.001e-13	0.0208e-3

is because of the small size of the test system considered. Moreover, it is attempted to produce a fair comparison since the procedure for the computationally efficient implementation of an existing algorithm is not reported in literature. Therefore, all the load flow algorithms are implemented without any special data processing so as to compare their performances in an equitable manner. The comparison of the computation time requirements of different methods is produced in Tables 6.4 and 6.5. Table 6.4 pertains to the current-balanced DG operation, whereas, Table 6.5 considers the voltage-balanced DG operation. In Table 6.5, the “BFS” column is left blank since the BFS technique cannot be used when DGs are operated in the voltage-balanced mode. Originally, the load flow algorithms proposed in [3] and [49] are also not applicable to the test system considered. However, those can also be enhanced by means of the transformer modeling proposed in this chapter.

Table 6.4: Comparison of computation time requirements among different methods for the current-balanced DG operation

DGs present	Computation time requirement (s)			
	BFS [39]	N-R [49]	Multi-slack Gauss- $Z_{bus}$ [3]	Single-slack Gauss- $Z_{bus}$
DG1	4.533552	4.286123	2.778956	0.742289
DG1-DG2	4.594869	6.202019	2.864205	0.868119
DG1-DG3	4.994428	8.498322	3.472297	0.892227
DG1-DG4	5.271945	9.247166	5.392867	0.979696
DG1-DG5	5.503950	9.938409	6.903485	0.954623

As expected, the use of N-R iterations for calculating bus voltages leads to much larger computation time requirement even if there is only a single DG in the sys-

Table 6.5: Comparison of computation time requirements among different methods for the voltage-balanced DG operation

DGs present	Computation time requirement (s)			
	BFS [39]	N-R [49]	Multi-slack Gauss- $Z_{bus}$ [3]	Single-slack Gauss- $Z_{bus}$
DG1	-	4.690115	2.591227	0.885246
DG1-DG2	-	6.321207	3.224062	0.952005
DG1-DG3	-	8.609402	4.156967	1.020091
DG1-DG4	-	9.251895	5.949058	1.023735
DG1-DG5	-	9.559601	6.481534	1.096659

tem. Although the multi-slack Gauss- $Z_{bus}$  technique shows low computation time in the presence of small number of DGs, its computational performance is drastically degraded as the number of DGs increases. The performance of the multi-slack Gauss- $Z_{bus}$  method is always found to be superior compared to the performance of the N-R method. Sometimes, even, the multi-slack Gauss- $Z_{bus}$  method outperforms the BFS method. However, in every situation, the methodology proposed in this chapter is found to deliver the overall superior performance.

In the present study, the computation times required by existing methodologies are found to be somewhat different from the values reported in literature for the similarly sized system. For example, lower computation times have been reported in [3] to carry out the ADLF calculation over a 123-bus network. It is, however, to be noted that the overall computation time requirement also depends upon the number of executions of the outermost loop. In this chapter, a modified 123-bus system has been considered with a number of steps in a voltage regulator or shunt capacitor bank. Therefore, the outermost loop is always found to execute more than twenty times. The number of executions of the outermost loop should not vary from one ADLF algorithm to another ADLF algorithm for the same system. On the other hand, voltage regulators might not have been considered in [3] since no procedure is suggested in [3] to incorporate voltage regulators within the Gauss- $Z_{bus}$  iterations. To the end, the addition of links may also increase the computation time of the load flow calculation.

### 6.6.3 Case Study 3 (Scalability Verification):

In order verify the scalability of the proposed ADLF algorithm, larger test systems are prepared by replicating the portion after Bus 2 of the above 123-bus system (with all the DGs connected) multiple times over a parallel connection as shown in Fig. 6.10.

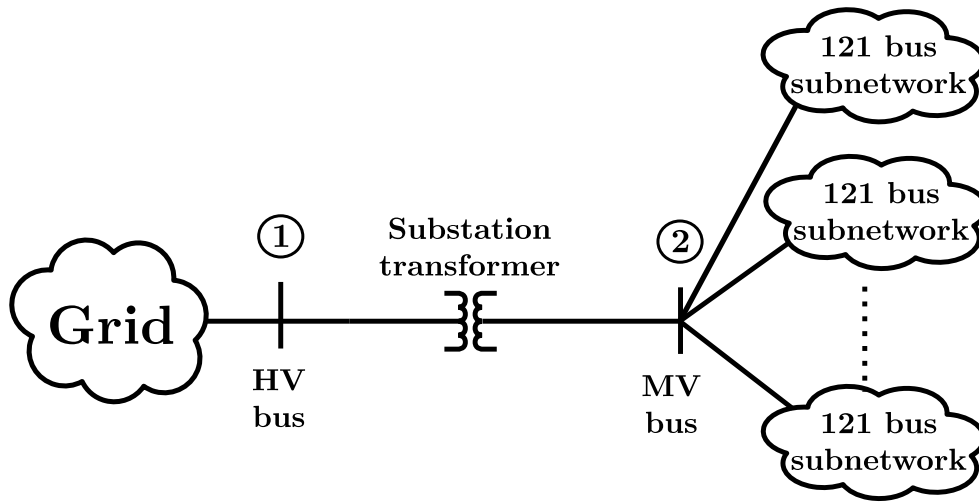


Figure 6.10: Network arrangement for the scalability test systems.

The sparse computation model of the proposed ADLF algorithm is implemented. The computation times reported in Table 6.6 demonstrates the capability of the proposed ADLF algorithm to make fast convergence even for a complex distribution network.

Table 6.6: Computational performance of the proposed ADLF algorithm in larger systems

System id.	Bus count	Generator count	Current-balanced DG		Voltage-balanced DG	
			Computation time (s)	Outer loop iteration count	Computation time (s)	Outer loop iteration count
123X5	607	25	6.787762	37	7.039174	38
123X10	1212	50	17.575100	41	18.206262	42
123X15	1817	75	31.019854	48	33.800819	49
123X20	2422	100	47.630410	55	50.136013	56

## 6.7 Summary

In this chapter, a novel load flow computation technique is proposed for the active distribution network. The Gauss- $Z_{bus}$  technique is applied in the symmetrical component domain by incorporating DG sequence impedances in network matrices instead of modeling those as external loads. In addition, the feeder network is modelled with only fixed parameters and without any blockage to zero sequence current flows. The parameter variation or the zero sequence current blockage caused by load or tap-changing transformers in the original distribution network is modelled externally via load currents. Thus, the load flow algorithm proposed is applicable to any feeder network with both voltage-balanced and current-balanced operations of DGs. Case

studies verify the computational efficiency of the proposed load flow algorithm. It is observed that the computation time requirements of existing methods radically increase with the increase in the number of DGs present in the system. In contrast, the methodology proposed always exhibits much lower computation time irrespective of the number of DGs present in the system. It is also found that the proposed Gauss- $Z_{bus}$  iterative calculation converge faster than the backward/forward sweeps (in the case the latter is applicable) for a system containing loops in the network. Furthermore, no solution inaccuracy results from the proposed modeling of DGs and transformers. A computationally efficient implementation of the proposed methodology is also shown for its application to a realistic distribution network. Results obtained from the study of large distribution systems confirm the practical applicability of the proposed load flow algorithm.

# Chapter 7

## Load Flow Analysis via Integrated DG and Transformer Modeling

### 7.1 Introduction

A DG may or may not have the capability to adjust its reactive power output in response to its terminal bus voltage variation. Harnessing DGs with variable reactive power outputs at the power distribution level leads to the flexibility of having some voltage-controlled buses in the feeder network [95,96]. Therefore, the load flow analysis techniques available for traditional passive distribution networks [35]- [42] are not directly applicable to active distribution networks. The load flow analysis of an active distribution network involves additional complexity with regard to the treatment of *PV* buses. In principle, the *PV* buses can be directly addressed by formulating nodal power balance equations and solving those through Newton-Raphson (N-R) iterations. The similar approach is followed in [48] and [49]. However, the N-R technique is, in general, not suitable for the distribution system because of high  $R/X$  ratios of feeder lines [1]. In [52], [68]- [70] the DG buses are indirectly modeled in the load flow analysis. The general approach that is followed in this regard is to add an outer loop of iteration for transforming the original system into a form that resembles a passive distribution network. In specific, the actual *PV* buses are iteratively represented as equivalent non-*PV* buses. Subsequently, the regular steps for the passive distribution network load flow analysis can be followed to determine the bus voltage profile. In each iteration of the outer loop, one passive distribution load flow (PDLF) problem is solved. Thus, the active distribution load flow (ADLF) problem is effectively formulated as a series of several PDLF problems. This, in turn, makes the computation

time requirement of the load flow analysis of an active distribution network several times higher than that for its passive counterpart.

This chapter contributes towards developing a novel algorithm for the load flow analysis of an active distribution network. The motivation behind this work is to improve the computational efficiency of the ADLF calculation so that the ADLF problem can be solved almost in the same time as is required for solving a traditional PDLF problem for the same system. The methodology proposed is based upon the following assumptions.

1. All the DGs are radially connected to the main feeder network.
2. There is no local load at a DG bus or, at least, the DG is operated under the voltage balancing control.

The first assumption is specifically true for power electronically interfaced DG units. The second assumption imposes only a minor restriction on the current-balanced operation of a DG unit. Implications of voltage-balanced and current-balanced operations are provided in later sections. Unlike the available techniques, the DG buses are not preserved in the proposed load flow calculation. Instead, the DG unit and the corresponding coupling transformer are combined together in the form of DG plant, which is subsequently represented as a voltage dependent negative load over the main feeder network.

## 7.2 Proposed DG Modeling

The organization of a power electronically interfaced DG unit is shown in Fig. 7.1 [90]-[91]. Here, the DC side of the DG unit is equivalently represented in the form of a fixed DC voltage source. Both the shunt capacitive filter and the DG side winding of the isolation/coupling transformer are either delta connected or star connected with neutral not grounded. This, in turn, ensures no zero sequence current flow on the DG side of the coupling transformer. The voltage at the point-of-connection (POC) to the main feeder network is indicated by  $\bar{V}_{poc}^{(abc)}$ . The main feeder network comprises of the normal feeder lines, load transformers and voltage regulators. A power electronically interfaced DG unit can be operated either in the voltage-balanced or in the current-balanced mode [3]. The voltage-balanced operation refers to the case when  $\bar{V}_{dg}^{(abc)}$  is perfectly in the positive sequence (i.e., negative and zero sequence components of terminal voltages are zeros). In the same way, the current-balanced

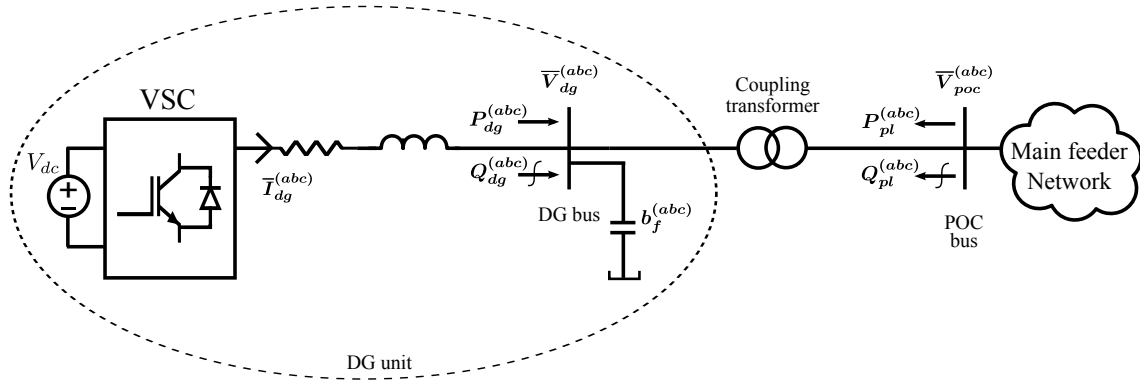


Figure 7.1: Organization of a power electronically interfaced DG unit.

operation indicates the absence of negative and zero sequence components in  $\bar{I}_{dg}^{(abc)}$ . The implementations of voltage balancing and current balancing controls are discussed in [91]- [97]. For both cases, the negative or zero sequence power supplied by the DG is zero. It is to be noted that, for the purpose of load flow analysis, the reactive power output of the DG is to be defined without including the shunt capacitor. The combined representation of the DG and the coupling transformer in positive, negative and zero sequence networks are shown in Fig. 7.2. In this chapter, the primary side of the coupling transformer is taken to be ungrounded-star, whereas the secondary side is taken to be grounded-star. The per-unit convention is followed in Fig. 7.2. The resistance and reactance of each phase of the coupling transformer is indicated by  $r_{tr}$  and  $x_{tr}$ , respectively. The capacitive phase susceptance of the shunt filter is symbolized as  $b_f$ . As mentioned previously, the zero sequence current on the DG side is always zero. Therefore, the DG always behaves as a zero current source in the zero sequence network. For the voltage-balanced operation, the negative sequence component of the DG terminal voltage is zero, which can be represented by a short circuit to the ground. In the case of the current-balanced operation, the only path through which the negative sequence current can flow is the shunt capacitor. In the positive sequence network, the DG should be represented as a single-phase AC generator with either of the following output specifications.

1. Fixed active power output and fixed terminal voltage magnitude (i.e.,  $P_{dg}^{sp}$  and  $V_{dg}^{sp(1)}$ ).
2. Both fixed active and reactive power outputs (i.e.,  $P_{dg}^{sp}$  and  $Q_{dg}^{sp}$ ).

For the first case, the DG is said to operate in the *PV* mode, whereas, in the second case, it is said to operate in the *PQ* mode. Since the Integrated DG plant (i.e.,

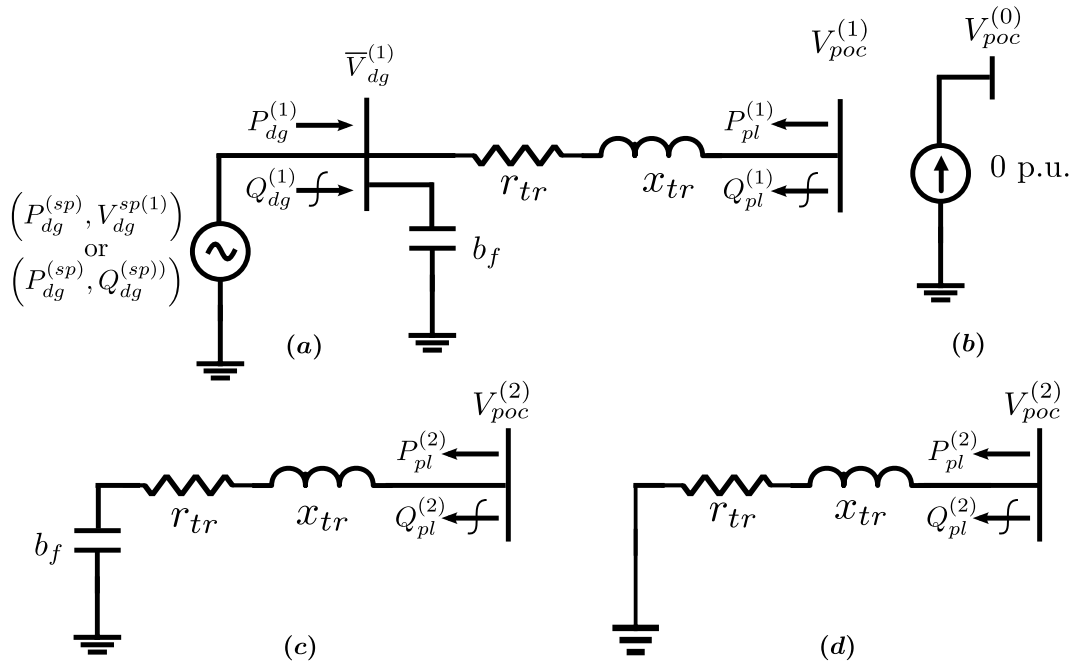


Figure 7.2: Symmetrical domain representation of the DG plant. a) Positive sequence, b) zero sequence, c) negative sequence under current balance, d) negative sequence under voltage balance.

the combination of the DG unit and the coupling transformer) is to be represented as a load on the main feeder network, the power flow on the secondary side of the transformer is shown in the reverse direction. Thus,  $\mathbf{P}_{pl}^{(abc)}$  is usually a negative vector. The secondary-side power flow of the transformer essentially indicates the power exchange between the DG plant and the main distribution network. In the negative or zero sequence network, the DG plant can straightaway be modeled as a constant impedance load. The basic working equations for deriving the equivalent voltage dependent load model of a DG plant in the positive sequence network are presented below.

$$P_{dg}^{(1)} = g_{tr} \left\{ V_{dg}^{(1)} \right\}^2 - y_{tr} V_{dg}^{(1)} V_{poc}^{(1)} \cos \left( \Delta\delta^{(1)} - \psi \right) \quad (7.1)$$

$$Q_{dg}^{(1)} = - \left( b_{tr} + b_f \right) \left\{ V_{dg}^{(1)} \right\}^2 - y_{tr} V_{dg}^{(1)} V_{poc}^{(1)} \sin \left( \Delta\delta^{(1)} - \psi \right) \quad (7.2)$$

$$P_{pl}^{(1)} = g_{tr} \left\{ V_{poc}^{(1)} \right\}^2 - y_{tr} V_{dg}^{(1)} V_{poc}^{(1)} \cos \left( \Delta\delta^{(1)} + \psi \right) \quad (7.3)$$

$$Q_{pl}^{(1)} = -b_{tr} \left\{ V_{poc}^{(1)} \right\}^2 + y_{tr} V_{dg}^{(1)} V_{poc}^{(1)} \sin \left( \Delta\delta^{(1)} + \psi \right) \quad (7.4)$$



where,

$$g_{tr} = \frac{r_{tr}}{x_{tr}^2 + r_{tr}^2} \quad (7.5)$$

$$b_{tr} = -\frac{x_{tr}}{x_{tr}^2 + r_{tr}^2} \quad (7.6)$$

$$y_{tr} = \sqrt{g_{tr}^2 + b_{tr}^2} \quad (7.7)$$

$$\psi = \tan^{-1} \left( \frac{g_{tr}}{b_{tr}} \right) \quad (7.8)$$

$$\Delta\delta^{(1)} = \delta_{dg}^{(1)} - \delta_{poc}^{(1)}. \quad (7.9)$$

The voltage angles at DG and POC buses are indicated by  $\delta_{dg}$  and  $\delta_{poc}$ , respectively. Primarily, two load models are possible for a DG plant in the positive sequence network. Those are discussed in the following subsections.

### 7.2.1 Load Model A

The particular load model corresponds to the *PV* mode of operation. From (7.1), the angle difference between the DG bus and POC bus voltage phasors, for a given voltage at the POC bus, can be determined as follows.

$$\Delta\delta^{(1)} = \psi + \cos^{-1} \left( \frac{g_{tr} \left\{ V_{dg}^{sp(1)} \right\}^2 - P_{dg}^{sp}}{y_{tr} V_{dg}^{sp(1)} V_{poc}^{(1)}} \right). \quad (7.10)$$

The value of  $\Delta\delta^{(1)}$  thus obtained can be replaced in (7.3) and (7.4) to obtain the active and reactive power drawn by the DG plant for the given POC bus voltage.

### 7.2.2 Load Model B

For the *PQ* mode of operation of the DG, Load Model B is derived. From (7.1) and (7.2), the following relationship can be obtained.

$$y_{pl}^2 \left\{ V_{dg}^{(1)} \right\}^4 + \zeta_{pl} \left\{ V_{dg}^{(1)} \right\}^2 + S_{dg}^2 = 0 \quad (7.11)$$

where,

$$y_{pl} = \sqrt{g_{tr}^2 + (b_{tr} + b_f)^2} \quad (7.12)$$

$$\zeta_{pl} = 2(b_{tr} + b_f) Q_{dg}^{sp} - 2g_{tr} P_{dg}^{sp} - y_{tr}^2 \left\{ V_{poc}^{(1)} \right\} \quad (7.13)$$

$$S_{dg} = \sqrt{\left\{ P_{dg}^{sp} \right\}^2 + \left\{ Q_{dg}^{sp} \right\}^2}. \quad (7.14)$$

The positive sequence voltage magnitude at the DG bus, for the given POC bus voltage, can be obtained by solving Equation (7.11). That is,

$$V_{dg}^{(1)} = \sqrt{\frac{-\zeta_{pl} + \sqrt{\zeta_{pl}^2 - 4y_{pl}^2 S_{dg}^2}}{2y_{pl}^2}}. \quad (7.15)$$

In order to obtain the solution for  $\Delta\delta^{(1)}$ , the value of  $V_{dg}^{(1)}$  obtained from (7.15) is to be substituted in Equation (7.10) at the place of  $V_{dg}^{sp(1)}$ . Subsequently, Equations (7.3) and (7.4) are again to be used to find the active and reactive power drawn by the DG plant.

Typically, the *PQ* mode corresponds to the operation of the DG at a reactive power limit. In this regard, the Load Model B can further be divided into two subcategories as follows.

1. Load Model B1:  $Q_{dg}^{sp} = Q_{dg,max}$ .
2. Load Model B2:  $Q_{dg}^{sp} = Q_{dg,min}$ .

Here,  $Q_{dg,max}$  and  $Q_{dg,min}$  indicate the maximum and minimum reactive power production limits of the DG. Ideally, the DG should operate in the *PV* mode. The switching to the *PQ* mode would take place when the reactive power to be supplied by the DG for maintaining operation in the *PV* mode surpasses the available limit. The reactive power output of the DG in the *PQ* mode should be set fixed to the limit that is exceeded under the *PV* mode.

### 7.3 ADLF Algorithm with the Proposed DG Modeling

Because of combining a DG unit and the corresponding coupling transformer into a single element, the DG buses are not to be preserved in the load flow calculation.

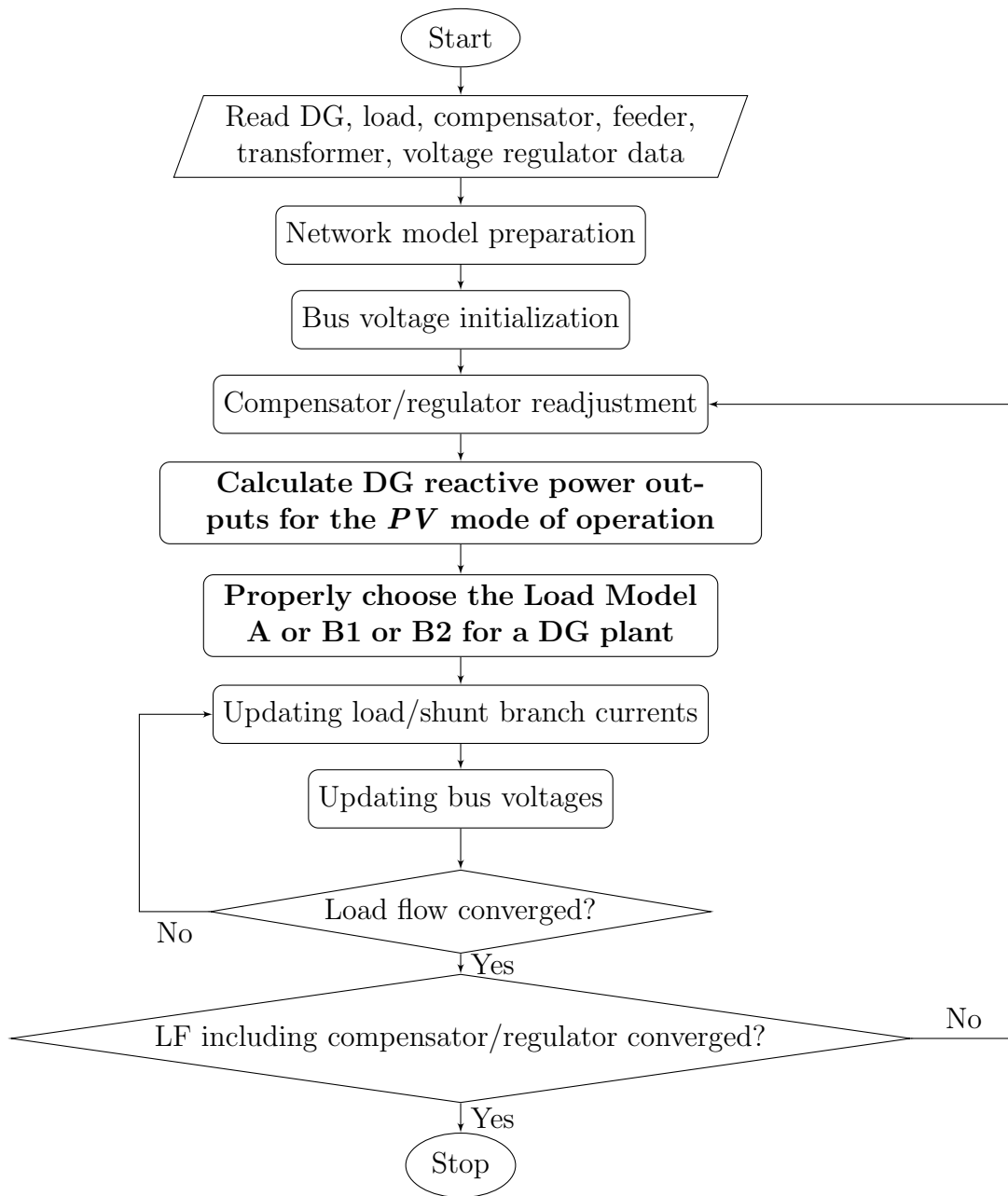


Figure 7.3: Flowchart of the proposed ADLF algorithm.

As mentioned previously, there should not be any local load at a current-balanced DG bus. For a voltage-balanced DG bus, the local loads can be included in the DG plant model itself by directly subtracting the load active power from the DG active power output. The flowchart of the proposed ADLF algorithm retains almost the same structure as that of the normal PDLF algorithm. The same is presented in Fig. 7.3.

Unlike Fig. 6.3, there is no extra loop in the flowchart presented in Fig. 7.3. In

fact, only a couple of simple blocks had to be added to convert a PDLF algorithm into an ADLF algorithm. The additional blocks incorporated are indicated by bolded texts. The respective blocks are required only to obey the reactive power capability of a DG. The procedure for the selection of a load model for the DG plant is explained in Section 7.2. In this chapter, the load current and bus voltage updates are carried out through FBS iterations in the phase domain. Apart from updating the load and compensator currents, the DG currents are also to be updated during the backward sweep. The DG currents are updated by following the same general procedure as was reported [69]. In the context of the proposed algorithm, the steps involved in updating the DG plant currents can be specifically stated as follows.

- Decompose the POC bus voltages into positive, negative and zero sequence components.
- Calculate the sequence currents of the DG plant by using its symmetrical domain models that are shown in Fig. 7.2.
- Transform the sequence currents of the DG plant into its phase currents.

In the negative or zero sequence network, the DG plant appears like a simple constant impedance load, whereas, in the positive sequence network, it can be represented via Load Model A or B1 or B2 derived in Section 7.2. Only one round of FBS iterations is required to obtain the final load flow solution after the voltage regulators and shunt capacitors are properly adjusted.

The load model selection for a DG plant can be further simplified by pre-evaluating its load characteristics. Typically, there exists a certain voltage range within which a particular load model remains valid. A similar result will be shown in the Case Study section. The load model to be employed can be directly identified through the voltage range that the present POC bus voltage lies in.

## 7.4 Case Study:

The methodology proposed needs to be verified with respect to its general convergence performance, computational efficiency and computational accuracy. Two different case studies are performed in this regard. The objective of the first case study is to investigate the characteristics of the equivalent load model of a DG plant in the positive sequence network. The main difference between the ADLF problem formulated and a PDLF problem is the deployment of new load models to represent a DG

plant. Therefore, the convergence of the load flow calculation can be affected only by any erratic characteristics of this new load model. The computational efficiency of the proposed methodology is verified through the second case study. All the calculations are carried out on an intel i5, 2.6-GHz processor with 4 GB of RAM.

### 7.4.1 Case Study 1 (Verification of the Convergence Performance)

For the particular study, only stand-alone DGs are considered. Five different DG plants are studied. The detailed information of respective DG plants is provided in Table 7.1. The ideal positive sequence voltage magnitude of the DG bus is taken as 1 p.u.

Table 7.1: DG plant information

DG Id.	$P_{dg}^{sp}$ (p.u.)	$Q_{g,max}$ (p.u.)	$Q_{g,min}$ (p.u.)	$b_f$ (p.u.)	$x_{tr}$ (p.u.)	$r_{tr}$ (p.u.)
DG1	0.10	0.100	-0.100	0.00100	0.100	0.020
DG2	0.09	0.075	-0.075	0.00095	0.110	0.025
DG3	0.08	0.100	-0.080	0.00090	0.120	0.030
DG4	0.15	0.125	-0.100	0.00150	0.095	0.018
DG5	0.20	0.150	-0.150	0.00200	0.080	0.015

The power characteristics of a DG plant are obtained by evaluating its positive sequence active and reactive power outputs for different values of the POC bus voltage magnitude (positive sequence). The positive sequence POC bus voltage magnitude is varied from 0.9 p.u. to 1.1 p.u. with a step size of 0.001 p.u. Each load characteristic comprises of three segments. In Segments 1 and 3, the DG unit operates in the  $PQ$  mode with its reactive power output being set to maximum and minimum limits, respectively. The second segment corresponds to the  $PV$  mode of operation.

After obtaining the load characteristics of a DG plant, each segment is fitted with a quadratic curve. In order words, the active and reactive power outputs of a DG plant, over each segment, are to be expressed as follows.

$$P_{pl}^{(1)} = \alpha_p \left\{ V_{poc}^{(1)} \right\}^2 + \beta_p V_{poc}^{(1)} + \gamma_p \quad (7.16)$$

$$Q_{pl}^{(1)} = \alpha_q \left\{ V_{poc}^{(1)} \right\}^2 + \beta_q V_{poc}^{(1)} + \gamma_q. \quad (7.17)$$

Equations (7.16) and (7.17) basically represent the power characteristics of a ZIP

load that is the commonly used load model for a distribution network. Thus, it is basically attempted to explore the similarity between a DG plant and a ZIP load from the point of view of power characteristics. The corresponding quadratic curve fitting results are produced in Table 7.2 and Table 7.3.

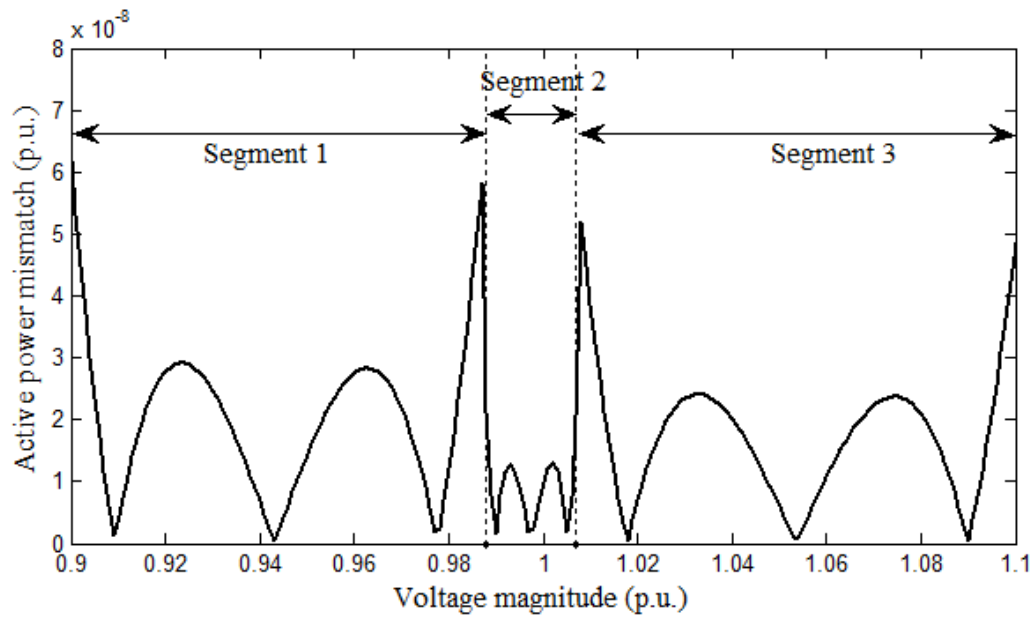
Table 7.2: Parameters of the quadratically approximated active power characteristics of DG plants

DG Id.	Segment 1			Segment 2			Segment 3		
	$\alpha_p$ (p.u.)	$\beta_p$ (p.u.)	$\gamma_p$ (p.u.)	$\alpha_p$ (p.u.)	$\beta_p$ (p.u.)	$\gamma_p$ (p.u.)	$\alpha_p$ (p.u.)	$\beta_p$ (p.u.)	$\gamma_p$ (p.u.)
DG1	0.0014	-0.0035	-0.0975	1.9923	-3.9769	1.8848	0.0010	-0.0029	-0.0978
DG2	0.0012	-0.0030	-0.0878	1.8820	-3.7558	1.7840	0.0009	-0.0024	-0.0881
DG3	0.0017	-0.0043	-0.0769	2.0740	-4.1382	1.9844	0.0010	-0.0027	-0.0779
DG4	0.0024	-0.0060	-0.1457	1.9844	-3.9584	1.8245	0.0015	-0.0042	-0.1467
DG5	0.0032	-0.0082	-0.1941	2.3303	-4.6473	2.1176	0.0024	-0.0067	-0.1947

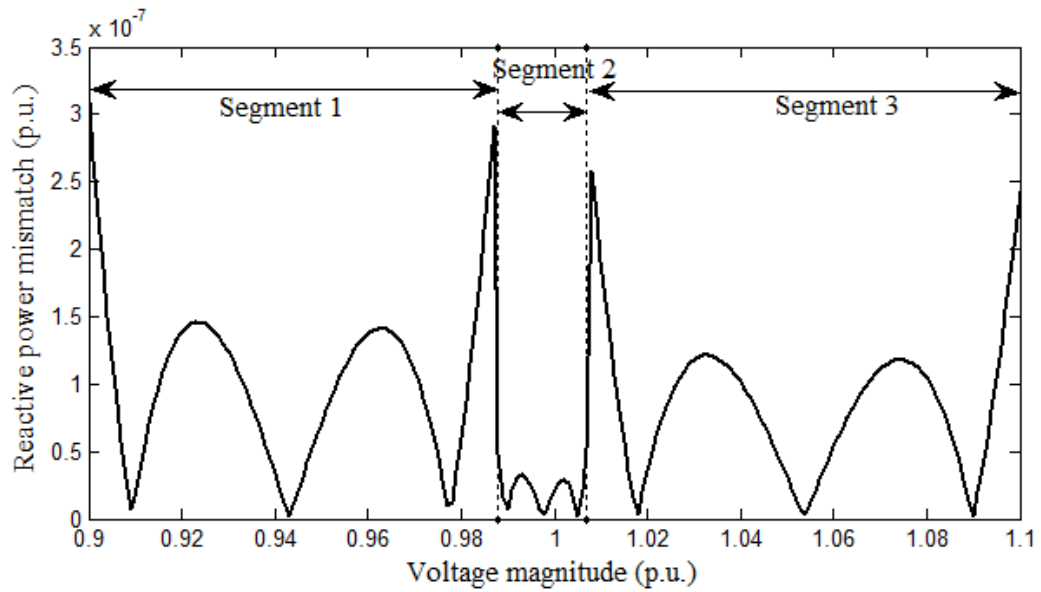
Table 7.3: Parameters of the quadratically approximated reactive power characteristics of DG plants

DG Id.	Segment 1			Segment 2			Segment 3		
	$\alpha_q$ (p.u.)	$\beta_q$ (p.u.)	$\gamma_q$ (p.u.)	$\alpha_q$ (p.u.)	$\beta_q$ (p.u.)	$\gamma_q$ (p.u.)	$\alpha_q$ (p.u.)	$\beta_q$ (p.u.)	$\gamma_q$ (p.u.)
DG1	0.0060	-0.0177	-0.0873	9.7816	-9.5446	-0.2165	0.0041	-0.0143	0.1112
DG2	0.0045	-0.0140	-0.0650	8.4719	-8.2301	-0.2218	0.0030	-0.0112	0.0838
DG3	0.0058	-0.0172	-0.0877	8.0554	-7.7591	-0.2759	0.0030	-0.0110	0.0886
DG4	0.0104	-0.0316	-0.1024	10.3117	-10.0709	-0.2113	0.0059	-0.0220	0.1173
DG5	0.0151	-0.0435	-0.1188	12.2458	-11.9572	-0.2495	0.0108	-0.0359	0.1782

In order to show the accuracy of the above mentioned quadratic approximation, the absolute errors between the actual power characteristics and the quadratically approximated power characteristics of DG1 are plotted in Fig. 7.4. The errors are almost negligible. Moreover, the DG plant active power does not significantly vary with the POC bus voltage since the power loss in the transformer impedance is negligible compared to the power output of the DG unit. The same phenomenon happens for the reactive power characteristics over Segments 1 and 3. Over Segment 2, the reactive power drawn by a DG plant monotonically increases with the POC bus voltage, which is the typical nature of a normal voltage dependent reactive power load. The plant active power and reactive power characteristics for DG1 are plotted in Fig. 7.5. Thus, in the positive sequence network, the DG plant behaves similarly to a ZIP load for both  $PV$  and  $PQ$  modes of operation. Therefore, there may not be any convergence issue in the load flow calculation because of the proposed DG modeling. It is, however, to be noted that the quadratic approximation of the DG plant power characteristics shown above is not for use during the actual load flow



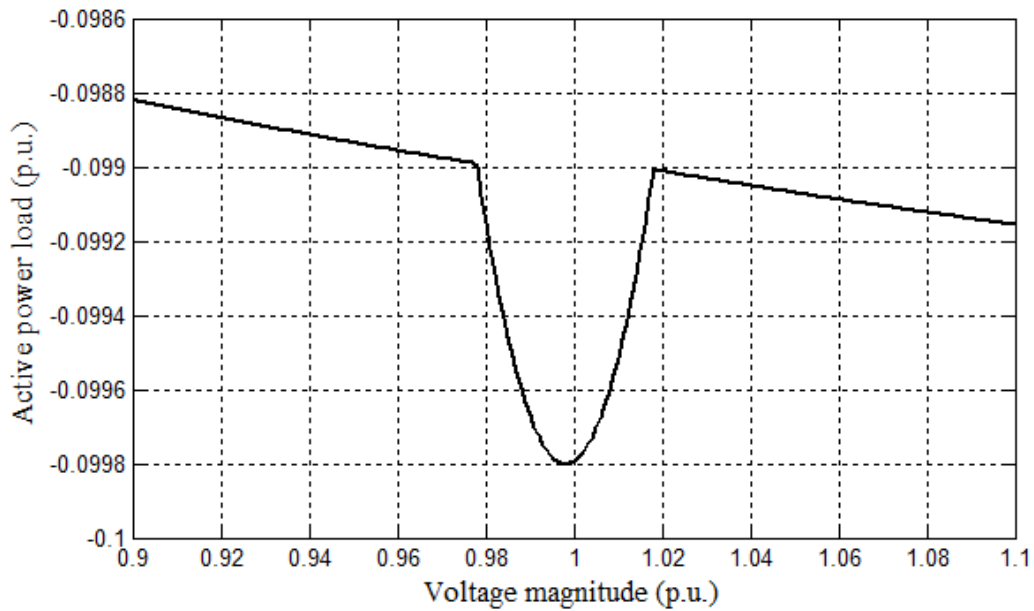
(a)



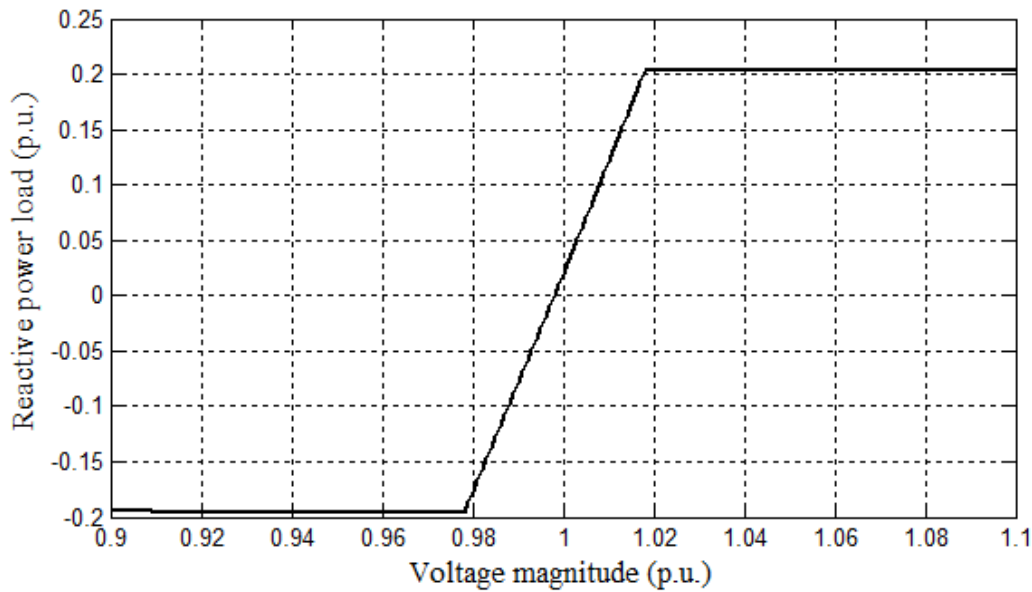
(b)

Figure 7.4: Absolute errors between actual and quadratically approximated load characteristics of DG1 for different POC bus voltages. a) Active power, b) reactive power.

calculation. The actual load flow calculation is performed by using the original power characteristics defined through (7.1)-(7.15).



(a)



(b)

Figure 7.5: Plant power characteristics for DG1. a) Active power, b) reactive power.

### 7.4.2 Case Study 2 (Verification of the Computational Efficiency and Solution Accuracy)

The particular case study is performed on a modified IEEE 123-bus distribution system. The original data of the particular system is available in [87]. The following modifications are performed.



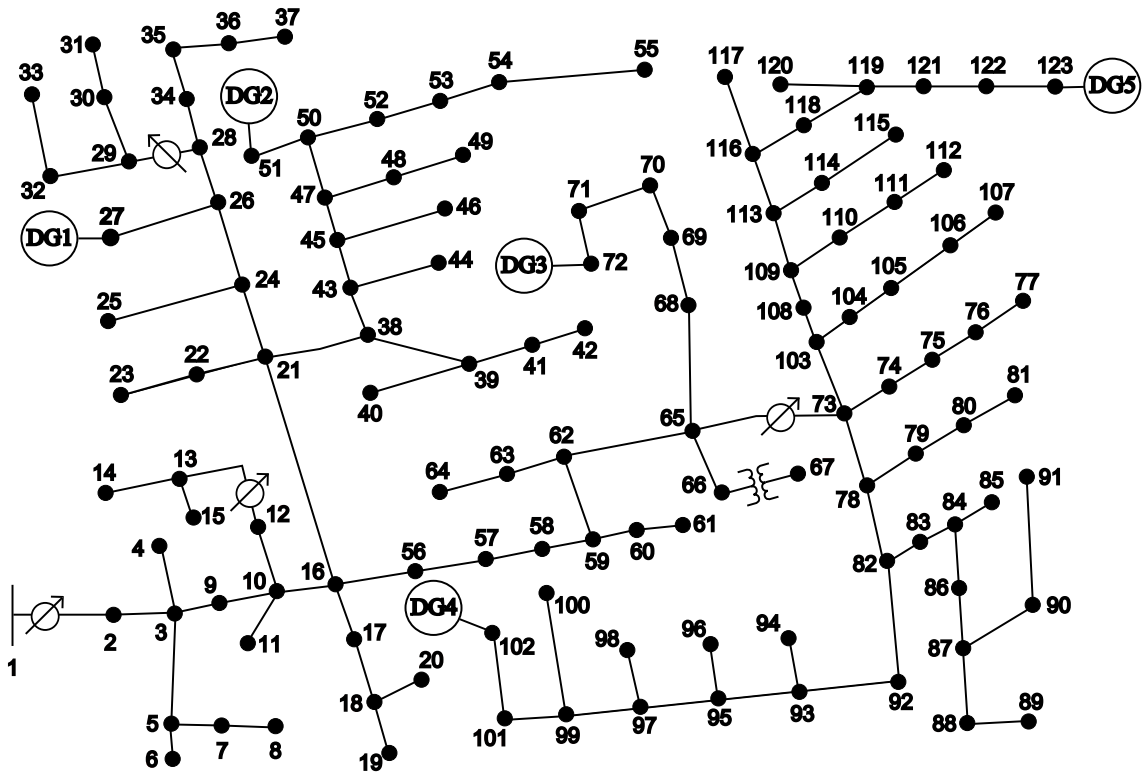


Figure 7.6: IEEE 123-bus system with the locations of DGs, transformers and regulators in referred bus numbering.

1. DGs are placed in the network.
2. The load (both active power and reactive power) at each phase of any bus is assumed to be composed 80% constant power load, 10% constant impedance load and 10% constant current load.
3. The capacitor bank placed at a bus is assumed to be composed of 10 equal sized capacitors.
4. The tap adjustment step size of a voltage regulator is taken to be 2%. The maximum permissible tap adjustment in either (i.e., positive or negative) direction is taken to be 4%.

The DGs placed are taken from Table 7.1. The specific locations at which DGs are placed are shown in Fig. 7.6. All the voltage regulators are assumed to be solidly grounded Y-connected autotransformers. The desired upper and lower limits of the bus voltage magnitude are set to 0.95 p.u. and 1.05 p.u., respectively. The capacitor switching or the voltage regulator tap adjustment action is called for if the voltage magnitude at any phase of a bus crosses a limit. Bus 1 is taken as the substation

bus. The precision index value chosen for the convergence of FBS iterations is 0.0001 p.u. Results are obtained by considering different numbers of DGs at a time. The computation time requirements of different ADLF algorithms to solve the given load flow problem with DGs being operated in the current-balanced fashion are reported in Table 7.4. Similar results for the voltage-balanced operation of DGs are produced in Table 7.5. Under all the scenarios, the methodology proposed performs far better than the other methods. Moreover, there is only some minor variation in the computation time requirement when a new DG is added to the system. On the other hand, all other methodologies (especially, [49] and [3]) are highly sensitive to the number of DGs present in the system. It is to be noted that the methodology proposed in [39] cannot be used if DGs are operated in the voltage-balanced mode. Therefore the second column of Table 7.5 is left blank except for the place in the first row.

Table 7.4: Comparison of computation time requirements by different ADLF algorithms corresponding to the current-balanced DG operation

DGs present	Computation time requirement (sec)			
	Method [39]	Method [49]	Method [3]	Proposed methodology
None	4.225699	3.9332520	4.225699	3.915974
DG1	6.143760	7.8876180	5.778869	4.442202
DG1-DG2	6.572797	9.5068830	6.808301	4.568433
DG1-DG3	7.438813	10.465520	9.838901	4.721951
DG1-DG4	7.532830	12.229112	10.111134	4.774331
All	8.507095	13.579844	10.169919	4.775672

Table 7.5: Comparison of computation time requirements by different ADLF algorithms corresponding to the voltage-balanced DG operation

DGs present	Computation time requirement (sec)			
	Method [39]	Method [49]	Method [3]	Proposed methodology
None	4.225699	3.933252	4.225699	3.915974
DG1	-	7.774976	5.961631	5.012618
DG1-DG2	-	8.580233	6.937760	5.856348
DG1-DG3	-	9.491023	7.963832	5.929896
DG1-DG4	-	11.839803	9.388106	5.984253
All	-	13.655837	10.263624	5.996570

In order to assess the accuracy of the proposed ADLF algorithm, bus power mismatches [93] are calculated for the final solution of bus voltage magnitudes and angles. The three-phase nodal power balance equations [94] to calculate bus power

mismatches. Table 7.6 presents results for the maximum (in absolute value) active power and reactive power mismatches observed over different buses and different phases. It can be seen that, for all the cases, the nodal power mismatches are very close to zero, which, in turn, confirms the accuracy of the proposed ADLF algorithm. There is no need to observe the voltage mismatch at a DG bus. This is because a DG bus is not included in the load flow calculation. Instead, the required DG bus voltage is enforced directly in the load equations of the DG plant.

Table 7.6: Results for the maximum bus power mismatch at the load flow solution

DGs present	Current-balanced operation		Voltage-balanced operation	
	Active power mismatch	Reactive power mismatch	Active power mismatch	Reactive power mismatch
	(p.u.)	(p.u.)	(p.u.)	(p.u.)
None	3.39E-08	3.31E-08	3.39E-08	3.31E-08
DG1	3.21E-08	3.95E-08	2.56E-08	2.50E-08
DG1-DG2	2.56E-08	2.77E-08	1.78E-08	1.75E-08
DG1-DG3	9.11E-08	8.78E-08	7.08E-08	8.43E-08
DG1-DG4	1.00E-07	1.03E-07	1.30E-07	1.47E-07
All	1.97E-07	5.27E-08	2.89E-08	3.23E-08

## 7.5 Summary

A novel load flow algorithm for active distribution networks is proposed in this chapter under some realistic assumptions. The distinct feature of the proposed algorithm is that the load flow analysis needs to be performed only over the main feeder network. It is shown that the DG plant can be represented similarly to a voltage dependent load. Thus, the DG buses are kept hidden while performing the load flow analysis. This, in turn, helps in eliminating an extra level of iteration in the ADLF calculation. The equivalent load representation of the DG-transformer assembly in the positive sequence network is found to closely match the form of a combination of constant power, constant current and constant impedance loads. In addition, the load models of a DG plant exhibits either negligible or monotonically increasing power variations with the POC bus voltage, which is in line of the traditional load characteristics. Thus, the convergence of the proposed load flow algorithm could be qualitatively ensured. Significant reduction in the computation time requirement is observed through the deployment of the proposed ADLF algorithm. The computation time required is also found to be negligibly sensitive to the number of DGs present in the system.

This, in turn, ensures convergences of ADLF and PDLF calculations almost in the same time scale. Similarly to the existing algorithms, the load flow solution obtained from the proposed algorithm is verified to be highly accurate.

# Chapter 8

## Conclusions

The general load flow analysis of a distribution network suffers with multiple issues related to accuracy and computational efficiency. These issues are inaccurate modeling of network components, inaccurate modeling of load, computationally inefficient load flow algorithms and limited scope to deal with DG integration. Problem further arises with the variation in the control strategy of integrated DGs. Therefore, by keeping these issues in mind solution of aforementioned problem are proposed in this thesis. The motivations behind these works are to improve computational efficiency and accuracy by modifying load flow algorithm and with accurate feeder components and load modeling.

### 8.1 Overall Summary

A thorough literature review is presented on distribution load flow analysis including both passive and active network. Precise modeling of network components is proposed along with load modeling. Modified versions of load flow algorithm are comprehensively discussed and thorough case studies are performed on both active/passive distribution test networks. The novel contributions of this thesis work are summarized as follows.

#### 8.1.1 Load flow Analysis with Accurate Modeling of IM Loads

The primary objective of this work is to carry out the load flow analysis of a distribution network in the case of the dominant presence of induction motor loads. For a given operating condition, the load representation of an induction motor on the distribution network is made by analyzing its exact equivalent circuit. Thus, the

induction motor is precisely represented as a voltage and frequency dependent load. The necessity of representing an induction motor by means of its precise load model is verified by means of a case study on 30-bus distribution network. In specific, the inaccuracy in load flow results that is introduced because of the conventional representation of the induction motor as a constant power load is investigated in the presence of both the *PV* and droop modes of generator operation.

The results verify the voltage magnitudes calculated with the constant power model of the induction model significantly differ from the actual values. The inaccurate calculation of bus voltage magnitudes and angles also has a strong concern with the stability of a renewable-driven microgrid. This, in turn, results in inappropriate parameter tuning with the final effect can degrade the system stability.

### 8.1.2 FBS Algorithm with Accurate Modeling of Zero Sequence Voltages

A novel technique is proposed in this work to improve the accuracy of the results obtained from the load flow analysis of a distribution network via forward-backward sweeps. Specific attention is paid to the two-port modeling of a transformer with precise consideration for the zero sequence components of its port voltages. A new two-port network model is derived, which is generalized enough for the accurate representation of a transformer in the cascaded connection. Based upon the novel two-port representation made, a new set of iteration rules is established to carry out the forward-backward sweeps for solving the load flow results. All possible transformer configurations are taken into account. It is shown that the load flow analysis technique proposed is suitable for both active and passive distribution networks. The accuracy analysis of the load flow results is also carried out, by assessing the nodal current imbalances of the network. The work starts with redefining the cascade and hybrid parameter representation of a 3-phase element through the introduction of some zero-sequence voltage offsets, whenever necessary. The zero sequence voltage offsets used during backward sweep which is derived from the results of the forward sweep in the previous iteration. It is to be emphasized once again the objective of this work is to improve the accuracy of the load flow solution. The accuracy assessment of load flow results is carried out by verifying the Kirchhoffs current law (KCL) at each bus. The load flow inaccuracy is quantified in terms of a bus current mismatch index (BCMI). With the presented result it can be verified that the proposed algorithm maintains almost zero BCMI at all the buses. Whether, the bus current

mismatches are prominent for the conventional algorithm, specially, at buses near the transformers.

### 8.1.3 Modified Gauss- $Z_{bus}$ Iterations for Solving ADLF Problem

The objective of this work is to develop a computationally efficient and generalised algorithm for the load flow calculation in an active distribution network. In proposed work, the load flow calculation is carried out by using the concept of Gauss- $Z_{bus}$  iterations, wherein the DG buses are modeled via the technique of power/current compensation. The specific distinctness of the proposed Gauss- $Z_{bus}$  formulation lies in overcoming the limitations imposed by DG control modes for the chosen DG bus modeling as well as in having optimized computational performance. The entire load flow calculation is carried out in the symmetrical component domain by decoupling all the sequence networks. Furthermore, a generalised network modeling is carried out to define decoupled and tap-invariant sequence networks along with maintaining the integrity of the zero sequence network under any transformer configurations.

Since, the Gauss- $Z_{bus}$  iterative technique is promising for building an ADLF algorithm that can take into account both the voltage-balanced and current-balanced operations of a DG. Therefore, the same principle is employed to build the proposed ADLF algorithm. The principal focus of this work is, thus, on attaining the following goals.

1. Prevention of blockages to the zero sequence current flow and elimination of the need for the repeated reconstruction of impedance matrices by means of some suitable modeling of transformers and voltage regulators.
2. Exploring a suitable modification of the Gauss- $Z_{bus}$  iterative formula so as to ensure faster computation and convergence of the ADLF calculation.

The direct use of Gauss- $Z_{bus}$  iterative equations may not be suitable for the large system application since the particular formulation involves a large number of computations. Therefore, a methodology is further proposed to convert the iterative equations into a computationally efficient format by means of the Doolittle's LU decomposition. Case studies are performed and results are validated in the form of solution accuracy, computational performance and scalability verification.

### **8.1.4 LF Analysis via Integrated DG and Transformer Modeling**

The objective of this work is to identify and eliminate unnecessary iteration loops in the load flow analysis of an active distribution network so as to improve its overall computational efficiency. The number of iteration loops is minimised through the integrated modeling of a distributed generator (DG) and the associated coupling transformer. The DG bus is not preserved in the load flow calculation and the aforementioned DG-transformer assembly is represented in the form of a voltage dependent negative load at the point of connection to the main distribution network. Thus, the iteration stage that is involved in indirectly preserving the DG in the form of a voltage source or negative constant power load can be eliminated. This, in turn, eliminates the need for multiple rounds of forward-backward sweep iterations to determine the bus voltages.

Because of combining a DG unit and the corresponding coupling transformer into a single element, the DG buses are not to be preserved in the load flow calculation. Because of DG merger into load flow only one round of FBS iterations is required to obtain the final load flow solution. This elimination of unnecessary step reduce computation time effectively. Also test case studies are performed and results are validated in the form of convergence performance, computational efficiency and solution accuracy.

### **8.1.5 Merits of Proposed Work**

Merits of above mentioned works can explained as follows. First work is only associated with induction motor modeling. Second work represents accurate modeling of zero sequence and best suited for radial distribution network. The third work, algorithm modification is specifically suitable for a meshed distribution network with local load to a DG. While, the fourth work's is specifically useful if there is no local load at a current/voltage balanced DG bus. Third work provide best algorithm for ADLF, while fourth work further reduce computation time. So, combining these works will improve accuracy and computational efficiency.

## **8.2 Future Scopes of Work**

There are following directions in which further research can be carried out.



### **8.2.1 OPF Analysis of an Unbalanced Active Distribution Network**

Using the finding of current work further research can be carried out for OPF analysis of unbalance distribution network. Further work can be done on DG modeling for OPF since current literatures do not consider proper modeling for unbalance DGs. Moreover, the computation time requirement is also a major concern in OPF analysis.

### **8.2.2 Network-Constrained Consumer Load Aggregation Over Distribution System**

Based on distribution network limitation further research can be proceed for load aggregation. Consumers' participation is to be more pragmatically defined and the provision for retail side completion is to be incorporated for load aggregation.

### **8.2.3 Power Flow Analysis of an AC-DC Distribution Network**

This topic is in line of the recent trend of hybrid microgrids. Current unbalanced AC network load flow distribution analysis can be expanded into AC-DC distribution network analysis.

# Appendix A

## Smaller Test System

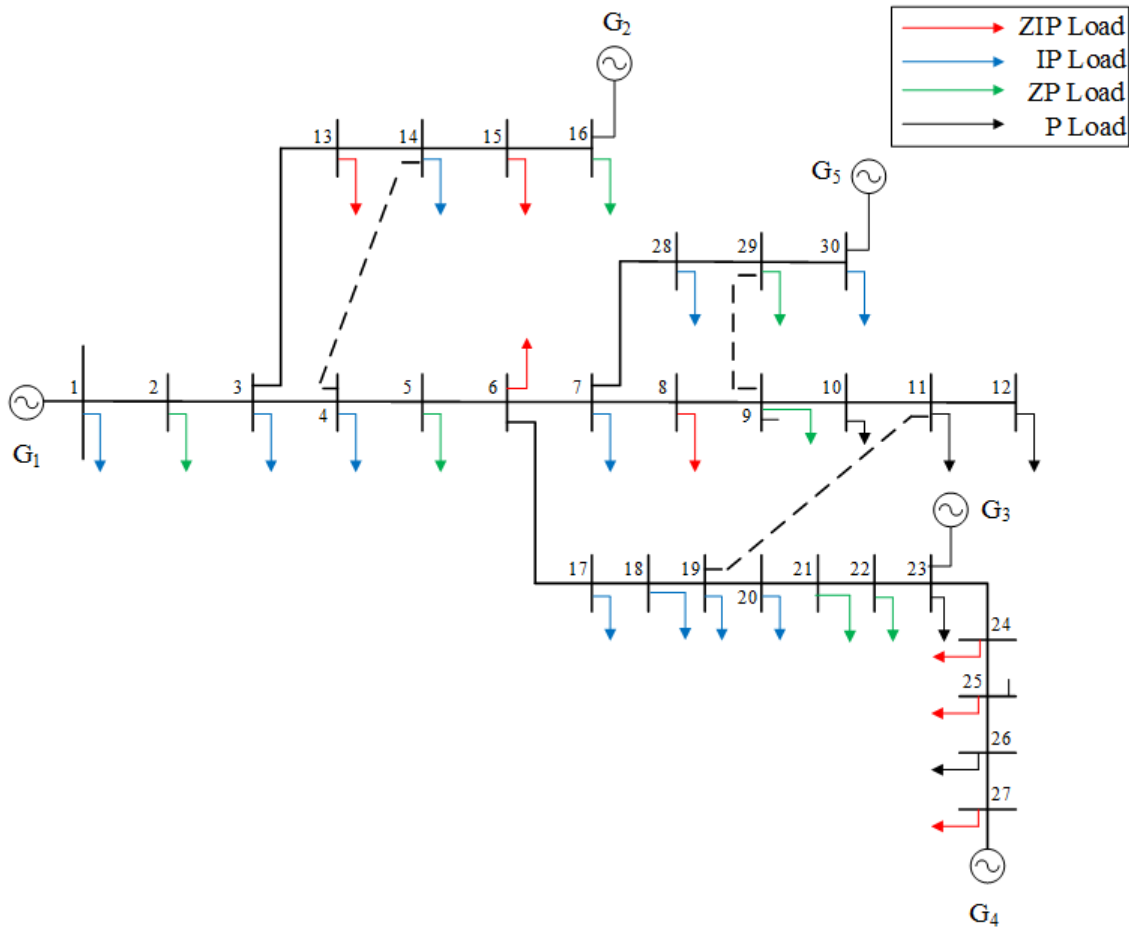


Figure A.1: 30 bus weakly meshed distribution system with induction motor and generator.

Table A.1: System line data

Branch number	From bus	To bus	Resistance (pu)	Reactance (pu)
1	1	2	0.0967	0.0397
2	2	3	0.0886	0.0364
3	3	4	0.1359	0.0377
4	4	5	0.1236	0.0343
5	5	6	0.1236	0.0343
6	6	7	0.2598	0.0446
7	7	8	0.1732	0.0298
8	8	9	0.2598	0.0446
9	9	10	0.1932	0.0298
10	10	11	0.2083	0.0186
11	11	12	0.0866	0.0149
12	3	13	0.1299	0.0223
13	13	14	0.1732	0.0298
14	14	15	0.0866	0.0149
15	15	16	0.0433	0.0074
16	6	17	0.1483	0.0412
17	17	18	0.1359	0.0377
18	18	19	0.1718	0.0291
19	19	20	0.1562	0.0355
20	20	21	0.1962	0.0355
21	21	22	0.2165	0.0372
22	22	23	0.3165	0.0372
23	23	24	0.2598	0.0446
24	24	25	0.1732	0.0198
25	25	26	0.1083	0.0186
26	26	27	0.0866	0.0149
27	7	28	0.1299	0.0223
28	28	29	0.2299	0.0223
29	29	30	0.1299	0.0273
30	4	14	0.1732	0.0298
31	9	29	0.0866	0.0149
32	11	19	0.0433	0.0074

Table A.2: System nominal load data

Bus No	Constant power load		Constant current load		Constant impedance load		Induction motor load	
	Active power (pu)	Reactive power (pu)	Active power (pu)	Reactive power (pu)	Active power (pu)	Reactive power (pu)	Active power (pu)	Reactive power (pu)
1	0.00367	0.00191	0.00044	0.00022	0	0	0	0
2	0.00307	0.00148	0	0	0.00083	0.00041	0	0
3	0.00368	0.00195	0.00014	0.00012	0	0	0	0
4	0.00268	0.00191	0.00027	0.00019	0	0	0	0
5	0.00469	0.00231	0	0	0.00015	5.23E-05	0.01491	0.00404
6	0.00368	0.00191	0.00064	0.00022	0.00037	0.00019	0	0
7	0.00368	0.00191	0.00094	0.00032	0	0	0	0
8	0.00268	0.00191	0.00043	0.00032	0.00063	0.00022	0	0
9	0.00468	0.00191	0	0	0.00025	0.00012	0.01491	0.00404
10	0.00368	0.00291	0	0	0	0	0	0
11	0.00307	0.00158	0	0	0	0	0	0
12	0.00261	0.00132	0	0	0	0	0.01491	0.00404
13	0.00158	0.00082	0.00016	8.24712E-05	0.00042	1.82E-05	0	0
14	0.00468	0.00191	0.00047	0.00019	0	0	0.01491	0.00404
15	0.00368	0.00291	0.00037	0.00029	0.00094	0.00033	0	0
16	0.00054	0.00033	0	0	5.40E-05	3.29E-05	0	0
17	0.00368	0.00191	0.00084	0.00022	0	0	0	0
18	0.00568	0.00191	0.00016	1.91379E-05	0	0	0.00746	0.00202
19	0.00368	0.00191	0.00037	0.00019	0	0	0	0
20	0.00368	0.00151	0.00037	0.00015	0	0	0	0
21	0.00768	0.00191	0	0	0.00028	0.00012	0.004028	0.00109
22	0.00368	0.00191	0	0	3.68E-05	1.91E-05	0	0
23	0.01268	0.00191	0	0	0	0	0	0
24	0.00368	0.00191	0.00014	2.19138E-05	0.00054	0.00022	0	0
25	0.00054	0.00033	6.53998E-05	3.32874E-05	5.40E-05	3.29E-05	0.01491	0.00404
26	0.00368	0.00191	0	0	0	0	0	0
27	0.00568	0.00191	0.00057	0.00019	0.00016	0.00012	0	0
28	0.00158	0.00082	0.00012	5.82471E-06	0	0	0.00746	0.00202
29	0.00368	0.00158	0	0	0.00031	0.00016	0	0
30	0.00158	0.00082	0.00016	8.24712E-05	0	0	0	0

# Appendix B

## Bigger Test System

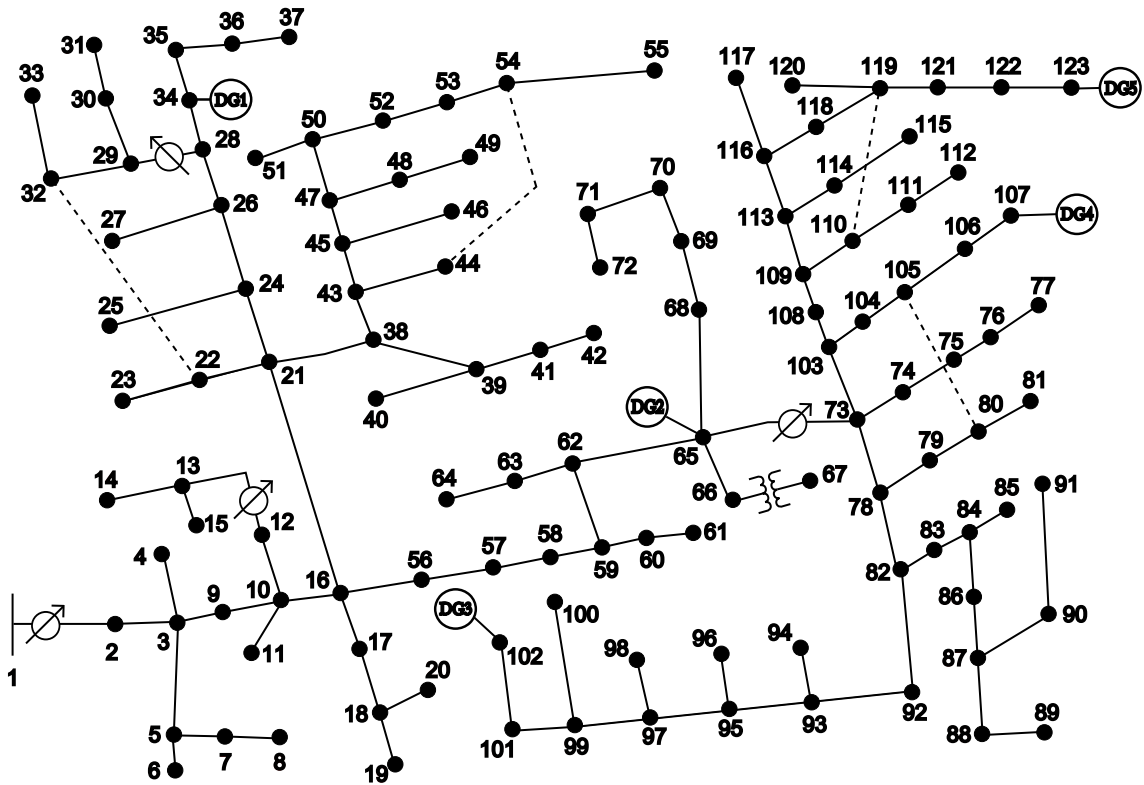


Figure B.1: Single line diagram of the modified 123-bus system with DGs and links.

# Bibliography

- [1] Das, D., Kothari, D.P., Kalam, A.: ‘Simple and efficient method for load flow solution of radial distribution networks’, *Int. J. Electr. Power Energy Syst.*, 1995, **17**, (5), pp. 335-346.
- [2] Sun, D.I.H., Abe, S., Shoults, R.R., Chen, M.S., Eichenberger, P.A.E.P., Farris, D.: ‘Calculation of energy losses in a distribution system’, *IEEE Trans. Power App. Syst.*, 1980, **PAS-99**, (4), pp. 1347-1356.
- [3] Ju, Y., Wu, W., Zhang, B., Sun, H.: ‘An extension of FBS three-phase power flow for handling PV nodes in active distribution networks’, *IEEE Trans. Smart Grid*, 2014, **5**, (4), pp. 1547-1555.
- [4] D’Adamo, C., Jupe, S., Abbey, C.: ‘Global survey on planning and operation of active distribution networks-update of CIGRE C6.11 working group activities’, *Proc. 20th Int. Conf. Exhib. Electr. Distrib.-Part 1*, 2009, pp. 1-4.
- [5] Ochoa, L.F., Dent, C.J., Harrison, G.P.: ‘Distribution network capacity assessment: Variable DG and active networks’, *IEEE Trans. Power Syst.*, 2010, **25**, (1), pp. 87-95.
- [6] Zhang, S., Cheng, H., Wang, D., Zhang, L., Li, F., Yao, L.: ‘Distributed generation planning in active distribution network considering demand side management and network reconfiguration’, *Applied energy*, 2018, **228**, pp. 1921-1936.
- [7] You, Y., Liu, D., Yu, W., Chen, F., Pan, F.: ‘Technology and its trends of active distribution network’, *Automation of Elect. Power Sys.*, 2012, **36**, (18), pp. 10-16.
- [8] McDonald, J.: ‘Adaptive intelligent power systems: Active distribution networks’, *Energy Policy*, 2008, **36**, (12), pp. 4346-4351.

- [9] Atteya, I.I., Ashour, H., Fahmi, N., Strickland, D.: ‘Radial distribution network reconfiguration for power losses reduction using a modified particle swarm optimisation’, *CIREOpen Access Proceedings Journal*, 2017, **2017**, (1), pp. 2505-2508.
- [10] Heidari, M. A.: ‘Optimal network reconfiguration in distribution system for loss reduction and voltage-profile improvement using hybrid algorithm of PSO and ACO’, *CIREOpen Access Proceedings Journal*, 2017, **2017**, (1), pp. 2458-2461.
- [11] Siti, M.W., Nicolae, D.V., Jimoh, A.A., Ukil, A.: ‘Reconfiguration and load balancing in the LV and MV distribution networks for optimal performance’, *IEEE Trans. Power Del.*, 2007, **22**, (4), pp. 2534-2540.
- [12] Morton, A.B., Mareels, J.M.Y.: ‘Overload prevention and loss minimization in managed distribution networks’, *IEEE Trans. Power Delivery*, **15**, (3), pp. 972-977.
- [13] Esmailian, H.R., Fadaeinedjad, R.: ‘Energy loss minimization in distribution systems utilizing an enhanced reconfiguration method integrating distributed generation’, *IEEE Systems Journal*, 2015, **9**, (4), pp. 1430-1439.
- [14] Peponis, G.J., Papadopoulos, M.P., Hatziargyriou, N.D.: ‘Distribution network reconfiguration to minimize resistive line losses’, *IEEE Trans. Power Delivery*, **10**, (3), pp. 1338-1342.
- [15] Borozan, V., Rajicic, D., Ackovski, R.: ‘Improved method for loss minimization in distribution networks. *IEEE Trans. Power Syst.*’, 1995, **10**, (3), pp. 1420-1425.
- [16] Coroamă, I., Chicco, G.: ‘Gavrilaş, M. and Russo, A.: ‘Distribution system optimisation with intra-day network reconfiguration and demand reduction procurement’, *Elect. Power Syst. Res.*, 2013, **98**, pp. 29-38.
- [17] Evangelopoulos, V.A., Georgilakis, P.S., Hatziargyriou, N.D., . ‘Optimal operation of smart distribution networks: A review of models, methods and future research’, *Elect. Power Syst. Res.*, 2016, **140**, pp.95-106.
- [18] Capitanescu, F., Bilibin, I., Ramos, E.R.: ‘A comprehensive centralized approach for voltage constraints management in active distribution grid’, *IEEE Trans. Power Syst.*, 2014, **29**, (2), pp. 933-942.

- [19] Marvasti, A.K., Fu, Y., DorMohammadi, S., Rais-Rohani, M.: ‘Optimal operation of active distribution grids: A system of systems framework’, *IEEE Trans. Smart Grid*, 2014, **5**, (3), pp. 1228-1237.
- [20] Degefa, M.Z., Lehtonen, M., Millar, R.J., Alahäivälä, A., Saarijärvi, E.: ‘Optimal voltage control strategies for day-ahead active distribution network operation’, *Elect. Power Syst. Res.*, 2015, **127**, pp. 41-52.
- [21] Ghasemi, M.A., Parniani, M.: ‘Prevention of distribution network overvoltage by adaptive droop-based active and reactive power control of PV systems’, *Elect. Power Syst. Res.*, 2016, **133**, pp. 313-327.
- [22] Li, P., Ji, H., Wang, C., Zhao, J., Song, G., Ding, F., Wu, J.: ‘Coordinated control method of voltage and reactive power for active distribution networks based on soft open point’, *IEEE Trans. Sust. Energy*, 2017, **8**, (4), pp. 1430-1442.
- [23] Hashim, T.T., Mohamed, A., Shareef, H.: ‘A review on voltage control methods for active distribution networks’, *Przeglad Elektrotechniczny (Electrical Review)*, 2012, **88**, (6).
- [24] Yuan, H., Li, F., Wei, Y., Zhu, J.: ‘Novel linearized power flow and linearized OPF models for active distribution networks with application in distribution LMP’, *IEEE Trans. Smart Grid*, 2018, **9**,(1), pp. 438-448.
- [25] Su, X., Masoum, M.A., Wolfs, P.J.: ‘Optimal PV inverter reactive power control and real power curtailment to improve performance of unbalanced four-wire LV distribution networks’, *IEEE Trans. Sustainable Energy*, 2014, **5**, (3), pp. 967-977.
- [26] Dolan, M.J., Davidson, E.M., Ault, G.W., Bell, K.R., McArthur, S.D.: ‘Distribution power flow management utilizing an online constraint programming method’, *IEEE Trans. Smart Grid*, 2013, **4**, (2), pp. 798-805.
- [27] Wei, W., Wang, J., Wu, L.: ‘Distribution optimal power flow with real-time price elasticity’, *IEEE Trans. Power Syst.*, 2018, **33**, (1), pp. 1097-1098.
- [28] Khonji, M., Chau, C.K., Elbassioni, K.: ‘Optimal power flow with inelastic demands for demand response in radial distribution networks’, *IEEE Trans. Control Netw. Syst.*, 2018, **5**, (1), pp. 513-524.



- [29] Tariq, M., Poor, H.V.: ‘Electricity theft detection and localization in grid-tied microgrids’, *IEEE Trans. Smart Grid*, 2018, **9**, (3), pp. 1920-1929.
- [30] Delgado, G.M., Contreras, J., Arroyo, J.M.: ‘Distribution network expansion planning with an explicit formulation for reliability assessment’, *IEEE Trans. Power Systems*, 2018, **33**, (3), pp.2583-2596.
- [31] Arrillaga, J., Arnold, C.P.: ‘Computer Analysis of Power Systems’(John Willey and Sons, Chichester, England, 1990).
- [32] Elsayed, A.M., Mishref, M.M., Farrag, S.M.: ‘Distribution system performance enhancement (Egyptian distribution system real case study)’, *Int. Trans. Electr. Energ. Syst.*, 2018, pp. 1-24. DOI: 10.1002/etep.2545.
- [33] Ramos, E.R., Expósito, A.G., Santos, J.R., Iborra, F.L.: ‘Path-based distribution network modeling: application to reconfiguration for loss reduction’, *IEEE Trans. Power Syst.*, 2005, **20**, (2), pp. 556-564.
- [34] Wu, F.F.: ‘Theoretical study of the convergence of the fast decoupled load flow’, *IEEE Trans. Power App. Syst.*, 1977, **PAS-96**, (1), pp. 268-275.
- [35] Kersting, W.H.: ‘Distribution system modeling and analysis’(CRC Press, New Mexico, 2012).
- [36] Yang, N.C., Chen, H.C.: ‘Three-phase power-flow solutions using decomposed quasi-Newton method for unbalanced radial distribution networks’, *IET Gener., Transm., Distrib.*, 2017, **11**, (4), pp. 3594-3600.
- [37] Ju, Y., Wu, W., Zhang, B., Su, H.: ‘Loop-analysis-based continuation power flow algorithm for distribution networks’, *IET Gener., Transm., Distrib.*, 2014, **8**, (7), pp. 1284-1292.
- [38] Xiao, P., Yu, D.C., Yan, Y.: ‘A unified three-phase transformer model for distribution load flow calculations’, *IEEE Trans. Power Syst.*, 2006, **21**, (1), pp. 153-159.
- [39] Cheng, C.S., Shlrmohammadi, D.: ‘A three-phase power flow method for real-time distribution system analysis’, *IEEE Trans. Power Syst.*, 1995, **10**, (2), pp. 671-679.
- [40] Kersting, W.H.: ‘A method to teach the design and operation of a distribution system’, *IEEE Trans. Power App. Syst.*, 1984, **103**, (7), pp. 1945-1952.

- [41] Augugliaro, A., Dusonchet, L., Favuzza, S.: ‘A backward sweep method for power flow solution in distribution networks’, *Int. J. Elect. Power Energy Syst.*, 2010, **32**, (4), pp. 271-280.
- [42] Chang, G.W., Chu, S.Y., Wang, H.L.: ‘An improved backward/forward sweep load flow algorithm for radial distribution systems’, *IEEE Trans. Power Syst.*, 2007, **22**, (2), pp. 882-884.
- [43] Losi, A., Russo, M.: ‘Object-oriented load flow for radial and weakly meshed distribution networks’, *IEEE Trans. Power Syst.*, 2003, **18**, (4), pp. 1265-1274.
- [44] Eminoglu, U., Hocaoglu, M.H.: ‘A new power flow method for radial distribution systems including voltage dependent load models’, *Elect. Power Syst. Res.*, 2005, **76**, (1-3), pp. 106-114.
- [45] Abdelaziz, M.M.A., Farag, H.E., El-Saadany, E.F., Mohamed, Y.A.R.I.: ‘A novel and generalized three-phase power flow algorithm for islanded microgrids using a newton trust region method’, *IEEE Trans. Power Syst.*, 2013, **28**,(1), pp. 190-201.
- [46] Chen, C.S., Hsu, C.T., Yan, Y.H.: ‘Optimal distribution feeder capacitor placement considering mutual coupling effect of conductors’, *IEEE Trans. Power Del.*, 1995, **10**, (2), pp. 987-994.
- [47] Lo, K.L. and Zhang, C.: , May. Decomposed three-phase power flow solution using the sequence component frame. *Proc. Inst. Elect. Eng., Gen., Transm., Distrib.*, 1993, **140**, (3), pp. 181-188.
- [48] Akher, M.A., Nor, K.M., Rashid, A.A.: ‘Improved three-phase power-flow methods using sequence components’, *IEEE Trans. Power Syst.*, 2005, **20**, (3), pp. 1389-1397.
- [49] Kamh, M.Z., Iravani, R.: ‘Unbalanced model and power-flow analysis of microgrids and active distribution systems’, *IEEE Trans. Power Del.*, 2010, **25**, (4), pp. 2851-2858.
- [50] Akher, M.A., Nor, K.M., Abdul-Rashid, A. H.: ‘Development of unbalanced three-phase distribution power flow analysis using sequence and phase components’, *Proc. 12th Int. Middle-East Power Syst. Conf.*, 2008, pp. 406-411.

- [51] Džafić, I., Neisius, H.T., Gilles, M., Henselmeyer, S., Landerberger, V.: ‘Three-phase power flow in distribution networks using fortescue transformation’, IEEE Trans. Power Syst., 2013, **28**, (2), pp. 1027-1034.
- [52] Luo, G.X., Semlyen, A.: ‘Efficient load flow for large weakly meshed networks’, IEEE Trans. Power Syst., 1990, **5**, (4), pp. 1309-1316.
- [53] Wu, W.C., Zhang, B.M.: ‘A three-phase power flow algorithm for distribution system power flow based on loop-analysis method’, Int. J. Electr. Power Energy Syst., 2008, **30**, (1), pp. 8-15.
- [54] Ju, Y., Wu, W., Zhang, B.: ‘Convergence problem in forward/backward sweep power flow method caused by non-positive-sequence impedance of distributed generators and its solution’, Int. J. Elect. Power Energy Syst., 2015, **65**, pp. 463-466.
- [55] Price, W.W., Wirgau, K.A., Murdoch, A., Mitsche, J.V., Vaahedi, E., El-Kady, M.A.: ‘Load modeling for power flow and transient stability computer studies’, IEEE Trans. Power Syst., 1988, **3**, (1), pp. 180-187.
- [56] Chen, T.H., Chen, M.S., Hwang, K.J., Kotas, P., Chebli, E.A.: ‘Distribution system power flow analysis-a rigid approach’, IEEE Trans. Power Del., 1991, **6**, (3), pp. 1146-1152.
- [57] Rajičić, D., Ačkovski, R., Taleski, R.: ‘Voltage correction power flow’, IEEE Trans. Power Del., 1994, **9**, (2), pp. 1056-1062.
- [58] Vieira, J.C.M., Freitas, W., Morelato, A.: ‘Phase-decoupled method for three-phase power-flow analysis of unbalanced distribution systems’, IEE Proc. Gener. Transm. Distrib., 2004, **151**, (5), pp. 568-574.
- [59] Shirmohammadi, D., Hong, H. W., Semlyen, A., Luo, G.X.: ‘A compensation-based power flow method for weakly meshed distribution and transmission networks’, IEEE Trans. Power Syst., 1988, **3**, (2), pp. 753-762.
- [60] Teng, J.H.: ‘A direct approach for distribution system load flow solutions’, IEEE Trans. Power Del., 2003, **18**, (3), pp. 882-887.
- [61] Irving, M.R., Al-Othman, A.K.: ‘Admittance matrix models of three-phase transformers with various neutral grounding configurations’, IEEE Trans. Power Syst., 2003, **18**, (3), pp. 1210-1212.

- [62] Verma, R., Sarkar, V.: ‘Accurate modeling of induction motor loads in the load flow analysis of a distribution network’, Proc. 6th Int. Conf. Power Syst., 2016, pp. 1-5.
- [63] Aree, P., Acha, E.: ‘Power flow initialisation of dynamic studies with induction motor loads’, IET Gener., Transm., Distrib., 2011, **5**, (4), pp. 417-424.
- [64] Aman, M.M., Jasmon, G.B., Bakar, A.H.A., Mokhlis, H., Naidu, K.: ‘Graph theory-based radial load flow analysis to solve the dynamic network reconfiguration problem’, Int. Trans. Electr. Energ. Syst., 2016, **26**, (1), pp. 783–808.
- [65] Ghatak, U., Mukherjee, V.: ‘An improved load flow technique based on load current injection for modern distribution system’, Int. J. Elect. Power Energy Syst., 2017, **84**, pp. 168-181.
- [66] Strezoski, V.C., Vidović, P.M.: ‘Power flow for general mixed distribution networks’, Int. Trans. Electr. Energ. Syst., 2014, **25**, (10), pp. 2455-2471.
- [67] Zimmerman, R.D., Chiang, H.D.: ‘Fast decoupled power flow for unbalanced radial distribution systems’, IEEE Trans. Power Syst., 1995, **10**, (4), pp. 2045-2052.
- [68] Li, H., Zhang, A., Shen, X., Xu, J.: ‘A load flow method for weakly meshed distribution networks using powers as flow variables’, Int. J. Elect. Power Energy Syst., 2014, **58**, pp. 291-299.
- [69] Khushalani, S., Solanki, J.M., Schulz, N.N.: ‘Development of three-phase unbalanced power flow using PV and PQ models for distributed generation and study of the impact of DG models’, IEEE Trans. Power Syst., 2007, **22**, (3), pp. 1019-1025.
- [70] Zhu, Y., Tomsovic, K.: ‘Adaptive power flow method for distribution systems with dispersed generation’, IEEE Trans. Power Del., 2002, **17**, (3), pp. 822-827.
- [71] Augugliaro, A., Dusonchet, L., Favuzza, S., Ippolito, M.G., Sanseverino, E.R.: ‘A new backward/forward method for solving radial distribution networks with PV nodes’, Elect. Power Syst. Res., 2008, **78**, (3), pp. 330-336.
- [72] Sun, H., Nikovski, D., Ohno, T., Takano, T., Kojima, Y.: ‘A fast and robust load flow method for distribution systems with distributed generations’, Proc. Smart Grid and Clean Energy Technol., 2011, **12**, (4), pp. 236-244.

- [73] Chen, H., Chen, J., Shi, D., Duan, X.: ‘Power flow study and voltage stability analysis for distribution systems with distributed generation’, Proc. IEEE Power Energy Soc. General Meeting, 2006, pp. 1-8.
- [74] Rajičić, D., Bose, A.: ‘A modification to the fast decoupled power flow for networks with high R/X ratios’, IEEE Trans. Power Syst., 1988, **3**, (2), pp. 743-746.
- [75] Rajicic, D., Bose, A.: ‘A modification to the fast decoupled power flow for networks with high R/X ratios’, IEEE Trans. Power Syst., 1988, **3**, (2), pp. 743-746.
- [76] Díaz, G., Aleixandre, J. G., Coto, J.: ‘Direct backward/forward sweep algorithm for solving load power flows in AC droop-regulated microgrids’, IEEE Trans. Smart Grid, 2016, **7**, (5), pp. 2208-2217.
- [77] Díaz, G., Gómez-Aleixandre, J., Coto, J.: ‘Direct backward/forward sweep algorithm for solving load power flows in AC droop-regulated microgrids’, IEEE Trans. Smart Grid, 2016, **7**, (5), pp. 2208-2217.
- [78] Chen, T.H., Chen, M.S., Inoue, T., Kotas, P., Chebli, E.A.: ‘Three-phase co-generator and transformer models for distribution system analysis’, IEEE Trans. Power Del., 1991, **6**, (4), pp. 1671-1681.
- [79] Grainger, J.J., Stevenson, W.D.: ‘Power System Analysis’(Tata-McGraw-Hill, New Delhi, 2003).
- [80] Stagg, G.W., El-Abiad, A.H.: ‘Computer methods in power system analysis’(McGraw-Hill, New York, 1968).
- [81] Liu, Y.H., Lee, W.J., Chen, M.S.: ‘Incorporating induction motor model in a load flow program for power system voltage stability study’, Proc. IEEE Int. Conf. Elect. Mach. and Drives, 1997, **3**, pp. 7.1-7.3.
- [82] Amin, B.: ‘Induction Motors: Analysis and Torque Control’ (Springer, Berlin, Germany, 2010).
- [83] Shakarami, M.R., Beiranvand, H., Beiranvand, A., Sharifipour, E.: ‘A recursive power flow method for radial distribution networks: Analysis, solvability and convergence’, Int. J. Electr. Power Energy Syst., 2017, **86**, pp. 71-80.

- [84] Džafić, I., Jabr, R.A., Neisius, H.T.: ‘Transformer modeling for three-phase distribution network analysis’, *IEEE Trans. Power Syst.*, 2015, **30**, (5), pp. 2604-2611.
- [85] Hong, Y.Y., Wang, F.M.: ‘Investigation of impacts of different three-phase transformer connections and load models on unbalance in power systems by optimization’, *IEEE Trans. Power Syst.*, 1997, **12**, (2), pp. 689-697.
- [86] ‘IEEE 34 Node Test Feeder’ ([Online], Available: <http://sites.ieee.org/pes-testfeeders/files/2017/08/feeder34.zip>).
- [87] ‘IEEE 123 Node Test Feeder’ ([Online], Available: <http://sites.ieee.org/pes-testfeeders/files/2017/08/feeder123.zip>).
- [88] Kamh, M.Z.: ‘Component modeling and three-phase power-flow analysis for active distribution systems’(PhD thesis, University of Toronto, 2011).
- [89] Wang, Y., Zhang, N., Li, H., Yang, J., Kang, C.: ‘Linear three-phase power flow for unbalanced active distribution networks with PV nodes’, *CSEE J. Power Energy Syst.*, 2017, **3**, (3), pp.321-324.
- [90] Pogaku, N., Prodanović, M., Green, T.C.: ‘Modeling, analysis and testing of autonomous operation of an inverter-based microgrid’, *IEEE Trans. Power Electron.*, 2007, **22**, (2), pp. 613-625.
- [91] Kallamadi, M., Sarkar, V.: ‘Enhanced real-time power balancing of an AC microgrid through transiently coupled droop control’, *IET Gener., Transm., Distrib.*, 2017, **11**, (8), pp. 1933-1942.
- [92] Yazdani, A., Iravani, R.: ‘Voltage-Sourced Converters in Power Systems’(IEEE/Wiley, Piscataway, NJ, USA, 2010).
- [93] Saddat, H.: ‘Power System Analysis’(Tata-McGraw-Hill, New Delhi, 2003).
- [94] Arrillaga, J., Arnold, C.P.: ‘Computer Analysis of Power Systems’(John Willey and Sons, Chichester, England, 1990).
- [95] Barr, J., Majumder, R.: ‘Integration of distributed generation in the volt/var management system for active distribution networks’, *IEEE Trans. Smart Grid*, 2015, **6**, (2), pp. 576-586.

- [96] Treballe, D., Hallberg, P., Lorenz, G., Mandatova, P., Guijarro, J.T.: 'Active distribution system management', In 22nd Int. Conf. Exh. Elect. Distribution (CIRED 2013), 2013, pp. 1-4.
- [97] Yazdani, A., Iravani, R.: 'A unified dynamic model and control for the voltage-sourced converter under unbalanced grid conditions', IEEE Trans. Power Del., 2006, **21**, (3), pp. 1620-1629.

# Author's Publications

## Journals:

- R. Verma and V. Sarkar, "Application of modified Gauss- $Z_{bus}$  iterations for solving the load flow problem in active distribution networks," *Electr. Power Syst. Res.*, vol. 168, no. 1, pp. 8-19, Mar. 2019.
- R. Verma and V. Sarkar, "Active distribution network load flow analysis through non-repetitive FBS iterations with integrated DG and transformer modelling," accepted for publication in *IET Gen., Transm., Distrib*, DOI: 10.1049/iet-gtd.2018.5478.

## Conferences:

- R. Verma and V. Sarkar, "Accurate modeling of induction motor loads in the load flow analysis of a distribution network," in *Proc. ICPS, New Delhi, 2016*, pp. 1-5.
- R. Verma and V. Sarkar, "An improved forward-backward sweep technique for the load flow analysis of a distribution network with accurate modeling of zero sequence voltages," in *Proc. ICITEE, Bali-Indonesia, 24-26 Jul. 2018*.
- R. Verma and V. Sarkar, "Power flow analysis of unbalanced distribution network with integration of various characteristics DGR," presented, *IICPE, Jaipur-India, 13-15 Dec. 2018*.